THERMODYNAMIC MODELING OF HVAC PLANT COOLING EQUIPMENT FOR QUANTIFICATION OF ENERGY SAVINGS THROUGH CONTINUOUS COMMISSIONING® MEASURES

A Thesis

by

STEVEN JAMES RIVERA

Submitted to the Office of Graduate Studies of
Texas A&M University
in partial fulfillment of the requirements for the degree of

MASTER OF SCIENCE

December 2011

Major Subject: Mechanical Engineering

Thermodynamic Modeling of HVAC Plant Cooling Equipment for Quantification of Energy Savings Through Continuous Commissioning® Measures

Copyright 2011 Steven James Rivera

THERMODYNAMIC MODELING OF HVAC PLANT COOLING EQUIPMENT FOR QUANTIFICATION OF ENERGY SAVINGS THROUGH CONTINUOUS COMMISSIONING® MEASURES

A Thesis

by

STEVEN JAMES RIVERA

Submitted to the Office of Graduate Studies of
Texas A&M University
in partial fulfillment of the requirements for the degree of

MASTER OF SCIENCE

Approved by:

Chair of Committee,	David E. Claridge
Committee Members,	Charles H. Culp
	Michael Pate
Head of Department,	Jerald Caton

December 2011

Major Subject: Mechanical Engineering

ABSTRACT

Thermodynamic Modeling of HVAC Plant Cooling Equipment for Quantification of Energy Savings Through Continuous Commissioning® Measures. (December 2011)
Steven James Rivera, B.S., The University of Notre Dame
Chair of Advisory Committee: Dr. David E. Claridge

The Continuous Commissioning® (CC®) process is applied to existing buildings in order to reduce energy consumption by optimizing HVAC system operation and improving occupant comfort. The CC® process consists of implementing energy saving measures for the air-side and plant-side of HVAC systems. Current development of a computer program (WinAM) by the Energy Systems Laboratory allows the expected energy savings from applying air-side CC® measures to a given building to be estimated. However, there is no means for quantifying the potential energy savings from applying plant-side CC® measures. The quasi-steady-state method and a regression of EnergyPlus library data were used for chiller modeling and the Merkel method was used for cooling tower modeling. Implementation of the models developed provides a means for quantifying the energy savings associated with plant cooling equipment CC® measures.

Chiller models have been developed for the following, with capacity range, average error, and standard deviation in parenthesis: air-cooled scroll chillers (15-168 tons, 8.07%, 9.13%), air-cooled screw chillers (69-513 tons, 7.38%, 6.13%), water-cooled scroll chillers (20-200 tons, 8.16%, 9.72%), water-cooled reciprocating chillers (20-364 tons, 10.30%, 7.81%), water-cooled screw chillers (194-498 tons, 9.87%, 3.65%), and water-cooled centrifugal chillers with inlet guide vane capacity control (233-677 tons, 12.07%, 5.96%) and with VSD capacity control (210-677 tons, 12.18%, 4.61%). From the chiller models developed, energy consumed by the chiller can be calculated as building cooling loads and fluid operating temperatures vary.

Cooling tower models have been developed to predict cooling tower energy consumption as building cooling loads, added load from chillers, fluid operating temperatures, and ambient air temperatures vary. The models developed provide for predicting energy consumption when fan operation is by single-speed, two-speed, variable-speed with modulating outlet dampers, or variable-speed with VFD control.

Implementation of the chiller and cooling tower models developed will allow WinAM users the ability to quantify the potential energy savings associated with changing plant cooling equipment operation.

DEDICATION

The work presented in this thesis is dedicated to those whose support and encouragement made it possible: my Mom, my Dad, and my sister, Nicole.

Dad, your words are those by which I try to live my life. You instilled in me an understanding of what is important in this world: God, family, and education. Thank you for the sacrifices you have made to allow me to grow mentally and spiritually at Holy Ghost, St. Pius X High School, and The University of Notre Dame.

Mom, your example of selfless giving has made a lasting impression on me. Whether staying up at night to help me with my math homework, shuttling me around to sporting events, or volunteering to read to first graders, you are the epitome of giving oneself for others. Thank you for your listening ear and understanding when things appeared hopeless.

Mom, Dad, and Nicole, I love you and try each and every day to make you proud.

ACKNOWLEDGEMENTS

First and foremost, I want to thank the Lord for blessing me with this opportunity, opening doors in times of angst, and blessing me with my family and the people below who guided me along the way.

I would like to thank my committee chair, Dr. Claridge, and my committee members, Dr. Culp and Dr. Pate, for their support and guidance throughout this project.

Dr. Claridge, your endless support and dedication to quality research has set a welcome example for me. Your help in teaching me not only energy principles, but also life lessons is much appreciated.

Dr. Culp, your open door and willingness to listen have helped give me perspective throughout my time at the Energy Systems Laboratory. I have no doubt that your openness and the sharing of your experiences will aid me throughout my own career.

I would also like to thank those at the Energy Systems Laboratory who have helped me along the way, especially Kevin Christman, Wes Van Rite, John Bynum, Oleksandr Tanskyi, and Iraj Solouki.

To my teachers at Holy Ghost Catholic School and St. Pius X High School, thank you for providing me with the fundamental principles upon which I have relied to get to this point. To my professors at the University of Notre Dame, especially Dr. Michael Stanisic and Dr. Frank Incropera, thank you for opening my eyes to the joys of engineering and the avenues through which it may be practiced to better the world.

I must also acknowledge The University of Notre Dame for a dedication to educating the mind, the spirit, and the heart. Our Lady's University has shaped my life beyond measure.

TABLE OF CONTENTS

Page

Page

LIST OF FIGURES

Page

Page

Page

Page

LIST OF TABLES

Page

1. INTRODUCTION

1.1 Motivation

The depletion of nonrenewable energy resources, coupled with increasing energy consumption, has spurred interest in energy efficiency measures. One of the most energy intensive sectors being targeted for improved energy utilization is the building sector. In 2006, the building sector alone consumed 39% of U.S. primary energy. By the year 2030, this sector is projected to increase its primary energy consumption by 29%, from 38.77 quadrillion Btu to 50.10 quadrillion Btu (Kelso 2009).

The 38.77 quadrillion Btu of energy consumed by the U.S. building sector in 2006 was used for space heating, water heating, space cooling, ventilation, lighting, electronics, refrigeration, computers, and cooking (Kelso 2009). Combining the energy associated with lighting, electronics, refrigeration, computers, and cooking into a general "other" category, Figure 1 shows the end-use of energy by the U.S. building sector in 2006.

The energy used for space heating, water heating, space cooling, and ventilation is required for the processes of heating, ventilation, and air conditioning (HVAC). As such, Figure 1 indicates that at 38%, HVAC systems are the single largest source of energy consumption in buildings. HVAC system operation has thus become an area of increasing interest as steps are taken to reduce the amount of energy consumed by the U.S. building sector.

This thesis follows the style of *HVAC&R Research*.

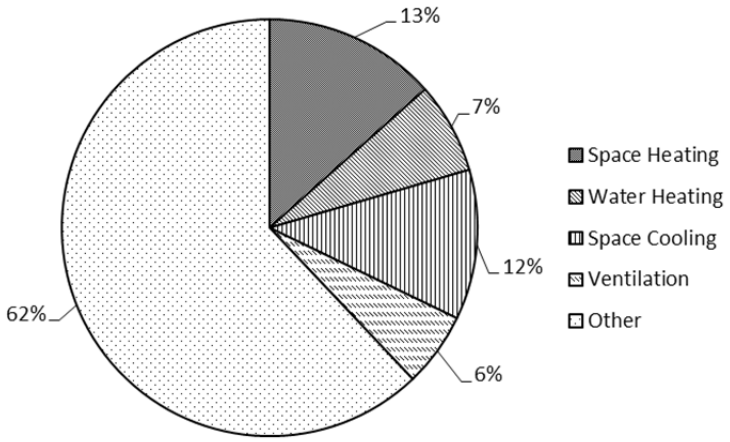

Figure 1. End-use of energy by the U.S. building sector in 2006 (adapted from Kelso 2009).

1.2 Continuous Commissioning®

In an effort to reduce the energy consumption of existing buildings and curtail the projected energy consumption increase of the building sector in the future, the U.S. Department of Energy's Federal Energy Management Program directed the Texas Engineering Experiment Station's Energy Systems Laboratory at Texas A&M University to develop documentation to accomplish such goals. The result was a guidebook published in 2002 that formally outlines methods and practices pertaining to a process known as Continuous Commissioning® (CC®) (Liu, Claridge, and W. Dan Turner 2002).

The CC® process focuses on optimizing the operation of HVAC systems such that building comfort is improved and energy consumption is reduced. By outlining methods that pertain to both the air-side and plant-side of HVAC systems, the guidebook presents a comprehensive strategy for optimizing building HVAC operation.

Results from the CC® process being employed on more than 130 buildings over a 10 year period by the Energy Systems Laboratory show an average reduction in utility consumption of 20% (Liu, Claridge, and W. Dan Turner 2002). During this time period, employing the CC® process on twenty-eight buildings provided annual savings ranging from $\$1.26/ft^2$ in medical research laboratories to $\$0.43/ft^2$ in university teaching and office buildings (Liu, M. 1999). While energy savings has been shown to vary with building usage, the underlying theme is that the CC® process results in reduced energy consumption.

Recognizing the potential for wide-spread energy savings by making the CC® process available on a large scale, the Energy Systems Laboratory currently offers interested parties the opportunity to obtain a CC® license. As a CC® licensee, access is provided to the latest research being done by the Energy Systems Laboratory to make the CC® process more efficient. With access to on-going developments, CC® licensees are provided the tools necessary for greater energy savings and reduced implementation time.

One of the most recent tools to be developed by the Energy Systems Laboratory is the WinAM program. Released in 2011, WinAM Version 4.1 allows CC® licensees to quantify potential energy savings from applying CC® measures, identify retrofits that may provide additional energy savings, and ensure that existing retrofits are performing as expected (ESL 2011). While a major step towards making the CC® process more manageable for CC® engineers, WinAM is limited in that it only takes into account the energy consumption associated with the air-side of HVAC systems. Therefore, at this stage of the programs' development, only the energy consumed by equipment tasked with conditioning and moving air within a building can be quantified.

1.3 Objective

The objective of this research is to provide a means for quantifying the potential energy savings resulting from CC® measures being applied to the cooling equipment associated with the plant-side of commercial HVAC systems.

In order to provide this additional functionality to WinAM, techniques for modeling water-cooled chillers, air-cooled chillers, and cooling towers must be developed. Based on the prevalence of their use in commercial buildings, water-cooled chillers with scroll, screw, centrifugal, and reciprocating compressors and air-cooled chillers with scroll and screw compressors will be modeled.

The addition of plant cooling equipment modeling will allow WinAM users to employ many of the plant-side CC® measures that cannot currently be accounted for in WinAM. The ability to quantify the energy savings associated with plant-side CC® measures will provide an additional tool for understanding the impact of such measures and ultimately provide CC® licensees with accurate energy savings estimates.

2. LITERATURE REVIEW

2.1 Energy Simulation Programs

The DOE-2 and Building Loads Analysis and System Thermodynamics (BLAST) programs were developed in the 1970's as design tools to aid engineers and architects in predicting HVAC loads. Many of the simulation tools developed by these programs were implemented in a program called EnergyPlus. EnergyPlus takes user inputs of building parameters and the HVAC system to calculate heating and cooling loads, plant energy consumption, and other conditions throughout the system (U.S. DOE 2010a). Simulations performed by EnergyPlus couple building characteristics, HVAC systems, and plant equipment to allow designers to understand the full effect of design choices on energy consumption (U.S. DOE 2010a).

WinAM is an energy simulation program that has been developed by the Energy Systems Laboratory for CC® engineers to accurately estimate potential energy savings resulting from the CC® process. It is with this tool that CC® engineers may provide customers with estimated cost savings, possible energy saving retrofits, and validation of existing retrofits (ESL 2011).

Currently, WinAM provides a means to quantify the potential energy savings resulting from applying air-side CC® measures. The air-side considerations made by WinAM are founded upon a thermodynamic analysis of the air required to meet the loads within a building. In order for an accurate estimate of the energy savings associated with instilling various air-side CC® measures, a two-step process is required (ESL 2011).

First, the WinAM user specifies data that characterizes the building, such as weather data, energy prices, plant efficiency, pump electric usage and control strategy, non-HVAC electric usage, and the air handler unit (AHU) types used in the building. The

AHU types accounted for include single-duct constant air volume (SDCAV) with reheat, single-duct variable air volume (SDVAV) with reheat, dual-duct constant air volume (DDCAV), and dual duct variable air volume (DDVAV) (ESL 2011).

Regardless of the AHU type, the following parameters describing the loads in the zone served by each AHU must be specified: preheat usage, return fan usage, occupancy schedule, conditioned floor area, interior zone percentage, area of external walls, windows, and roof, peak lighting and plug usage, peak occupancy, sensible and latent heat per person, outside air (OA) usage, economizer usage, and the hourly fraction of max load experienced during a day (ESL 2011).

For the SDCAV and DDCAV systems, the user must specify the zone temperature setpoint, the volumetric air flow rate, the temperature rise across the supply fan, the fan electricity usage, and the supply air temperature reset schedule from the cooling coil based on outside air temperature. The DDCAV system also requires the supply air temperature reset schedule from the heating coil based on outside air temperature (ESL 2011).

For the SDVAV and DDVAV systems, the user must specify the zone temperature setpoint, the minimum and maximum volumetric air flow rate, the maximum fan electricity usage, whether the air volume is controlled by a variable frequency drive or inlet guide vanes, and the supply air temperature reset schedule from the cooling coil based on outside air temperature. The DDVAV system also requires the supply air temperature reset schedule from the heating coil based on outside air temperature (ESL 2011).

Once a user has specified the parameters describing the building, its usage, and its HVAC system, WinAM uses a series of energy balances to simulate the hourly heating

and cooling loads placed on the HVAC system to meet the conditions specified by the user (ESL 2011).

The second step required to ensure that estimated energy savings resulting from applied air-side CC® measures are valid is to calibrate the building model created during the first step. Calibration of the building model requires that the user input measured heating and cooling utility data in the form of electricity, gas, district chilled water, or district hot water/steam. It is imperative that the measured utility data corresponds to the same time period as the weather data specified during the first step in order to perform an accurate calibration. By comparing the simulated heating and cooling loads to the measured utility data, WinAM guides the user to vary the parameters set in step one to reduce the error between the simulated and measured consumption (ESL 2011).

The building model is considered calibrated when the simulated and measured consumption are in close agreement and the parameter variations recommended by WinAM to further reduce the error are unrealistic or contrary to what is known about the building operation. There is no prescribed value of error below which the building model is guaranteed to be calibrated, but many projects have shown that a total error of 10% to 15% between simulated and measured consumption is attainable (ESL 2011).

Having obtained a calibrated building model, air-side CC® measures can be employed by applying many of the methods outlined in the *Continuous Commissioning℠ Guidebook* (Liu, Claridge, and W. Dan Turner 2002).

2.2 Plant Cooling

In the case of cooling loads, return air (RA) from the conditioned space is mixed with the required amount of outside air (OA) to ensure that ventilation standards set by ASHRAE 62 are met (Kreider et al. 2002). In order to maintain the proper air volumetric flow rate, a portion of the RA (equal to the amount of OA introduced) is

treated as exhaust air (EA) and rejected from the building. The remaining RA and the introduced OA form what is known as mixed air (MA) (Kreider et al. 2002).

The MA embodies thermal energy in the form of sensible and latent heat. The amount of heat that must be dissipated from the MA depends on the supply air (SA) conditions needed to provide cooling to the building. The SA must have a dry-bulb temperature less than that of the space to be cooled in order to remove sensible heat and the SA must also have a moisture content low enough to remove latent heat from the space. The thermal energy that must be removed from the MA in order to provide the desired SA conditions is known as the cooling load placed on the cooling coil, $\dot{Q}_{cc}$. The cooling load generated within a building is met by the thermal energy of the MA being transferred to a liquid, typically water, at a lower temperature flowing through the cooling coil of an AHU (Kreider et al. 2002). The preceding process is shown in Figure 2.

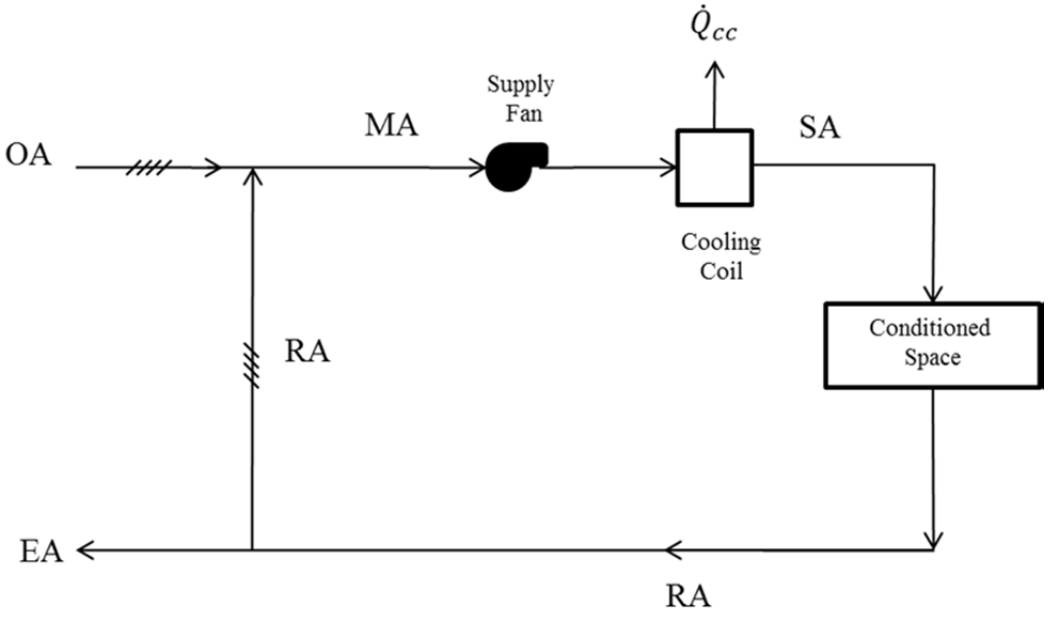

Figure 2. Diagram of a simple building cooling process.

The water circulating through the cooling coil is referred to as chilled water (CHW) and is part of a closed loop that connects the cooling coil to the cooling plant. At the cooling plant, the CHW must reject the absorbed thermal energy before it returns to the cooling coil. This task is performed by a set of equipment that forms what is known as a chiller (Kreider et al. 2002).

There are two common methods by which a chiller is used to remove thermal energy from the CHW. These methods are termed the vapor compression cycle and the absorption cycle (Kreider et al. 2002). Reciprocating, centrifugal, screw, and scroll chillers all utilize the vapor compression cycle for achieving the required heat transfer (Kreider et al. 2002).

A chiller that utilizes the vapor compression cycle requires an evaporator, compressor, condenser, and expansion device. These components, as well as the energy input and output terms pertinent to the operation of a vapor compression cycle, are shown in Figure 3.

The ideal vapor compression cycle begins when the CHW enters the evaporator and rejects thermal energy, $\dot{Q}_{evap}$, (equivalent to the cooling load, $\dot{Q}_{cc}$) to the working fluid of the chiller. Upon absorption of thermal energy from the CHW, the chiller fluid changes from a liquid to a saturated vapor. The saturated vapor then enters the compressor, where shaft work, $\dot{W}_{shaft}$, is input to raise the pressure and temperature of the fluid.

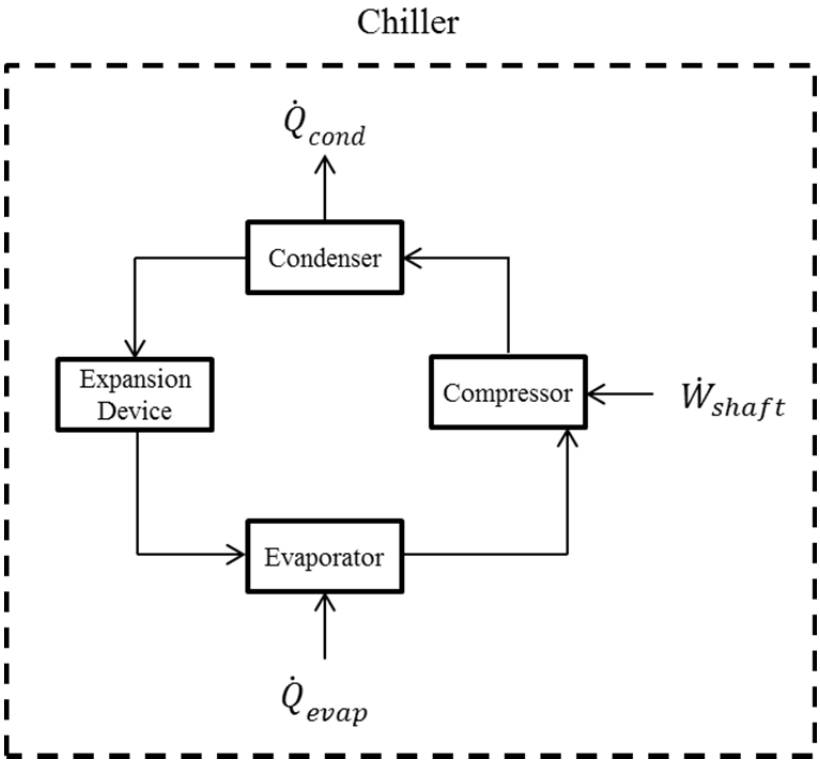

Figure 3. Diagram of a chiller utilizing the vapor compression cycle (Kreider et al. 2002).

The increase in temperature and pressure allows thermal energy, $\dot{Q}_{cond}$, to be rejected from the fluid at the condenser. The fluid exits the condenser as a saturated liquid, resulting from thermal energy being rejected. As the fluid passes through an expansion device, it becomes a saturated liquid-vapor mixture with a reduced temperature that allows it to repeat the cycle (Kreider et al. 2002).

The vapor compression cycle relies on the ability of the condenser to effectively transfer thermal energy from the chiller fluid so that it may be used to cool the incoming CHW. By means of a simple energy balance, the thermal energy that must be removed at the condenser, $\dot{Q}_{cond}$, is equal to the sum of the thermal energy absorbed at the evaporator, $\dot{Q}_{evap}$, and the compressor work, $\dot{W}_{shaft}$ (Kreider et al. 2002).

The two most common strategies for dissipating thermal energy at the condenser are provided by air-cooled and water-cooled systems. Air-cooled systems simply expose the chiller fluid to outside air as it passes through tubes in the condenser (Kreider et al. 2002). Figure 4 shows the relationship between a building's cooling load and an air-cooled system.

Water-cooled systems rely on a separate water loop for rejecting thermal energy from the condenser. In such systems, the condenser serves as a heat exchanger where by thermal energy is transferred from the chiller fluid to water flowing in a separate stream called condenser water (CW). The CW, having absorbed thermal energy from the chiller fluid, is then pumped to a cooling tower (Kreider et al. 2002).

A cooling tower employs atmospheric air as a cooling medium to remove heat from a water-cooled system (SMACNA 1995). When CW reaches the cooling tower, it is sprayed over a fill. The fill is used to improve heat transfer efficiency by uniformly distributing the water throughout the tower (Drbal et al. 1996).

Three common fill configurations are film, splash, and trickle. Film fills allow a thin layer of water to run down their surface, splash fills are designed to separate the water into smaller streams, and trickle fills utilize a combination of film and splash techniques.

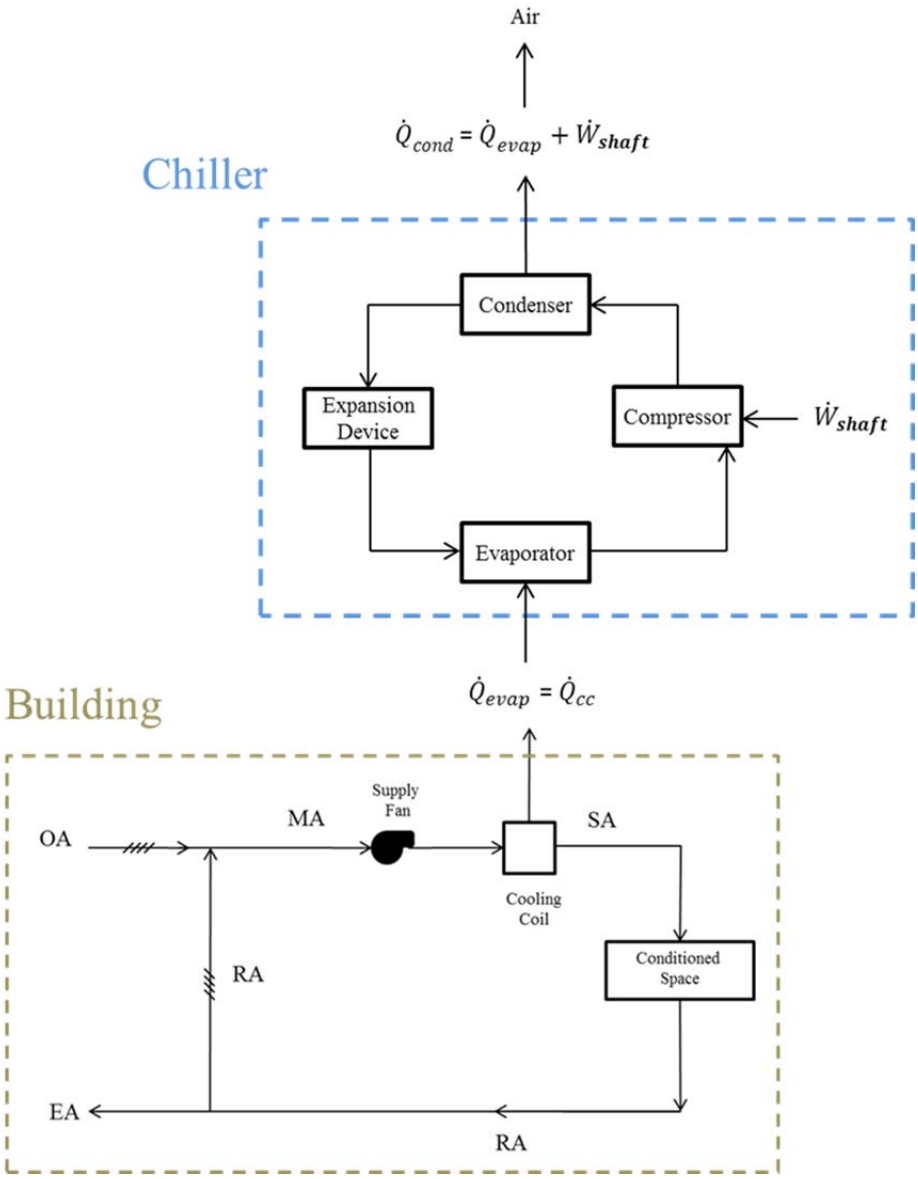

Figure 4. Diagram showing the relationship between a building's cooling load and an air-cooled system.

Regardless of the fill type employed, the goal is to increase the water surface area that can come into contact with the air and thus induce a greater potential for heat transfer and cooling (Kloppers et al. 2005).

The water-air interaction causes evaporation to occur, thus resulting in thermal energy being released from the water. The cooled CW may then be pumped back to the chiller condenser to absorb thermal energy from the chiller fluid (Kreider et al. 2002).

The need to remove large quantities of thermal energy has led to towers being commonly configured as forced-draft, where by fans blow air, or induced-draft, where by fans draw air, into crossflow or counterflow directions relative to the water (Kreider et al. 2002). In either case, releasing thermal energy by means of evaporation is the fundamental principle.

In addition to forced-draft and induced-draft cooling towers, natural-draft cooling towers exist and rely on the physics of air to rise as a result of being heated. As more heat is transferred from the water to the air, the air velocity increases and the same principles of forced-draft and induced-draft cooling towers apply (Fisenko et al. 2002). However, natural-draft cooling tower performance is subject to changing environmental conditions, like unpredictable wind velocities. This has made mechanically controlled cooling towers most common (SMACNA 1995).

Figure 5 shows the relationship between a building's cooling load and a water-cooled system.

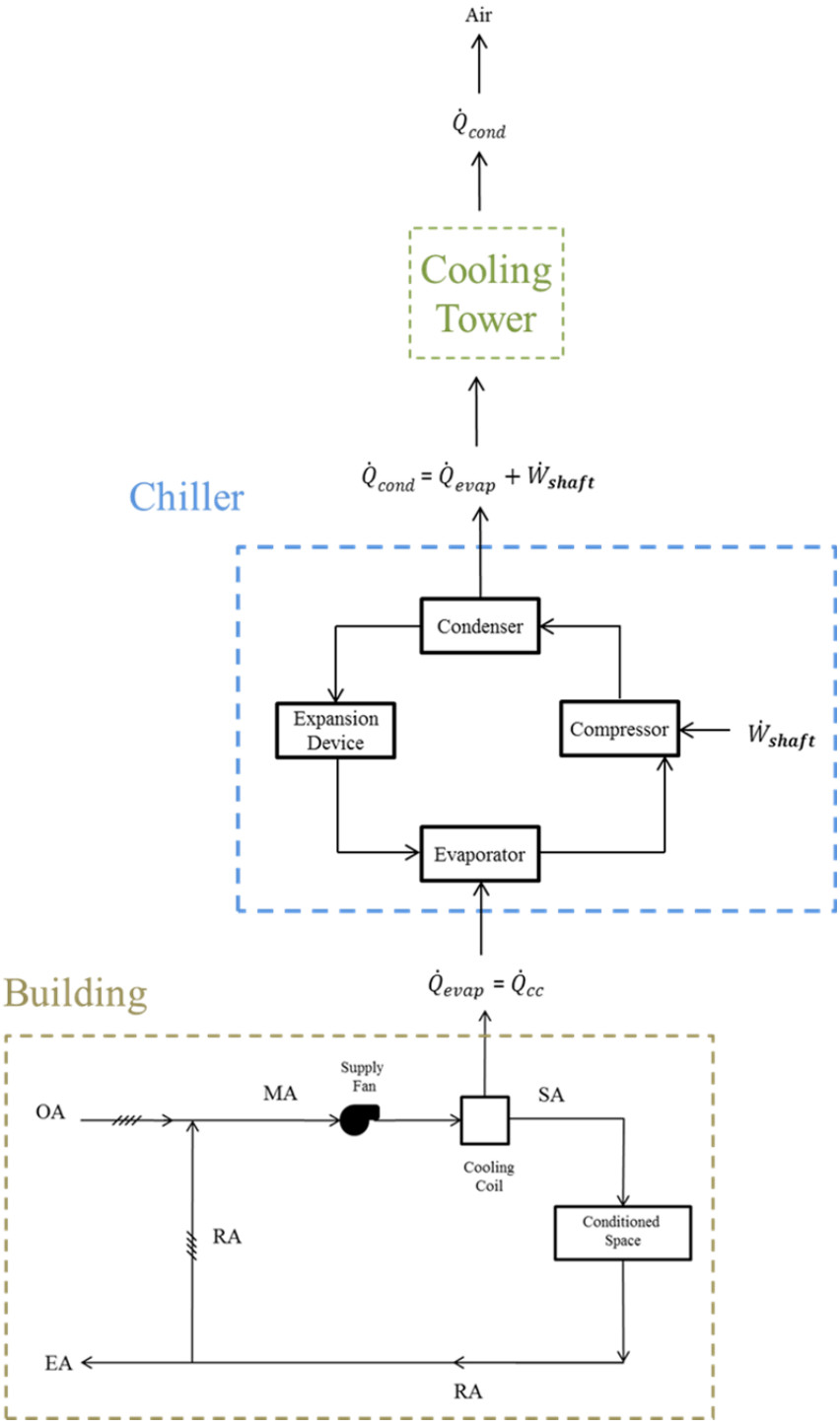

Figure 5. Diagram showing the relationship between a building's cooling load and a water-cooled system.

2.3 Plant-Side CC® Measures

The plant-side CC® measures documented in the CC® Guidebook and in direct relation to cooling equipment include using the most efficient chillers, increasing the CHW supply temperature, decreasing the condenser water (CW) return temperature, and properly staging multiple chiller systems (Liu, Claridge, and W. Dan Turner 2002). The ramifications of each of the preceding measures are described below.

Using the most efficient chillers refers to one objective of the CC® process: identify possible retrofits for a system that may help reduce energy consumption (Liu, Claridge, and W. Dan Turner 2002). The efficiency of a chiller is expressed in terms of the efficiency of its refrigeration cycle. This value is termed the coefficient of performance (COP) and represents the amount of cooling provided divided by the amount of work performed by the compressor on the chiller fluid (Leff et al. 1978).

Chiller age and designed operating load both affect chiller efficiency. Older chillers are often subject to reduced efficiency and an inability to provide the rated capacity (Liu, Claridge, and W. Dan Turner 2002). This results from the buildup of fluid deposits that form a layer and increase resistance to heat transfer in the evaporator and condenser heat exchangers, ultimately reducing efficiency (Cengel et al. 2011). In the case of operating load, manufacturers provide chillers with peak operating efficiencies at different percentages of full load (Liu, Claridge, and W. Dan Turner 2002).

Increasing the CHW supply temperature refers to the CHW that exits the evaporator of a chiller. It has been shown that for a 1°F increase, the required shaft work input to the chiller compressor is reduced by 1.7%. One implementation strategy for increasing the CHW supply temperature is based on the cooling load. As the cooling load decreases from 100% to 40%, the CHW supply temperature increases linearly from the design value up to 5°F above the design value. When the cooling load is less than 40% of the chillers design load, the CHW supply temperature remains 5°F above the design

temperature. A second strategy is to base the CHW supply temperature on ambient conditions. As the ambient temperature decreases from the value designed for to 60°F, the CHW supply temperature increases linearly from the design value up to 5°F above the design value. When the ambient temperature is less than 60°F, the CHW supply temperature remains 5°F above the design temperature. The 5°F temperature increase mentioned in both cases is a starting point and may be adjusted so long as air dehumidification is maintained (Liu, Claridge, and W. Dan Turner 2002).

Decreasing the CW return temperature refers to the CW that leaves the cooling tower and enters the condenser of a chiller. It has been shown that a reduction of 1°F in CW return temperature results in improved chiller efficiency and reduces chiller energy consumption by approximately 2% (Burger 2005). As long as several guidelines are adhered to for decreasing the CW return temperature, energy savings can be expected. First, increased cooling tower fan power consumption may be avoided by maintaining a CW return temperature at least 5°F above the ambient wet-bulb temperature. Second, limitations should be placed on the amount by which the CW return temperature may be lowered. Specifically, chillers made prior to 1999 should have a lower limit of 65°F and newer chillers should have a lower limit of 55°F (Liu, Claridge, and W. Dan Turner 2002).

Properly staging multiple chiller systems focuses on optimizing the control strategy of existing chillers. Chiller efficiency is dependent on the percentage of full-load operation. When the cooling load placed on a chiller is much less than the full-load, typically less than 40%, chiller efficiency decreases. A properly staged chiller system should be designed to control multiple chillers such that a greater portion of time is spent operating under part-load conditions that offer greater efficiency (Liu, Claridge, and W. Dan Turner 2002).

2.4 Chillers

2.4.1 Quasi-Steady-State Modeling

Presented in Section 2.2, a chiller's vapor compression cycle utilizes an evaporator, compressor, condenser, and expansion device. Commercially available chillers are designed around the compressor, as their operating characteristics are the primary concern for meeting design constraints. For example, different compressors have different size constraints, generate different amounts of noise, and provide different cooling capacities (ASHRAE 2008). Of the compressor types employed in vapor compression cycles, the greatest cooling capacity is typically provided by centrifugal compressors, followed by screw, reciprocating, and scroll compressors (in descending order) (Kreider et al. 2002). Considering the dependence of chiller performance on compressor specification, techniques for modeling scroll, screw, centrifugal, and reciprocating compressors used in water-cooled and air-cooled chillers have been studied.

One approach for modeling water-cooled and air-cooled chillers employing the vapor compression cycle is to perform a detailed analysis of each component in a chiller assembly and subsequently relating their interactions. Such modeling is commonly performed by chiller manufacturers as part of the design process. However, the complexities and time requirements associated with a detailed model of this type make it impractical for the purposes of simulating energy consumption by cooling equipment (Leverenz et al. 1983).

Another method is to treat the chiller as a quasi-steady-state system such that an energy balance may be used to describe the performance of the chiller. This method was originally developed for and found to work well in hourly building energy simulation programs. The utility of this method stems from the fact that inputs to the model are tied directly to fluctuations in the cooling load and from the inputs, the energy balance allows the outputs from the chiller to be calculated. This method takes existing data that is

provided by chiller manufacturers, derives parameters that relate the manufacturers' data to the quasi-steady-state model, and normalizes the parameters so that they may be applied to different model capacities (Leverenz et al. 1983).

Models developed using the quasi-steady-state method allow the performance of a chiller to be predicted when operating with varying CW temperatures, CHW temperatures, and cooling loads (Gordon et al. 1994).

2.4.1.1 Reciprocating Chillers

The quasi-steady-state method has been utilized in the past to account for irreversibilities and to predict the performance of reciprocating chillers (Gordon et al. 1994). The thermodynamic model developed results in Equation 1,

$$\frac{1}{\mathrm{COP}} = -1 + \frac{T_{cond}^{in}}{T_{evap}^{out}} + \frac{-A_0 + A_1\left(T_{cond}^{in}\right) - A_2\left(\frac{T_{cond}^{in}}{T_{evap}^{out}}\right)}{Q_{evap}} \qquad (1)$$

where COP is the chiller coefficient of performance, T_{cond}^{in} is the temperature of the entering CW from the cooling tower in Kelvin, and T_{evap}^{out} is the temperature of the CHW exiting the evaporator in Kelvin. A_0, A_1, and A_2 are constants that account for the irreversibilities associated with the chiller. A_0 has units of kW, A_1 has units of kW/K, and A_2 has units of kW. The cooling load placed on the chiller evaporator, Q_{evap}, has units of kW. Equation 1 may similarly be written with T_{cond}^{in} replaced by T_{cond}^{out}, the temperature of the CW leaving the condenser (Gordon et al. 1994).

The constants A_0, A_1, and A_2required to effectively model the reciprocating chiller are obtained by using performance data from the manufacturer. An example of the performance data that manufacturers commonly provide is shown in Table 1.

Table 1. Example of performance data provided by a chiller manufacturer (York 2011d).

LCWT (°F)	Air Temperature on Condenser (°F)											
	75		80		85		90		95		100	
	Tons	kW	Tons	kW	Tons	kW	Tons	kW	Tons	kW	Tons	kW
40	149.1	131.5	148.0	141.8	146.7	152.6	145.4	164.1	143.9	176.0	142.2	189.4
42	153.7	132.5	152.5	142.6	151.2	153.5	149.8	165.0	148.2	177.0	146.5	190.5
44	158.3	133.5	157.1	143.6	155.7	154.4	154.3	165.9	152.6	177.9	150.8	191.5
45	160.7	134.0	159.4	144.1	158.1	154.9	156.5	166.4	154.9	178.4	153.0	192.0
46	163.1	134.6	161.8	144.6	160.4	155.4	158.8	166.9	157.1	178.9	155.2	192.5
48	167.9	135.7	166.6	145.7	165.1	156.5	163.5	167.9	161.7	180.0	159.7	193.6
50	172.8	137.0	171.4	146.9	169.9	157.7	168.2	169.0	166.4	181.1	164.3	194.7
52	177.8	138.4	176.4	148.2	174.8	158.9	173.1	170.2	171.2	182.3	168.6	195.6
55	185.4	140.6	184.0	150.3	182.3	160.8	180.5	172.1	178.5	184.1	175.0	196.8

From this data, COP may be calculated, T_{cond}^{in} is equivalent to the air temperature on the condenser, T_{evap}^{out} is equivalent to the leaving chilled water temperature (LCWT), and the only unknowns in Equation 1 are A_0, A_1, and A_2.

By plotting $\left(1/\mathrm{COP} + 1 - T_{cond}^{in}/T_{evap}^{out}\right)Q_{evap}$ against $T_{cond}^{in}/T_{evap}^{out}$, a set of approximately parallel straight lines are obtained, with the average slope corresponding to A_2. An example of this plot is shown in Figure 6.

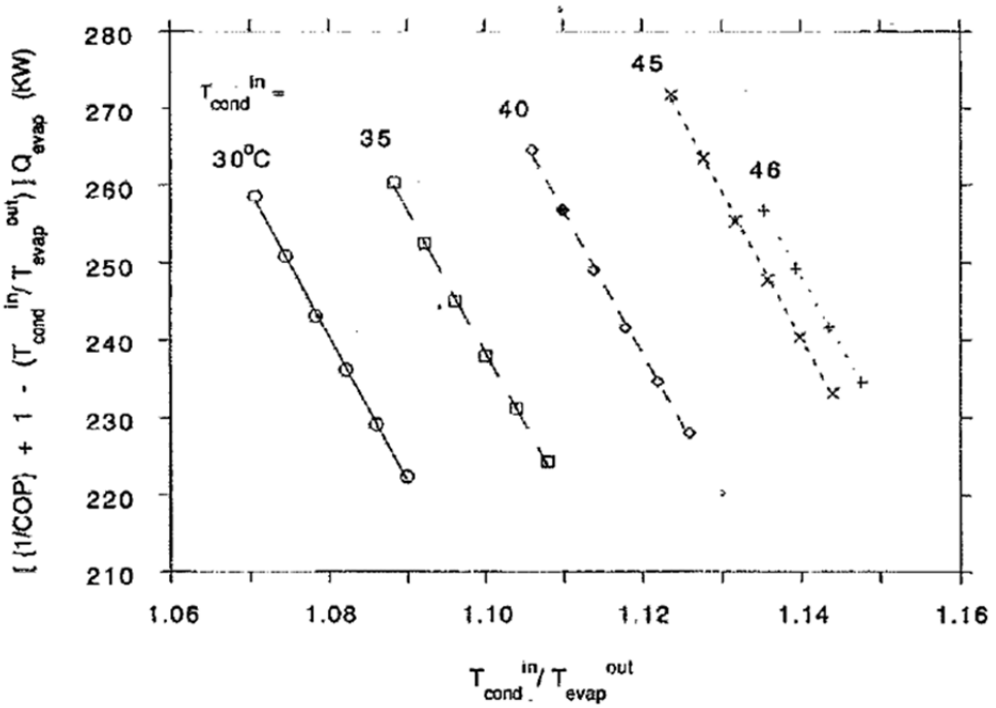

Figure 6. Example of plot used to obtain constant A_2 (Gordon et al. 1994).

Using the value of A_2 and plotting $\left(1/\mathrm{COP} + 1 - T_{cond}^{in}/T_{evap}^{out}\right)Q_{evap} + A_2\left(T_{cond}^{in}/T_{evap}^{out}\right)$ against T_{cond}^{in} yields a single line. An example of this plot is shown in Figure 7.

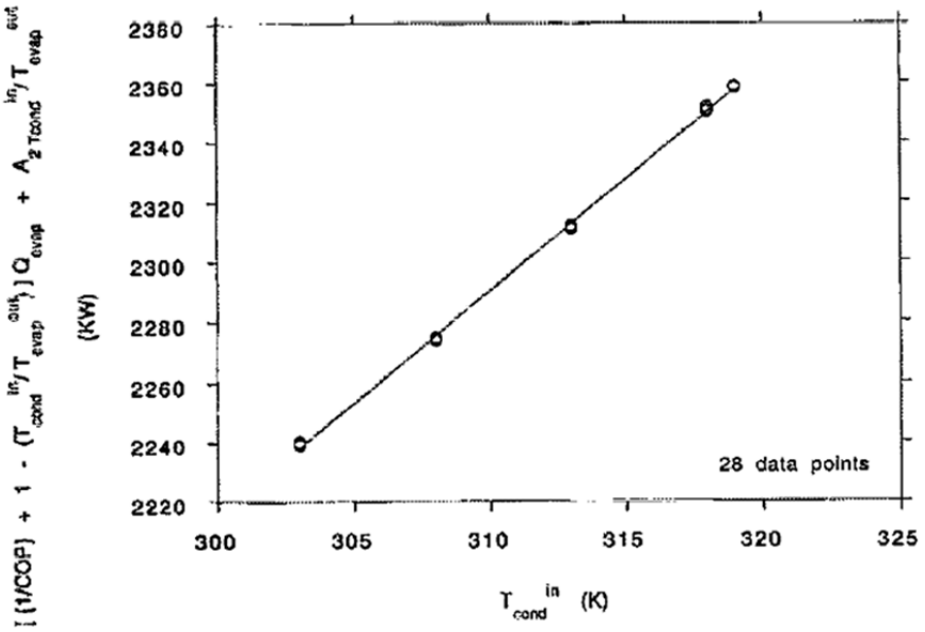

Figure 7. Example of plot used to obtain constants A_0 and A_1 (Gordon et al. 1994).

A linear fit of this line provides the slope, which corresponds to A_1, and the y-intercept, which corresponds to A_0. Using A_0, A_1, A_2, and the same values presented in the manufacturer's data for T_{cond}^{in} and T_{evap}^{out}, Equation 1 is used to calculate the predicted COP resulting from the model (Gordon et al. 1994). The application of A_0, A_1, and A_2 to the entire set of chiller operating conditions is based on the assumption that, for reciprocating and centrifugal compressors, the total entropy generated by irreversibilities is approximately constant over the range of operating conditions (Graves 2003).

The preceding method was applied to 30 reciprocating chillers and the predicted COP was compared to the manufacturers reported COP. The average root mean square error (RMSE) between the predicted and measured COP for all of the chillers was calculated to be 0.4%. Considering that the uncertainty associated with the manufacturers performance data is ±3%, the quasi-steady-state method was found to be valid for modeling reciprocating chillers (Gordon et al. 1994).

2.4.1.2 Centrifugal Chillers

The quasi-steady-state model shown to accurately predict reciprocating chiller performance was extended to centrifugal chillers by means of a diagnostic study. Instead of using manufacturers data to obtain A_0, A_1, and A_2 in Equation 1, this study obtained the cooling rate, power input, entering CW temperature, and CHW temperature exiting the evaporator over the course of two time periods: before and after cleaning the interiors of the evaporator and condenser tubes to improve chiller efficiency. The data collected was for a 100 ton water-cooled centrifugal chiller serving part of the Engineering Faculty building at the National University of Singapore. Using a thermodynamic model and approach identical to that presented in Section 2.4.1.1, the study found that the predicted COP and measured COP were in agreement as they both indicated improved efficiency after maintenance was performed (Gordon et al. 1995).

2.4.1.3 Screw Chillers

A screw chiller was modeled and coupled with the model of a cooling tower to develop a control strategy to optimize the performance of a chiller plant. Unlike reciprocating and centrifugal chillers, the total amount of entropy generated by screw chillers is not constant for different operating conditions. Rather, the entropy produced was shown to depend on the change in pressure across the screw compressor (Graves 2003).

An improved model was developed to take into consideration the entropy associated with the pressure rise across the compressor. Using measured performance data for a screw chiller, the improved model resulted in an error of 2-5% between predicted and measured power consumption. For comparative purposes, the screw chiller was also modeled under the assumption that the total entropy generated remains constant for a range of conditions (the modeling technique shown to be valid for reciprocating chillers in Section 2.4.1.1 and centrifugal chillers in Section 2.4.1.2). This model resulted in an error of 4-12% between the predicted and measured power consumption (Graves 2003).

2.4.1.4 Scroll Chillers

The scroll compressor used in scroll chillers is similar to a reciprocating compressor in that both are positive-displacement compressors that reduce fluid volume as a means to increase pressure (ASHRAE 2008).

2.4.2 EnergyPlus Modeling

The quasi-steady-state modeling technique may be employed as described in Section 2.4.1 as long as manufacturers data may be obtained. While manufacturers data is still provided for water-cooled and air-cooled reciprocating and scroll chillers, it is no longer provided for water-cooled centrifugal and screw chillers (Hydeman et al. 2002). Instead, manufacturers are required by the Air-Conditioning, Heating, and Refrigeration Institute (AHRI) to specify chiller part-load performance in terms of an Integrated Part-Load Value (IPLV) or Non-Standard Part-Load Value (NPLV). These values are obtained by applying weighting factors to the chiller efficiency at 100%, 75%, 50%, and 25% full-load. The weighting factors represent the average amount of time that a chiller spends operating at each load percentage and are 1% at 100% full-load, 42% at 75% full-load, 45% at 50% full-load, and 12% at 25% full-load. The direct result is a single value indicative of chiller part-load performance (AHRI 2003).

While part-load performance data is no longer provided for water-cooled centrifugal and screw chillers, the EnergyPlus building energy simulation program has used past data and data provided from chiller sales representatives to develop a library of such chillers (Hydeman et al. 2002). EnergyPlus uses the approach for chiller modeling developed for the DOE-2.1 building energy simulation program. This empirical approach uses chiller performance data at reference conditions and three curve fits to determine chiller performance at part-load conditions. More than 160 total chillers, primarily centrifugal and screw type, have been modeled in the program so that users may select a chiller with similar reference characteristics to that found in their building and apply it to their

simulation. Each chiller is characterized in the library by its reference capacity and reference COP. These reference values are based on an entering CW temperature into the condenser of 29.4°C (85°F) and a leaving CHW temperature from the evaporator of 6.67°C (44°F) (U.S. DOE 2010b).

The three curves pertaining to each chiller are generated by obtaining regression coefficients from manufacturers performance data. The first curve, CAPFT, uses 6 coefficients to calculate chiller full-load capacity as a function of condenser and evaporator fluid temperatures. The second curve, EIRFT, uses 6 coefficients to calculate chiller efficiency as a function of evaporator and condenser fluid temperatures (Hydeman et al. 2002). The chiller efficiency is expressed as the energy input to cooling output ratio (EIR), which is the inverse of the COP (U.S. DOE 2010b). The third curve, EIRFPLR, uses 3 coefficients to calculate chiller efficiency as a function of the part-load ratio (PLR) (Hydeman et al. 2002).

The sequence of operation for chiller modeling in EnergyPlus is as follows. A user selects a chiller from the EnergyPlus library that has a reference capacity and reference COP similar to that used in their building. The chiller selected has 3 sets of predefined coefficients, one set for each performance curve. EnergyPlus first uses the CAPFT coefficients to obtain the fraction of reference capacity that the chiller can provide for the current evaporator and condenser fluid temperatures. By multiplying this fraction by the reference capacity, the full-load capacity is obtained. EnergyPlus then calculates the PLR by dividing the actual building cooling load by the full-load capacity. The PLR is then used with the EIRFPLR coefficients to obtain the fraction of reference EIR for the current PLR. EnergyPlus simultaneously uses the EIRFT coefficients and the current evaporator and condenser fluid temperatures to calculate the fraction of reference EIR for the current evaporator and condenser fluid temperatures. The fractions resulting from the EIRFPLR and EIRFT calculations are multiplied to obtain the total fraction of reference EIR. This total fraction is multiplied by the reference EIR (1/reference COP)

to obtain the actual EIR for the current PLR and evaporator and condenser fluid temperatures (U.S. DOE 2010b).

Based on the definition of COP in Section 2.3, the actual power consumption of the chiller may be calculated by multiplying the actual EIR by the actual building cooling load.

2.5 Cooling Towers

2.5.1 Modeling Approaches

2.5.1.1 Merkel, Poppe, and e-NTU Methods

Three common approaches exist for modeling the performance of cooling towers in terms of the amount of heat rejected and the amount of water evaporated. A comparative study was performed to determine the validity of these approaches: the Merkel, Poppe, and e-number-of-transfer-units (e-NTU) methods (Kloppers et al. 2005).

The Merkel method provided the first thermal analysis of cooling towers and was introduced in 1925. In order to simplify the analysis of evaporative cooling within a cooling tower, the Merkel method assumes that the Lewis factor is equal to 1, the air exiting the cooling tower is saturated, and the effects of water loss through evaporation are ignored (Kloppers et al. 2005).

The Lewis factor is the ratio of sensible heat transfer to mass transfer at the interface of the water and main airstream (ASHRAE 2008). The value specified for the Lewis factor was proven to be irrelevant when concerned with predicting exiting water temperature from the cooling tower and the amount of heat rejected as long as the specified value remained the same during the analysis (Kloppers et al. 2005).

The Merkel method is prohibitive in that the actual moisture content of the air leaving the cooling tower cannot be calculated as a result of the second assumption. However, this assumption (that the air exiting the cooling tower is saturated) allows the exiting air temperature to be calculated (Kloppers et al. 2005).

The third assumption used in the Merkel method, that water loss effects through evaporation are negligible, provides added simplification to the modeling technique. It has been shown that for every 10°F of cooling range (difference between inlet and outlet cooling tower water temperatures), 1.2% of the CW is lost as vapor (Burger 2005). Considering water loss through evaporation being 1.2%, the third assumption has been accepted and employed in other cooling tower models (Graves 2003).

Although not considered in the Merkel method, cooling tower drift is another source of water loss and reduced cooling efficiency. Drift occurs when water droplets become sufficiently small, causing the force imparted by the fan to exceed that of gravity and blow partially cooled water into the atmosphere. Drift eliminators have been incorporated in cooling towers to prevent such losses, resulting in the volume of water lost being less than 0.02% (Burger 2005).

The e-NTU method provides a simplified numerical solution and is based on the same assumptions made by the Merkel method. As a result of these assumptions, the e-NTU method does not provide an accurate model of the exiting air conditions (Kloppers et al. 2005).

The Poppe method was introduced in the 1970's and deviates from the Merkel and e-NTU methods by not employing the three assumptions previously presented. By means of a detailed mass and energy balance procedure the actual air and water interaction during the evaporative cooling process is accounted for. Application of the mass and

energy balances is employed as an iterative approach that allows the actual air conditions exiting the cooling tower to be calculated (Kloppers et al. 2005).

A comparison of the Merkel, Poppe, and e-NTU methods was performed, with the results independent of the type of fill used in the cooling tower and indicative of natural-draft and mechanical-draft cooling towers. The results for all three methods were compared for ambient air temperatures ranging from 280 to 310 K and ambient air humidity ranging from dry to completely saturated (Kloppers et al. 2005).

The comparison considered the predicted exiting air temperature, rate of evaporation, and exiting water temperature. Results indicated that the Poppe method was the most accurate predictor of exiting air temperature and rate of evaporation. As such, it was recommended that for the design of hybrid cooling towers and cases in which the amount of water vapor present in the exiting air is important, the Poppe method should be employed. In the case of exiting water temperature, it was shown that the Merkel, e-NTU and Poppe methods predict nearly identical values (Kloppers et al. 2005).

2.5.1.2 EnergyPlus

The EnergyPlus building energy simulation program provides users with the ability to specify cooling towers serving condenser loops. Users may choose between single-speed, two-speed, and variable-speed cooling towers, depending on the fan being used. All three cooling tower models are based on the Merkel method presented in Section 2.5.1.1 (U.S. DOE 2010b).

Capacity control is implemented by the following description. The simulation calculates the required CW temperature that must be output from the cooling tower in order to provide for adequate heat transfer from the condenser (U.S. DOE 2010b). The required heat transfer from the condenser is known to be the sum of the building cooling load and the work input by the compressor (Kreider et al. 2002). If the user has specified that free

convection is used when possible, the cooling tower model predicts the outlet CW temperature under free convection conditions. If the predicted CW temperature is equal to or less than the required CW temperature to meet the load, then the tower fan is modeled as off during that period of operation. This initial routine, however, requires that the user input either the air volumetric flow rate and heat transfer-area product (UA) or the tower capacity under free convection conditions. If the user does not know these values, then the free convection operation routine is skipped (U.S. DOE 2010b).

If the predicted outlet CW temperature resulting from free convection is greater than the required outlet CW temperature to meet the load, or the user has not specified free convection parameters, then the fan is modeled as 100% on (single-speed), at the lowest fan speed setting (two-speed), or the fan speed is calculated based on the air flow rate needed to achieve the desired outlet CW temperature (variable-speed). In the case of a two-speed cooling tower, if the predicted outlet CW temperature at low speed remains above the required outlet CW temperature, then the fan is modeled at the high speed setting (U.S. DOE 2010b).

For specification of a two-speed cooling tower, the user inputs the fan power consumption at low speed and high speed. If only the high speed power consumption value is known, the program sets the low speed power consumption to 16% of that specified for high speed operation (U.S. DOE 2010b).

The detailed cooling tower implementation by EnergyPlus also provides for modeling water consumption. The default setup calculates evaporation loss by assuming the leaving air is saturated. An alternative option allows users to input a factor of evaporation in terms of water loss percent per degree Kelvin, with the default value being 0.2%/K. This factor is multiplied by the CW temperature change to obtain the evaporation rate (U.S. DOE 2010b).

EnergyPlus also allows for water lost through drift effects to be calculated by assuming a constant percentage of CW is lost. With typical cooling tower values being between 0.002% and 0.2% of the CW flow rate, the default setting is 0.008% (U.S. DOE 2010b).

The specification of cooling tower cells is also provided by EnergyPlus. However, the number of cells does not affect the cooling tower performance. Rather, this feature allows users modeling existing systems to understand the sequence of operation, or users designing a new system to understand how many cells should be incorporated into the design. Users have two options for viewing these outputs, as they may specify minimum or maximum cell control. In either case, the model calculates the required water flow rate to meet the cooling load. For minimum cell control, the model operates one cell until 250% of the design water flow rate is reached, in which case another cell is turned on. For maximum cell control, the model operates as many cells as possible until 33% of the design water flow rate is reached, in which case one cell is turned off. This feature allows users to understand how many cells are operating in a cooling tower and their sequence of operation. If the number of cooling tower cells is not specified, the model assumes there is only one, and this functionality is lost. However, cooling tower performance remains unaffected as the model is independent of the number of cells (U.S. DOE 2010b).

2.5.2 Capacity Control

When capacity control is employed by cooling towers, adjustment of water flow rate is discouraged (Kreider et al. 2002). Water distribution systems used in cooling towers are designed for maximum efficiency by assuming a relatively constant water flow rate. If the water flow rate is too high, the system may become over pressurized and collecting basins may overflow. If the water flow rate is too low, the system may not provide enough water to cover the fill, thus reducing the heat transfer rate. A by-product of this reduction in heat transfer rate is an increase in fan power consumption to compensate and provide the necessary cooling (SPX 2009). For these reasons, it is advised that the

water flow rate remain at the design specification. A typical cooling tower is designed with a flow rate of 3 gpm per ton of cooling (U.S. DOE 2010b; ASHRAE 2008; Kreider et al. 2002). Capacity control may therefore be attained by varying the fan speed (SPX 2009).

Considering that cooling towers consume energy by powering fans and pumping water (SPX 2009), energy savings can be expected when capacity control reduces fan power. Regarding energy consumption, the energy consumed by cooling tower fans is much greater than the power expended by the water pumps (Kreider et al. 2002).

When a cooling tower uses a single-speed fan motor, the options for capacity control are limited. In order to avoid fan motor short-cycling between on and off, such cooling towers often incorporate a hot water by-pass system. This design allows the fan to remain on and the desired exiting water temperature to be provided by mixing by-passed water with the cooled water collected in the basin. These systems are limited in their usage because in freezing conditions, the reduced flow rate of cooled water may not be enough to prevent freezing within the tower. In order to provide better capacity control, cooling towers are designed with two-speed or variable-speed fans (SPX 2009).

While two-speed fans provide better capacity control than single-speed fans, variable-speed fans are ideal for providing the greatest capacity control and energy savings under part-load conditions. Originally, centrifugal fans with modulating outlet dampers were used to provide variable-speed capacity control, but they are being replaced by less expensive variable frequency drives (VFDs). When VFDs are used for cooling tower capacity control, the speed should be prevented from being less than 25% of the maximum speed in order to maintain air and water distribution (ASHRAE 2008).

2.6 Fan Power

The fan laws provide a means for quantifying the variation of rotational speed, air flow rate, power, and produced head as a result of one of the other parameters changing. With subscripts 1 and 2 designating before and after conditions, respectively, the relationship between volumetric air flow rate, $\dot{V}$, rotational speed, N, and fan power, $\dot{W}$, are shown below (Kreider et al. 2002).

$$\dot{V}_2 = \dot{V}_1 \left(\frac{N_2}{N_1}\right) \tag{2}$$

$$\dot{W}_2 = \dot{W}_1 \left(\frac{N_2}{N_1}\right)^3 \tag{3}$$

When relating fan volumetric flow rate and power consumption, the fan efficiency must also be accounted for. The total fan efficiency is assumed to be 0.5 in the EnergyPlus building energy simulation program (U.S. DOE 2010b).

Variable-volume air flow has been used in commercial HVAC systems to meet changing loads and reduce power consumption, as a change in flow is proportional to a cubic change in power. One method for controlling flow is the use of fan outlet dampers to introduce resistance. When fan outlet dampers are applied for flow control, the actual fan power, $\dot{W}$, may be expressed as a function of the fan power at design flow, $\dot{W}_{rated}$, and the part-load ratio (actual volumetric air flow rate divided by rated volumetric air flow rate), PLR, as shown below (Kreider et al. 2002).

$$\frac{\dot{W}}{\dot{W}_{rated}} = 0.371 + 0.973(PLR) - 0.342(PLR)^2 \tag{4}$$

An alternative method for controlling air flow is the use of variable-speed fan motors. When variable-speed drives (VSDs) are used for flow control, the actual fan power may

similarly be expressed as a function of the fan power at design flow and the part-load ratio, as shown below (Kreider et al. 2002).

$$\frac{\dot{W}}{\dot{W}_{rated}} = 0.00153 + 0.0052(PLR) + 1.1086(PLR)^2 - 0.1164(PLR)^3 \quad (5)$$

2.7 Psychrometric Equations

Relationships between air dry-bulb temperature, T_{db}, air wet-bulb temperature, T_{wb}, saturation pressure at wet-bulb temperature, $p_{sat,wb}$, saturation pressure at dry-bulb temperature, $p_{sat,db}$, partial pressure, p_m, relative humidity, ϕ, humidity ratio, ω, and enthalpy, h, are all expressed by psychrometric equations (Kreider et al. 2002).

The enthalpy of moist air may be expressed as (Kreider et al. 2002)

$$h = c_{pa}T_{db} + w\left(h_{g,ref} + c_{pw}T_{db}\right) \quad (6)$$

Substituting appropriate values for the specific heat of dry air, c_{pa}, (0.240 Btu/lb-°F), the enthalpy of saturated water vapor, $h_{g,ref}$, (1061.2 Btu/lb), and the specific heat of superheated water, c_{pw}, (0.444 Btu/lb-°F), Equation 6 may be expressed as (Kreider et al. 2002)

$$h = 0.240T_{db} + w(1061.2 + 0.444T_{db}) \quad (7)$$

where T_{db} is in degrees Fahrenheit and h is in Btu/lb_{da}.

The humidity ratio may be obtained by (Kreider et al. 2002)

$$w = 0.622\left(\frac{\phi p_{sat,db}}{p - \phi p_{sat,db}}\right) \quad (8)$$

where the atmospheric pressure, p, is approximately 14.696 psia.

The relative humidity may be calculated by (Kreider et al. 2002)

$$\phi = \frac{p_{sat,wb} - p_m}{p_{sat,db}} \tag{9}$$

Replacing T with absolute T_{wb} to calculate $p_{sat,wb}$ or absolute T_{db} to calculate $p_{sat,db}$, the saturation pressure may be obtained by (Kreider et al. 2002)

$$p_{sat} = p_c\left(10^{K(1-T_c/T)}\right) \tag{10}$$

where the critical pressure of water, p_c, is approximately 3226 psia and the critical temperature, T_c, is approximately 1165.67°R. The parameter K is calculated from the absolute T_{wb} when calculating $p_{sat,wb}$ and the absolute T_{db} when calculating $p_{sat,db}$ by (Kreider et al. 2002)

$$K = 4.39553 - 3.469\left(\frac{T}{1000}\right) + 3.072\left(\frac{T}{1000}\right)^2 - 0.8833\left(\frac{T}{1000}\right)^3 \tag{11}$$

The partial pressure may be calculated from the absolute temperatures by (Kreider et al. 2002)

$$p_m = p\left(\frac{T_{db} - T_{wb}}{2725}\right)\left(1 + \frac{T_{wb} - 492}{1571}\right) \tag{12}$$

where the atmospheric pressure, p, is approximately 14.696 psia.

3. CHILLER MODEL DEVELOPMENT

The methodology employed to obtain chiller models that may be implemented in WinAM to quantify potential energy savings from plant cooling equipment CC® measures is presented in the following sections. It will be shown how the quasi-steady-state method and EnergyPlus library of data have been extended for application to this research.

3.1 Air-Cooled Chillers

3.1.1 Scroll Chillers

Manufacturer's data for scroll chillers with reference capacities between 15 and 168 tons was obtained from York (York 2011c; York 2011b). Likewise, manufacturer's data for scroll chillers with reference capacities between 20 and 60 tons was obtained from Trane (Trane 2002a). This data has been compiled and is shown in Appendix A.

The data provided for each York chiller included entering condenser air temperatures (T_{cond}^{in}) of 75°F, 80°F, 85°F, 90°F, and 95°F. For each value of T_{cond}^{in}, exiting CHW temperatures (T_{evap}^{out}) of 40°F, 42°F, 44°F, 45°F, 46°F, 48°F, and 50°F were provided. For each of the 35 data points, the measured compressor power consumption and full-load capacity were also given. The actual chiller COP for each data point was calculated by dividing the full-load capacity by the required power. The chiller reference capacities for which such data was provided were 15, 19, 26, 29, 37, 39, 46, 56, and 66 tons for model YCAL and 72, 78, 86, 96, 114, 120, 127, 140, 143, and 168 tons for model YLAA. In total, 665 data points were provided to describe the York chillers.

The quasi-steady-state method, as presented in Section 2.4.1, was used to obtain the A_0, A_1, and A_2 constants for each chiller reference capacity. The constant values were then plotted vs. reference capacity, as shown in Figure 8.

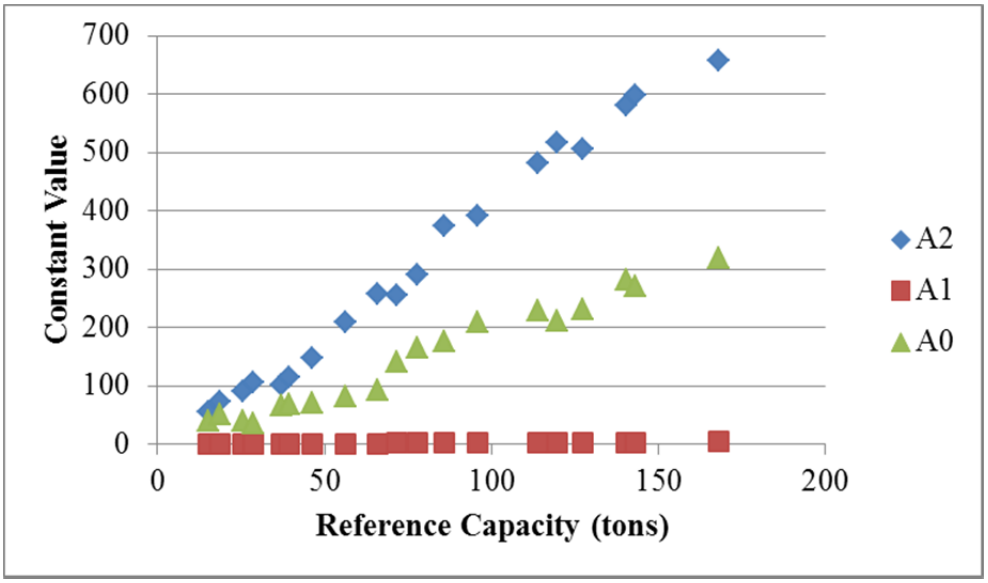

Figure 8. Plot of A_0, A_1, and A_2 constants vs. reference capacity for selected York air-cooled scroll chillers.

A linear regression of the preceding plot provided the following functions relating the constants to the reference capacity, cap_{ref}:

$$A_0{}^* = 1.96 * cap_{ref} - 5.56 \quad (13)$$

$$A_1{}^* = 0.02 * cap_{ref} - 0.12 \quad (14)$$

$$A_2{}^* = 4.28 * cap_{ref} - 27.04 \quad (15)$$

Using the linear functions, $A_0{}^*$, $A_1{}^*$, and $A_2{}^*$ were calculated for each chiller reference capacity. These constant values were then used with the set of temperatures and full-load capacities provided by the manufacturer's 665 data points to calculate the predicted COP by using Equation 1. Comparing the actual and predicted COP values for all 665 data points showed an average error of 3.53% with a standard deviation of 3.89%.

These results indicate that the linear functions closely predict chiller COP at full-load capacity.

The data provided for each Trane chiller included entering condenser air temperatures (T_{cond}^{in}) of 75°F, 85°F, 95°F, 105°F, and 115°F. For each value of T_{cond}^{in}, exiting CHW temperatures (T_{evap}^{out}) of 40°F, 42°F, 44°F, 45°F, 46°F, 48°F, and 50°F were provided. For each of the 35 data points, the measured compressor power consumption and full-load capacity were also given. The actual chiller COP for each data point was calculated by dividing the full-load capacity by the required power. The chiller reference capacities for which such data was provided were 20, 25, 30, 40, 50, and 60 tons for model CGAF. In total, 210 data points were provided to describe the Trane chillers.

The quasi-steady-state method, as presented in Section 2.4.1, was used to obtain the A_0, A_1, and A_2 constants for each chiller reference capacity. The constant values were then plotted vs. reference capacity, as shown in Figure 9.

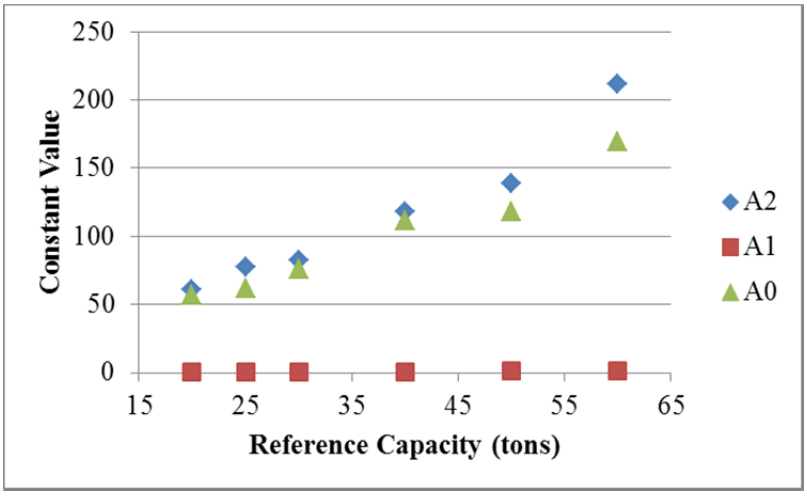

Figure 9. Plot of A_0, A_1, and A_2 constants vs. reference capacity for selected Trane air-cooled scroll chillers.

A linear regression of the preceding plot provided the following functions relating the constants to the reference capacity, cap_{ref}:

$$A_0{}^* = 2.72 * cap_{ref} - 2.98 \quad (16)$$

$$A_1{}^* = 0.02 * cap_{ref} - 0.07 \quad (17)$$

$$A_2{}^* = 3.49 * cap_{ref} - 15.75 \quad (18)$$

Using the linear functions, $A_0{}^*$, $A_1{}^*$, and $A_2{}^*$ were calculated for each chiller reference capacity. These constant values were then used with the set of temperatures and full-load capacities provided by the manufacturer's 210 data points to calculate the predicted COP by using Equation 1. Comparing the actual and predicted COP values for all 210 data points showed an average error of 2.91% with a standard deviation of 0.76%. These results indicate that the linear functions closely predict chiller COP at full-load capacity.

Having developed manufacturer-dependent models for air-cooled scroll chillers, the development of a manufacturer-independent model for air-cooled scroll chillers utilized the same methodology.

The A_0, A_1, and A_2 constants obtained for each York and Trane chiller reference capacity were plotted vs. reference capacity, as shown in Figure 10.

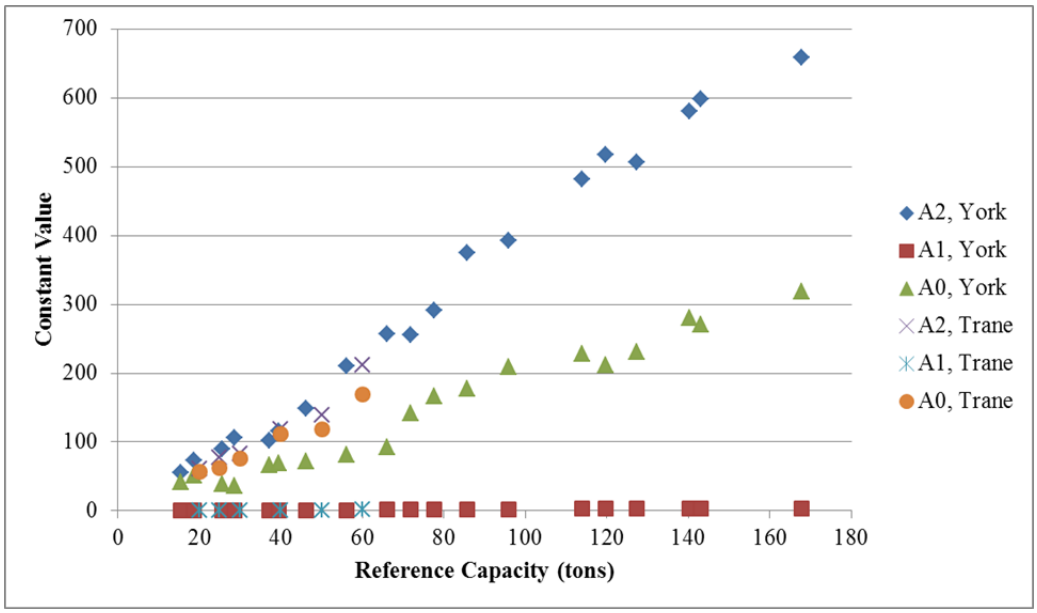

Figure 10. Plot of A_0, A_1, and A_2 constants vs. reference capacity for York and Trane air-cooled scroll chillers.

A linear regression of the preceding plot provided the following functions relating the constants to the reference capacity, cap_{ref}:

$$A_0{}^* = 1.85 * cap_{ref} + 8.75 \quad (19)$$

$$A_1{}^* = 0.02 * cap_{ref} - 0.10 \quad (20)$$

$$A_2{}^* = 4.33 * cap_{ref} - 34.93 \quad (21)$$

Using the linear functions, $A_0{}^*$, $A_1{}^*$, and $A_2{}^*$ were calculated for each chiller reference capacity. These constant values were then used with the set of temperatures and full-load capacities provided by the both manufacturers' 875 data points to calculate the predicted COP by using Equation 1. Comparing the actual and predicted COP values for all 875 data points showed an average error of 3.91% with a standard deviation of 2.68%. These results indicate that the linear functions closely predict chiller COP at full-load capacity.

Equations 19, 20, and 21 may thus be used to calculate $A_0{}^*$, $A_1{}^*$, and $A_2{}^*$ for a given air-cooled scroll chiller reference capacity (independent of manufacturer) between 15 and 168 tons. Use of these constants, the cooling load, and evaporator and condenser fluid temperatures in Equation 1 allows the chiller COP at full-load conditions to be predicted.

Considering that the majority of chiller operation occurs at part-load conditions, as presented in Section 2.4.2, it is necessary to be able to characterize chiller COP at part-load.

The manufacturer's data provided for the York set of chillers included chiller COP values at different PLR conditions. However, a correlation between COP and PLR could not be obtained directly from the provided data because the reported values are at different condenser fluid temperatures.

For a constant evaporator outlet temperature, T_{evap}^{out}, of 44°F, the manufacturer's data provided the chiller COP at a given condenser inlet temperature, T_{cond}^{in}, and PLR. In order to obtain an accurate correlation describing the behavior of COP with respect to PLR, a curve specific to one set of fluid temperatures was required. The manufacturer's data provided one data point for a PLR between 1 and 0. A second data point was obtained by recognizing that COP=0 when PLR=0. Having previously shown the ability of the chiller model developed by the quasi-steady-state method to accurately predict chiller full-load COP, the evaporator and condenser fluid temperature were input to the model in order to obtain a third data point (COP at PLR=100%). This method was used to obtain a temperature-specific curve representing the behavior of COP with respect to PLR.

The following description provides an example of the methodology presented in the preceding paragraph. For a 66 ton air-cooled scroll chiller, the manufacturer provided

the chiller COP for a PLR of 0.75 when T_{cond}^{in}=82.6°F and the chiller COP for a PLR of 0.5 when T_{cond}^{in}=69.3°F. Using the quasi-steady-state model, the chiller full-load COP (when PLR=1) was calculated for the given T_{cond}^{in} temperatures and for T_{evap}^{out}=44°F. The resulting curves are shown in Figure 11.

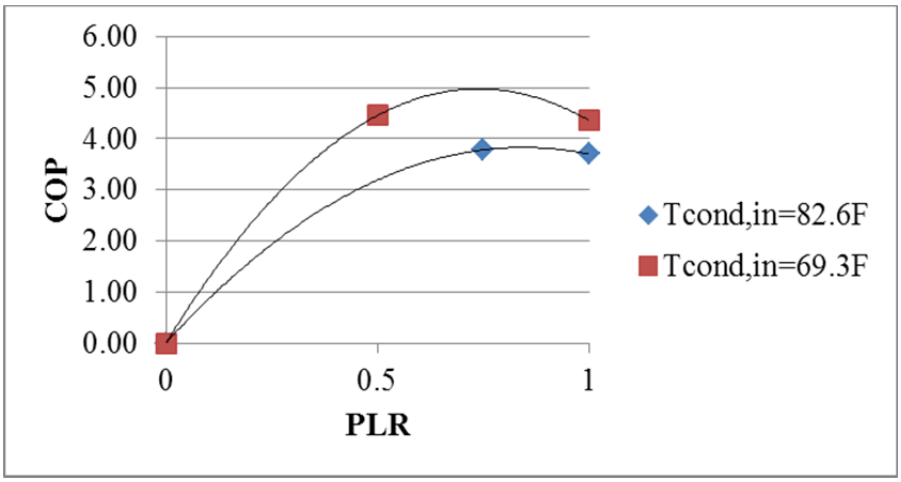

Figure 11. COP vs. PLR for a 66 ton air-cooled scroll chiller at two condenser inlet temperatures and a constant evaporator outlet temperature.

In order to normalize the behavior observed in the preceding figure for the two condenser fluid temperatures, the fraction of full-load COP was plotted vs. PLR, as shown in Figure 12.

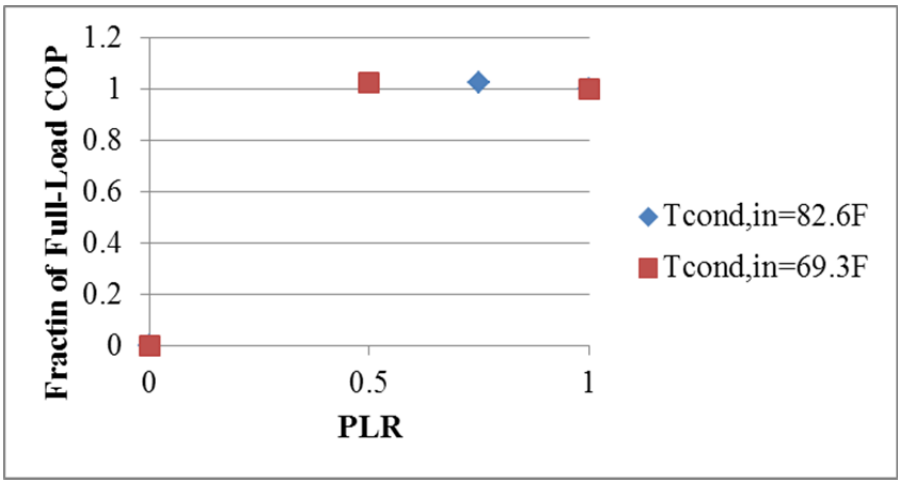

Figure 12. Fraction of full-load COP vs. PLR for a 66 ton air-cooled scroll chiller at two condenser inlet temperatures and a constant evaporator outlet temperature.

The preceding figure indicates that for different PLRs, chiller COP varies as a fraction of the full-load COP in a similar manner for different fluid temperature conditions.

The preceding steps were performed for the York chillers with the part-load data shown in Appendix B and the fraction of full-load COP was plotted vs. PLR, as shown in Figure 13.

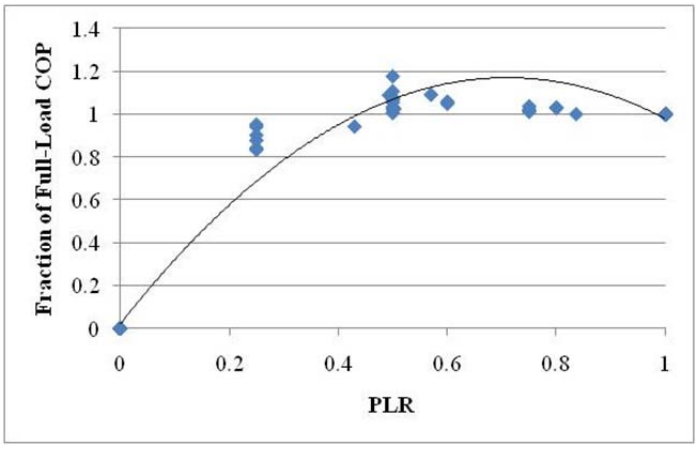

Figure 13. Fraction of full-load COP vs. PLR for all York air-cooled scroll chillers.

Analysis of the preceding figure indicates that a single curve approximates the behavior of the chillers. Specifically, the fraction of full-load COP increases as PLR decreases from 1 and peaks around PLR=0.5.

A polynomial curve was found to best fit the data shown in the preceding figure, and provided the following function relating fraction of full-load COP ($COP_{FL,frac}$) to PLR,

$$COP_{FL,frac} = -2.275(PLR)^2 + 3.233(PLR) + 0.021 \qquad (22)$$

The preceding equation was used to calculate the predicted fraction of full-load COP for different PLR values and the results were compared to the manufacturer's reported values. This comparison yielded an average error of 4.16% with a standard deviation of 6.45%. These results indicate that the polynomial function closely predicts variation in chiller COP under part-load conditions.

Given the cooling load and the chiller reference capacity, the PLR may be calculated and used in Equation 22 to obtain the multiplier that must be applied to the predicted full-load chiller COP. The resulting value provides the chiller COP at current operating conditions with a total (combined full-load and part-load) average error of 8.07% and standard deviation of 9.13%.

3.1.2 Screw Chillers

Manufacturer's data for screw chillers with reference capacities between 153 and 513 tons was obtained from York (York 2011d). Likewise, manufacturer's data for screw chillers with reference capacities between 69 and 386 tons was obtained from Trane (Trane 1999, RLC-DS-2). This data has been compiled and is shown in Appendix C.

The data provided for each York chiller included entering condenser air temperatures (T_{cond}^{in}) of 75°F, 80°F, 85°F, 90°F, and 95°F. For each value of T_{cond}^{in}, exiting CHW temperatures (T_{evap}^{out}) of 40°F, 42°F, 44°F, 45°F, 46°F, 48°F, and 50°F were provided. For each of the 35 data points, the measured compressor power consumption and full-load capacity were also given. The actual chiller COP for each data point was calculated by dividing the full-load capacity by the required power. The chiller reference capacities for which such data was provided were 153, 168, 184, 198, 215, 236, 258, 273, 303, 343, 385, 410, 439, 471, 492, and 513 tons for model YCAV. In total, 560 data points were provided to describe the York chillers.

The quasi-steady-state method, as presented in Section 2.4.1, was used to obtain the A_0, A_1, and A_2 constants for each chiller reference capacity. The constant values were then plotted vs. reference capacity, as shown in Figure 14.

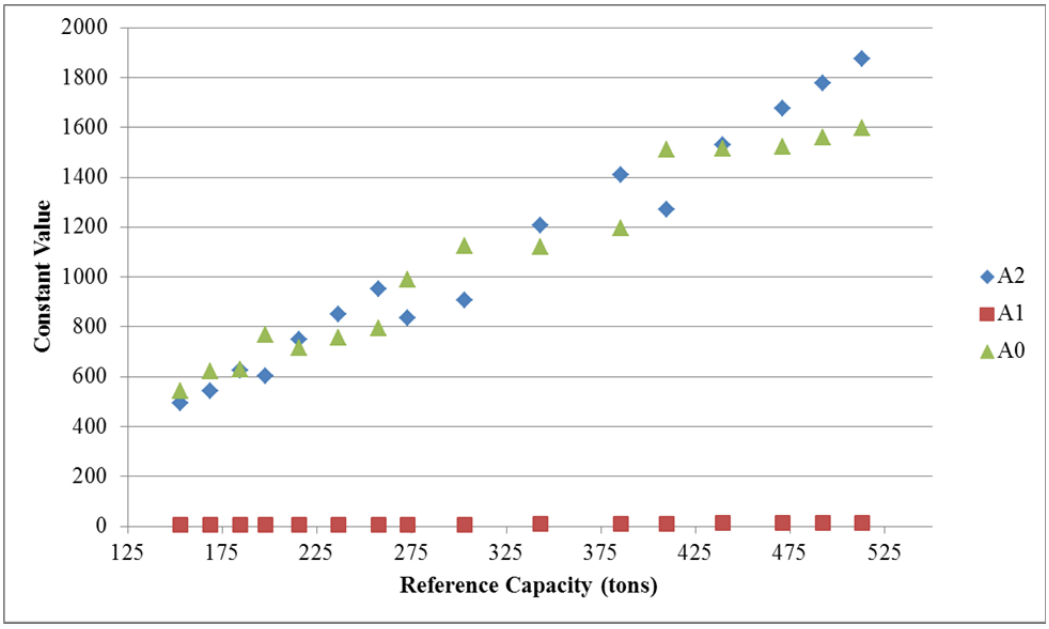

Figure 14. Plot of A_0, A_1, and A_2 constants vs. reference capacity for selected York air-cooled screw chillers.

A linear regression of the preceding plot provided the following functions relating the constants to the reference capacity, cap_{ref}:

$$A_0{}^* = 3.08 * cap_{ref} + 90.09 \quad (23)$$

$$A_1{}^* = 0.03 * cap_{ref} + 0.001 \quad (24)$$

$$A_2{}^* = 3.70 * cap_{ref} - 84.87 \quad (25)$$

Using the linear functions, $A_0{}^*$, $A_1{}^*$, and $A_2{}^*$ were calculated for each chiller reference capacity. These constant values were then used with the set of temperatures and full-load capacities provided by the manufacturer's 560 data points to calculate the predicted COP by using Equation 1. Comparing the actual and predicted COP values for all 560 data points showed an average error of 0.92% with a standard deviation of 0.41%. These results indicate that the linear functions closely predict chiller COP at full-load capacity.

The data provided for each Trane chiller included entering condenser air temperatures (T_{cond}^{in}) of 75°F, 85°F, 95°F, 105°F,and 115°F. For each value of T_{cond}^{in}, exiting CHW temperatures (T_{evap}^{out}) of 40°F, 42°F, 44°F, 46°F, 48°F, 50°F, and 55°F were provided. For each of the 35 data points, the measured compressor power consumption and full-load capacity were also given. The actual chiller COP for each data point was calculated by dividing the full-load capacity by the required power. The chiller reference capacities for which such data was provided were 69, 80, 91, 101, 108, 120, 132, 143, 151, 166, 175, 190, 195, 235, 262, 287, 333, 360, and 386 tons for model RTAA. In total, 665 data points were provided to describe the Trane chillers.

The quasi-steady-state method, as presented in Section 2.4.1, was used to obtain the A_0, A_1, and A_2 constants for each chiller reference capacity. The constant values were then plotted vs. reference capacity, as shown in Figure 15.

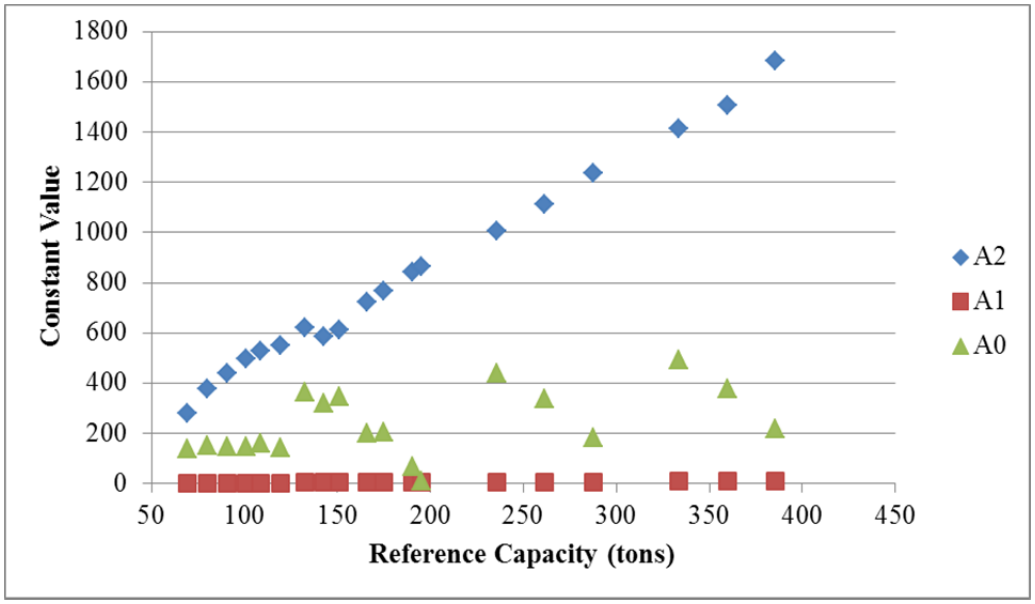

Figure 15. Plot of A_0, A_1, and A_2 constants vs. reference capacity for selected Trane air-cooled screw chillers.

Figure 15 indicates that a linear correlation for A_0 is not as definite as for air-cooled scroll chillers. It is believed that the behavior of A_0 reflects the conclusions made by previous research regarding the use of the quasi-steady-state method for modeling screw chillers. Specifically, the total amount of entropy generated by screw chillers is not constant for different operating conditions. Rather, the entropy produced was shown to depend on the change in pressure across the screw compressor (Graves 2003). A_0 may therefore be the constant through which this variation in entropy generation is manifested.

However, the same research found that modeling screw chillers under the assumption that the total entropy generated remains constant for a range of conditions (the quasi-steady-state method), resulted in an error of 4-12% between predicted and measured power consumption (Graves 2003). Due to the utility of the form of Equation 1 for

predicting chiller COP, and the limited error shown, the applicability of the quasi-steady-state method was explored.

A linear regression of the preceding plot provided the following functions relating the constants to the reference capacity, cap_{ref}:

$$A_0{}^* = 0.62 * cap_{ref} + 117.53 \quad (26)$$

$$A_1{}^* = 0.02 * cap_{ref} + 0.51 \quad (27)$$

$$A_2{}^* = 4.14 * cap_{ref} + 41.86 \quad (28)$$

Using the linear functions, $A_0{}^*$, $A_1{}^*$, and $A_2{}^*$ were calculated for each chiller reference capacity. These constant values were then used with the set of temperatures and full-load capacities provided by the manufacturer's 665 data points to calculate the predicted COP by using Equation 1. Comparing the actual and predicted COP values for all 665 data points showed an average error of 3.27% with a standard deviation of 1.19%. These results indicate that the linear functions closely predict chiller COP at full-load capacity.

Having developed manufacturer-dependent models for air-cooled screw chillers, the development of a manufacturer-independent model for air-cooled screw chillers utilized the same methodology.

The A_0, A_1, and A_2 constants obtained for each York and Trane chiller reference capacity were plotted vs. reference capacity, as shown in Figure 16.

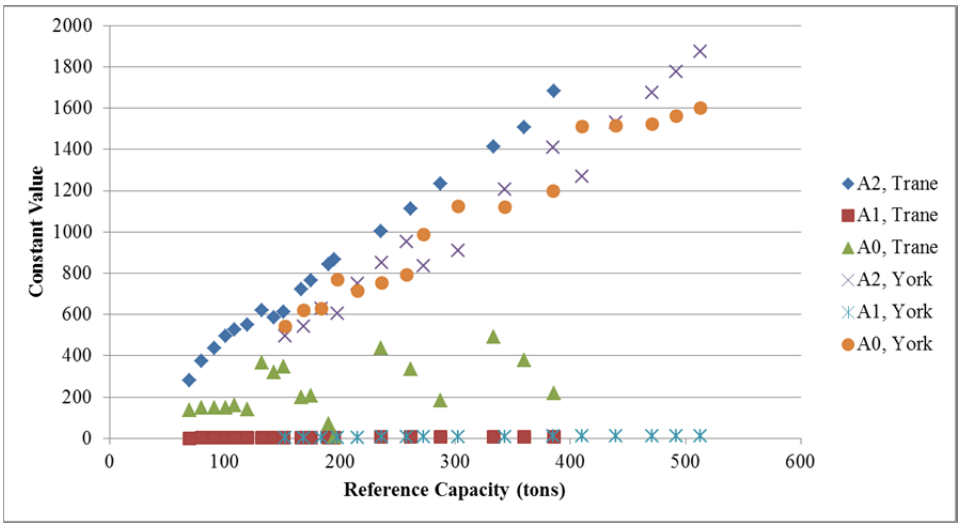

Figure 16. Plot of A_0, A_1, and A_2 constants vs. reference capacity for York and Trane air-cooled screw chillers.

A linear regression of the preceding plot provided the following functions relating the constants to the reference capacity, cap_{ref}:

$$A_0{}^* = 3.20 * cap_{ref} - 177.26 \quad (29)$$

$$A_1{}^* = 0.03 * cap_{ref} - 0.20 \quad (30)$$

$$A_2{}^* = 3.41 * cap_{ref} + 101.29 \quad (31)$$

Using the linear functions, $A_0{}^*$, $A_1{}^*$, and $A_2{}^*$ were calculated for each chiller reference capacity. These constant values were then used with the set of temperatures and full-load capacities provided by the both manufacturers' 1225 data points to calculate the predicted COP by using Equation 1. Comparing the actual and predicted COP values for all 1225 data points showed an average error of 4.53% with a standard deviation of 2.34%. These results indicate that the linear functions closely predict chiller COP at full-load capacity.

The resulting error from applying the quasi-steady-state method to screw chillers, even though entropy generation is not constant for different operating conditions, is similar to the 4-12% previously reported (Graves 2003).

Equations 29, 30, and 31 may thus be used to calculate $A_0{}^*$, $A_1{}^*$, and $A_2{}^*$ for a given air-cooled screw chiller reference capacity (independent of manufacturer) between 69 and 513 tons. Use of these constants, the cooling load, and evaporator and condenser fluid temperatures in Equation 1 allows the chiller COP at full-load conditions to be predicted.

Considering that the majority of chiller operation occurs at part-load conditions, as presented in Section 2.4.2, it is necessary to be able to characterize chiller COP at part-load.

The manufacturer's data provided for the Trane set of chillers included chiller COP values at different PLR conditions. However, a correlation between COP and PLR could not be obtained directly from the provided data because the reported values are at different evaporator and condenser fluid temperatures, as required by the AHRI (AHRI 2003). Specifically, COP is reported for PLRs with the fluid temperatures shown in Table 2.

Table 2. AHRI standard conditions for reporting air-cooled chiller COP at varying PLRs.

PLR	**$T_{evap,out}$ (°F)**	**$T_{cond,in}$ (°F)**
100%	44	95
75%	44	80
50%	44	65
25%	44	55

In order to obtain an accurate correlation describing the behavior of COP with respect to PLR, a curve specific to one set of fluid temperatures was required. One curve was

generated for the temperature conditions of T_{evap}^{out} = 44°F and T_{cond}^{in} = 80°F. Two data points were known: COP at PLR=75% (provided by the manufacturer's data) and COP=0 at PLR=0. Having previously shown the ability of the chiller model developed by the quasi-steady-state method to accurately predict chiller full-load COP, the evaporator and condenser fluid temperature were input to the model in order to obtain a third data point (COP at PLR=100%).

A second curve was generated for the temperature conditions of T_{evap}^{out} = 44°F and T_{cond}^{in} = 65°F. Two data points were known: COP at PLR=50% (provided by the manufacturer's data) and COP=0 at PLR=0. Having previously shown the ability of the chiller model developed by the quasi-steady-state method to accurately predict chiller full-load COP, the evaporator and condenser fluid temperature were input to the model in order to obtain a third data point (COP at PLR=100%).

The two curves are shown in Figure 17 as an example for a 175 ton chiller.

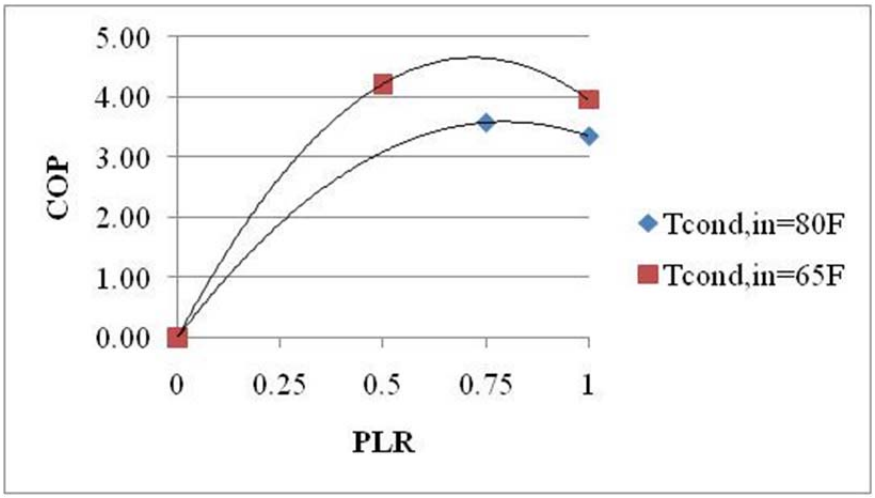

Figure 17. COP vs. PLR for a 175 ton air-cooled screw chiller at two condenser inlet temperatures and a constant evaporator outlet temperature.

In order to normalize the behavior observed in the preceding figure for the two condenser fluid temperatures, the fraction of full-load COP was plotted vs. PLR, as shown in Figure 18.

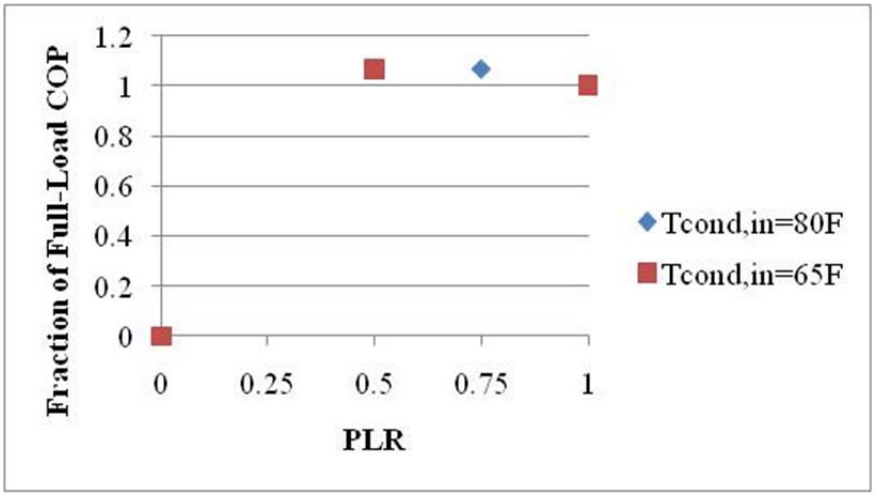

Figure 18. Fraction of full-load COP vs. PLR for a 175 ton air-cooled screw chiller at two condenser inlet temperatures and a constant evaporator outlet temperature.

The preceding figure indicates that for different PLRs, chiller COP varies as a fraction of the full-load COP in a similar manner for different fluid temperature conditions.

The preceding steps were performed for the Trane chillers with the part-load data shown in Appendix D and the fraction of full-load COP was plotted vs. PLR, as shown in Figure 19.

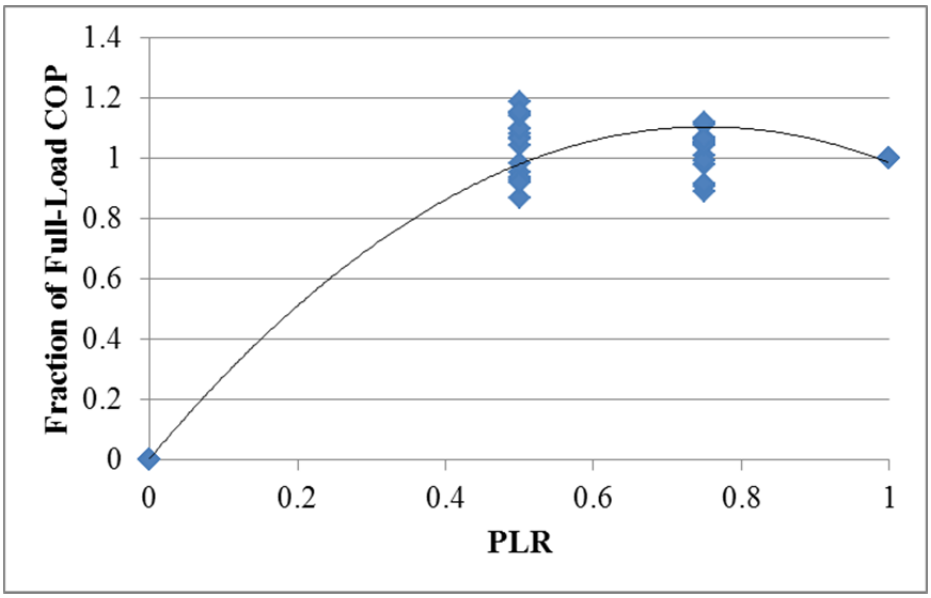

Figure 19. Fraction of full-load COP vs. PLR for all Trane air-cooled screw chillers.

Analysis of the preceding figure indicates that a single curve is not representative of all chillers. Specifically, for some chillers, the full-load COP is the maximum COP, whereas for other chillers the maximum COP occurs at a lower PLR.

It was identified that the PLR at which maximum COP is observed is dependent on the chiller capacity. Figure 20 shows that for air-cooled screw chillers, capacities less than 151 tons reach maximum COP at full-load and capacities greater than 151 tons reach maximum COP at lower PLRs.

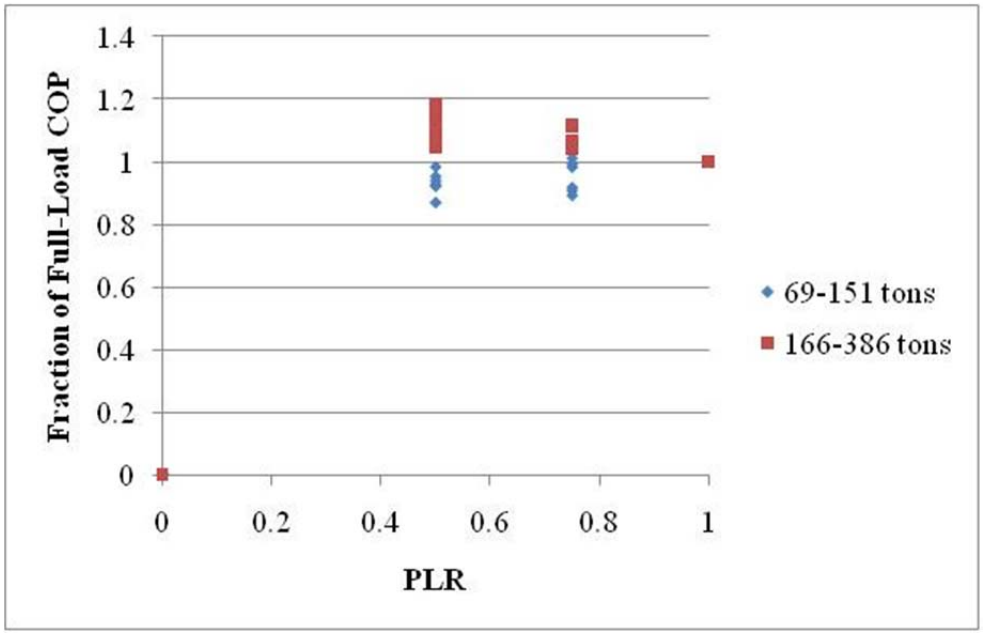

Figure 20. Fraction of full-load COP vs. PLR for two sets of Trane air-cooled screw chillers.

Polynomial curves were found to best fit the data shown in the preceding figure, and provided the following functions relating fraction of full-load COP ($COP_{FL,frac}$) to PLR for capacities less than or equal to 151 tons

$$COP_{FL,frac} = -1.515(PLR)^2 + 2.496(PLR) + 0.005 \quad (32)$$

and

$$COP_{FL,frac} = -2.197(PLR)^2 + 3.176(PLR) + 0.005 \quad (33)$$

for capacities greater than 151 tons.

The preceding equations were used to calculate the predicted fraction of full-load COP for different PLR values and the results were compared to the manufacturer's reported values. This comparison yielded an average error of 2.88% with a standard deviation of

4.04% for capacities less than or equal to 151 tons and an average error of 2.81% with a standard deviation of 3.53% for capacities greater than 151 tons. For all capacities, the average error is 2.85% with a standard deviation of 3.79%. These results indicate that the polynomial functions closely predict variation in chiller COP under part-load conditions.

Given the cooling load and the chiller reference capacity, the PLR may be calculated and used in Equation 32 or 33 to obtain the multiplier that must be applied to the predicted full-load chiller COP. The resulting value provides the chiller COP at current operating conditions with a total (combined full-load and part-load) average error of 7.38% and standard deviation of 6.13%.

3.2 Water-Cooled Chillers

3.2.1 Scroll Chillers

Manufacturer's data for scroll chillers with reference capacities between 52 and 200 tons was obtained from York (York 2011a). Likewise, manufacturer's data for scroll chillers with reference capacities between 20 and 59 tons was obtained from Trane (Trane 2002b). This data has been compiled and is shown in Appendix E.

The data provided for each York chiller included leaving condenser water temperatures (T_{cond}^{out}) of 85°F, 95°F, and 105°F. As presented in Section 2.4.1.1, Equation 1 may be similarly written in terms of T_{cond}^{out} if such data is provided. For each value of T_{cond}^{out}, exiting CHW temperatures (T_{evap}^{out}) of 40°F, 42°F, 44°F, 46°F, 48°F, and 50°F were provided. For each of the 18 data points, the measured compressor power consumption and full-load capacity were also given. The actual chiller COP for each data point was calculated by dividing the full-load capacity by the required power. The chiller reference capacities for which such data was provided were 52, 60, 68, 77, 86, 93, 110,

127, 141, 144, 168, and 200 tons for model YCWL. In total, 216 data points were provided to describe the York chillers.

The quasi-steady-state method, as presented in Section 2.4.1, was used to obtain the A_0, A_1, and A_2 constants for each chiller reference capacity. The constant values were then plotted vs. reference capacity, as shown in Figure 21.

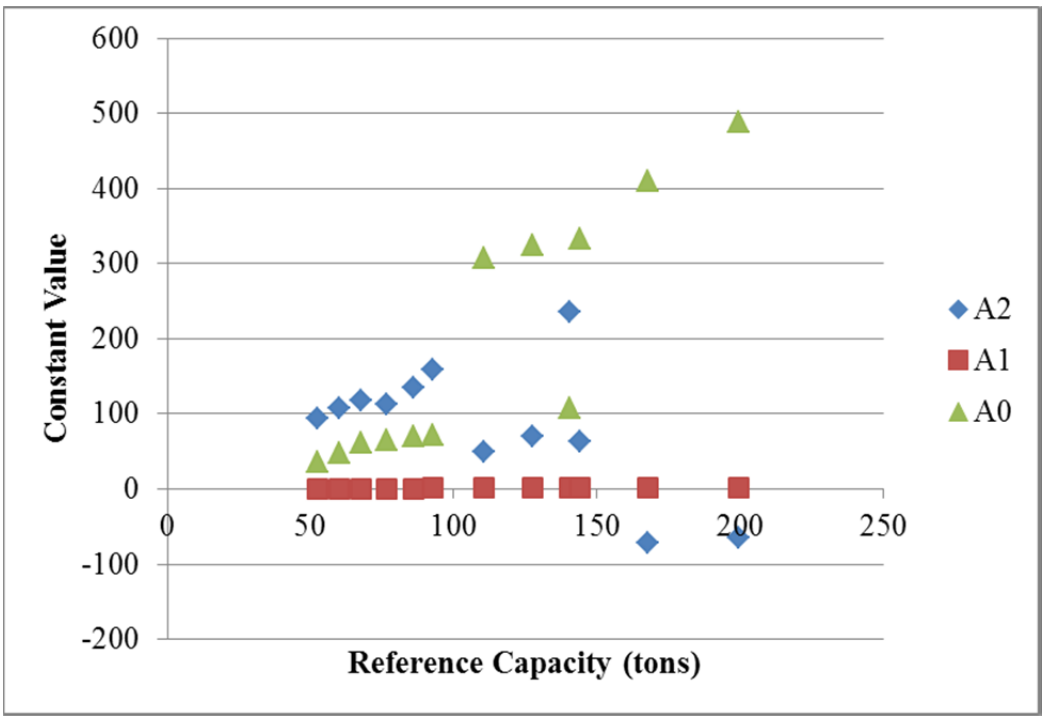

Figure 21. Plot of A_0, A_1, and A_2 constants vs. reference capacity for selected York water-cooled scroll chillers.

Referring to Figure 21, the constant A_2 appears to increase linearly up to a reference capacity of 100 tons, then decrease. However, applying a linear regression to the values was not found to compromise the accuracy of predicting chiller COP. Experimentation showed that Equation 1 was sensitive to the A_0 constant, while the A_2 constant did not significantly affect the predicted COP accuracy. The error associated with applying a

linear regression to the A_2 constant will be shown to be similar to that obtained for modeling air-cooled scroll and screw chillers.

A linear regression of the preceding plot provided the following functions relating the constants to the reference capacity, cap_{ref}:

$$A_0{}^* = 3.19 * cap_{ref} - 159.22 \quad (34)$$

$$A_1{}^* = 0.01 * cap_{ref} + 0.23 \quad (35)$$

$$A_2{}^* = -1.09 * cap_{ref} + 204.33 \quad (36)$$

Using the linear functions, $A_0{}^*$, $A_1{}^*$, and $A_2{}^*$ were calculated for each chiller reference capacity. These constant values were then used with the set of temperatures and full-load capacities provided by the manufacturer's 216 data points to calculate the predicted COP by using Equation 1. Comparing the actual and predicted COP values for all 216 data points showed an average error of 2.25% with a standard deviation of 1.32%. These results indicate that the linear functions closely predict chiller COP at full-load capacity.

The data provided for each Trane chiller included entering condenser water temperatures (T_{cond}^{in}) of 75°F, 80°F, 85°F, 90°F,and 95°F. For each value of T_{cond}^{in}, exiting CHW temperatures (T_{evap}^{out}) of 40°F, 42°F, 44°F, 46°F, 48°F, and 50°F were provided. For each of the 30 data points, the measured compressor power consumption and full-load capacity were also given. The actual chiller COP for each data point was calculated by dividing the full-load capacity by the required power. The chiller reference capacities for which such data was provided were 20, 25, 29, 39, 49, and 59 tons for model CGWE. In total, 180 data points were provided to describe the Trane chillers.

The quasi-steady-state method, as presented in Section 2.4.1, was used to obtain the A_0, A_1, and A_2 constants for each chiller reference capacity. The constant values were then plotted vs. reference capacity, as shown in Figure 22.

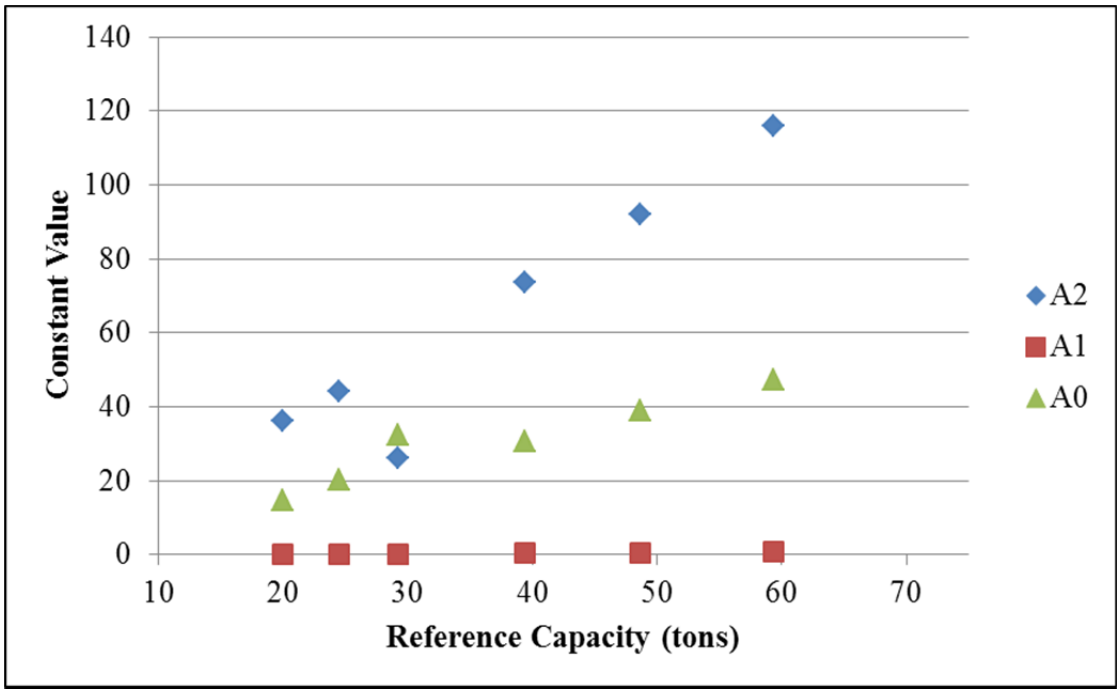

Figure 22. Plot of A_0, A_1, and A_2 constants vs. reference capacity for selected Trane water-cooled scroll chillers.

A linear regression of the preceding plot provided the following functions relating the constants to the reference capacity, cap_{ref}:

$$A_0{}^* = 0.74 * cap_{ref} + 3.42 \quad (37)$$

$$A_1{}^* = 0.01 * cap_{ref} - 0.05 \quad (38)$$

$$A_2{}^* = 2.20 * cap_{ref} - 16.18 \quad (39)$$

Using the linear functions, A_0^*, A_1^*, and A_2^* were calculated for each chiller reference capacity. These constant values were then used with the set of temperatures and full-load capacities provided by the manufacturer's 180 data points to calculate the predicted COP by using Equation 1. Comparing the actual and predicted COP values for all 180 data points showed an average error of 0.99% with a standard deviation of 0.35%. These results indicate that the linear functions closely predict chiller COP at full-load capacity.

Having developed manufacturer-dependent models for water-cooled scroll chillers, the development of a manufacturer-independent model for water-cooled scroll chillers utilized the same methodology.

The A_0, A_1, and A_2 constants obtained for each York and Trane chiller reference capacity were plotted vs. reference capacity, as shown in Figure 23.

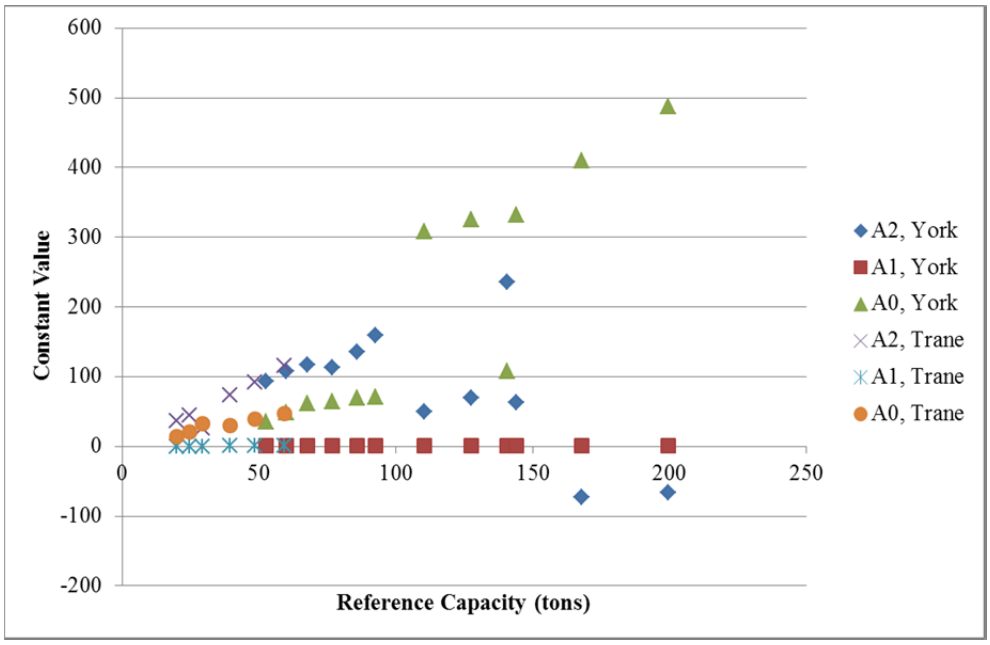

Figure 23. Plot of A_0, A_1, and A_2 constants vs. reference capacity for York and Trane water-cooled scroll chillers.

A linear regression of the preceding plot provided the following functions relating the constants to the reference capacity, cap_{ref}:

$$A_0{}^* = 2.67 * cap_{ref} - 90.30 \quad (40)$$

$$A_1{}^* = 0.01 * cap_{ref} + 0.12 \quad (41)$$

$$A_2{}^* = -0.37 * cap_{ref} + 109.63 \quad (42)$$

Using the linear functions, $A_0{}^*$, $A_1{}^*$, and $A_2{}^*$ were calculated for each chiller reference capacity. These constant values were then used with the set of temperatures and full-load capacities provided by the both manufacturers' 396 data points to calculate the predicted COP by using Equation 1. Comparing the actual and predicted COP values for all 396 data points showed an average error of 4.95% with a standard deviation of 4.90%. These results indicate that the linear functions closely predict chiller COP at full-load capacity.

Equations 40, 41, and 42 may thus be used to calculate $A_0{}^*$, $A_1{}^*$, and $A_2{}^*$ for a given water-cooled scroll chiller reference capacity (independent of manufacturer) between 20 and 200 tons. Use of these constants, the cooling load, and evaporator and condenser fluid temperatures in Equation 1 allows the chiller COP at full-load conditions to be predicted.

Considering that the majority of chiller operation occurs at part-load conditions, as presented in Section 2.4.2, it is necessary to be able to characterize chiller COP at part-load.

The manufacturer's data provided for the York set of chillers included chiller COP values at different PLR conditions. However, a correlation between COP and PLR could not be obtained directly from the provided data because the reported values are at

different evaporator and condenser fluid temperatures, as required by the AHRI (AHRI 2003). Specifically, COP is reported for PLRs with the fluid temperatures shown in Table 3.

Table 3. AHRI standard conditions for reporting water-cooled chiller COP at varying PLRs.

PLR	**$T_{evap,out}$ (°F)**	**$T_{cond,in}$ (°F)**
100%	44	85
75%	44	75
50%	44	65

In order to obtain an accurate correlation describing the behavior of COP with respect to PLR, a curve specific to one set of fluid temperatures was required. One curve was generated for the temperature conditions of T_{evap}^{out} = 44°F and T_{cond}^{in} = 75°F. Two data points were known: COP at PLR=75% (provided by the manufacturer's data) and COP=0 at PLR=0. Having previously shown the ability of the chiller model developed by the quasi-steady-state method to accurately predict chiller full-load COP, the evaporator and condenser fluid temperatures were input to the model in order to obtain a third data point (COP at PLR=100%).

A second curve was generated for the temperature conditions of T_{evap}^{out} = 44°F and T_{cond}^{in} = 65°F. Two data points were known: COP at PLR=50% (provided by the manufacturer's data) and COP=0 at PLR=0. Having previously shown the ability of the chiller model developed by the quasi-steady-state method to accurately predict chiller full-load COP, the evaporator and condenser fluid temperatures were input to the model in order to obtain a third data point (COP at PLR=100%).

The two curves are shown in Figure 24 as an example for an 86 ton chiller.

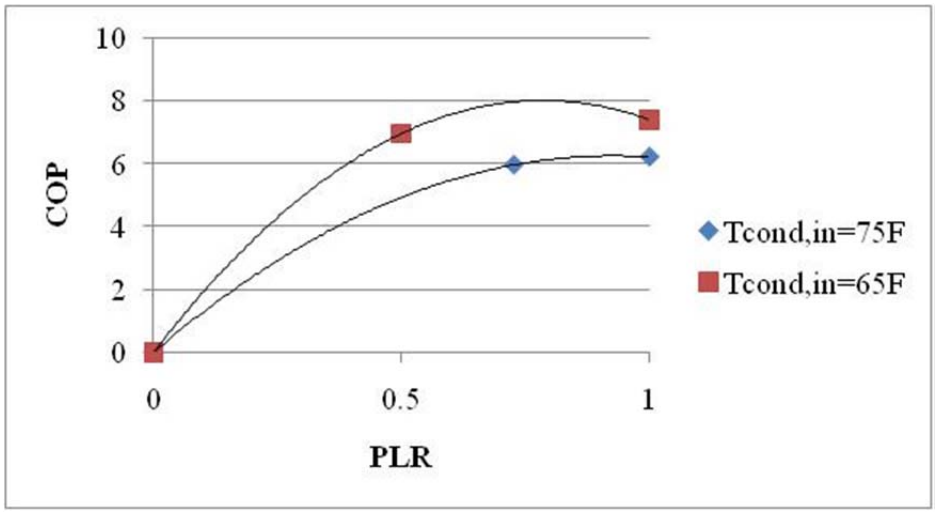

Figure 24. COP vs. PLR for an 86 ton water-cooled scroll chiller at two condenser inlet temperatures and a constant evaporator outlet temperature.

In order to normalize the behavior observed in the preceding figure for the two condenser fluid temperatures, the fraction of full-load COP was plotted vs. PLR, as shown in Figure 25.

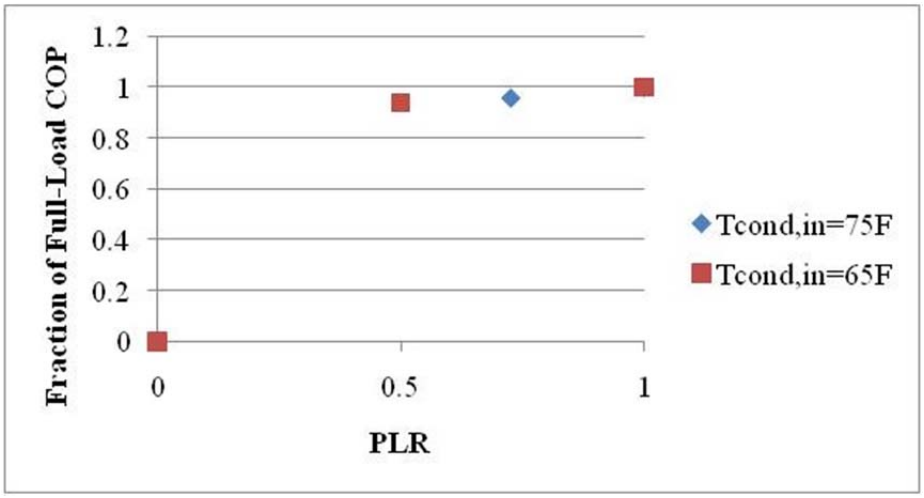

Figure 25. Fraction of full-load COP vs. PLR for an 86 ton water-cooled scroll chiller at two condenser inlet temperatures and a constant evaporator outlet temperature.

The preceding figure indicates that for different PLRs, chiller COP varies as a fraction of the full-load COP in a similar manner for different fluid temperature conditions.

The preceding steps were performed for the York chillers with part-load data shown in Appendix F and the fraction of full-load COP was plotted vs. PLR, as shown in Figure 26.

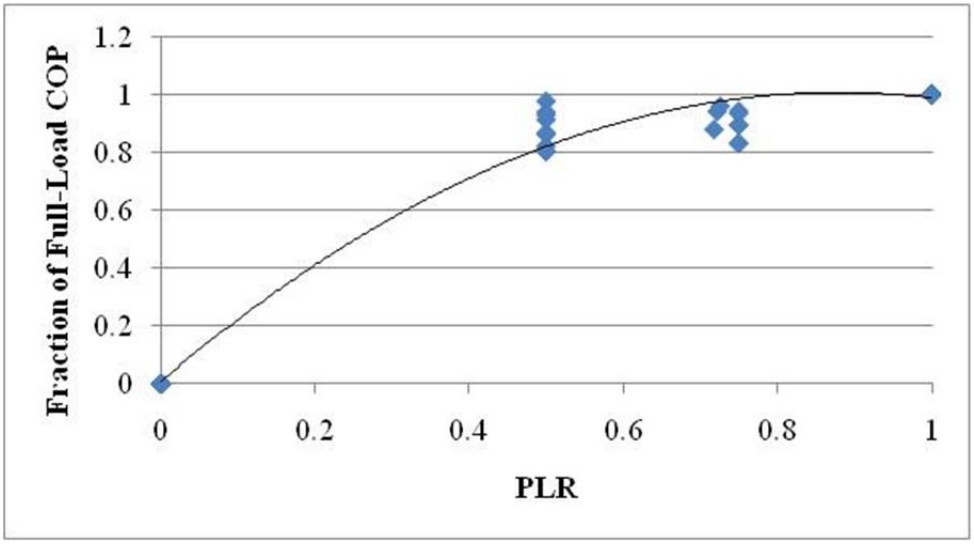

Figure 26. Fraction of full-load COP vs. PLR for York water-cooled scroll chillers.

Analysis of the preceding figure indicates that a single curve approximates the behavior of the chillers. Specifically, the fraction of full-load COP decreases as PLR decreases, with the peak COP occurring at PLR=1.

A polynomial curve was found to best fit the data shown in the preceding figure, and provided the following function relating fraction of full-load COP ($COP_{FL,frac}$) to PLR,

$$COP_{FL,frac} = -1.295(PLR)^2 + 2.276(PLR) + 0.005 \quad (43)$$

The preceding equation was used to calculate the predicted fraction of full-load COP for different PLR values and the results were compared to the manufacturer's reported values. This comparison yielded an average error of 3.21% with a standard deviation of 4.82%. These results indicate that the polynomial function closely predicts variation in chiller COP under part-load conditions.

Given the cooling load and the chiller reference capacity, the PLR may be calculated and used in Equation 43 to obtain the multiplier that must be applied to the predicted full-load chiller COP. The resulting value provides the chiller COP at current operating conditions with a total (combined full-load and part-load) average error of 8.16% and standard deviation of 9.72%.

3.2.2 Reciprocating Chillers

Referring to the product brochures of three large chiller manufacturers (Trane, Carrier, and York), reciprocating chillers are no longer in production (Trane 2006; Carrier 2005, Cat. No. 04-819192-25; York 2010). As a result, product data required for implementation of the quasi-steady-state method could not be obtained.

While new reciprocating chillers are not being installed, it remains essential that WinAM be able to model such chillers considering that CC® engineers are likely to encounter them in existing HVAC systems.

The quasi-steady-state method was first introduced in a study focused on reciprocating chillers alone (Gordon et al. 1994). This study used manufacturers' data for 11 Carrier chillers and 16 Trane chillers to determine the ability of the quasi-steady-state method to predict reciprocating chiller COP. Documentation of this study includes the A_0, A_1, and A_2 constants derived for each chiller, the rated capacities at reference evaporator outlet

and condenser inlet temperatures, and the root mean square error in COP. This data has been compiled and is shown in Appendix G.

The study concluded that because the average root mean square error in predicted COP for all of the chillers was 0.4%, and that manufacturers' experimental uncertainty was ±3%, the quasi-steady-method was capable of predicting reciprocating chiller COP under various operating conditions (Gordon et al. 1994). Considering that the A_0, A_1, and A_2 constants were derived according to the quasi-steady-state procedure described in Section 2.4.1.1, the documented constants from the study served as the basis for developing a correlation between A_0, A_1, and A_2 and chiller reference capacity.

The A_0, A_1, and A_2 constants were reported for Carrier chillers with reference capacities of 14, 18, 23, 34, 46, 55, 68, 90, 102, 125, and 137 tons. The A_0, A_1, and A_2 constants were reported for Trane chillers with reference capacities of 69, 73, 73, 73, 84, 84, 94, 105, 115, 127, 167, 243, 265, 303, 334, and 364 tons. The reference capacities listed are all for a reference entering condenser water temperature (T_{cond}^{in}) of 95°F and exiting CHW temperature (T_{evap}^{out}) of 50°F. For each reference capacity, the reference water temperatures and the A_0, A_1, and A_2 constants reported were used to calculate the COP by Equation 1. These COP values will be referred to as the "reported COP" values.

The constant values reported for each reference capacity were plotted vs. reference capacity, as shown in Figure 27.

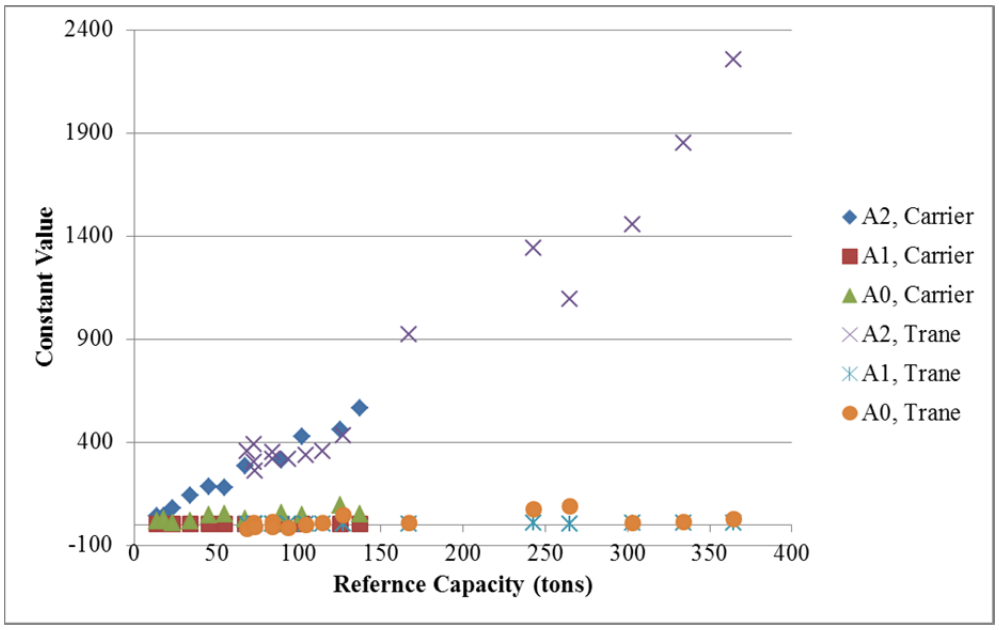

Figure 27. Plot of A_0, A_1, and A_2 constants vs. reference capacity for Carrier and Trane reciprocating chillers.

A linear regression of the preceding plot provided the following functions relating the constants to the reference capacity, cap_{ref}:

$$A_0{}^* = 0.02 * cap_{ref} + 15.33 \quad (44)$$

$$A_1{}^* = 0.01 * cap_{ref} - 0.47 \quad (45)$$

$$A_2{}^* = 1.62 * cap_{ref} - 136.46 \quad (46)$$

Using the linear functions, $A_0{}^*$, $A_1{}^*$, and $A_2{}^*$ were calculated for each chiller reference capacity. These constant values were then used with the reference water temperatures and reference capacities reported for the 27 chillers to calculate the predicted COP by using Equation 1. Comparing the reported and predicted COP values for the 27 chillers showed an average error of 16.40% with a standard deviation of 29.39%. The magnitude of error observed was reason for further analysis.

Figure 28 indicates that the linear functions are able to predict full-load COP accurately for medium and large reference capacities. However, for smaller reference capacities, the predicted full-load COP results in significant error. For this reason, the applicability of the model was limited to reciprocating chillers with reference capacities greater than 20 tons.

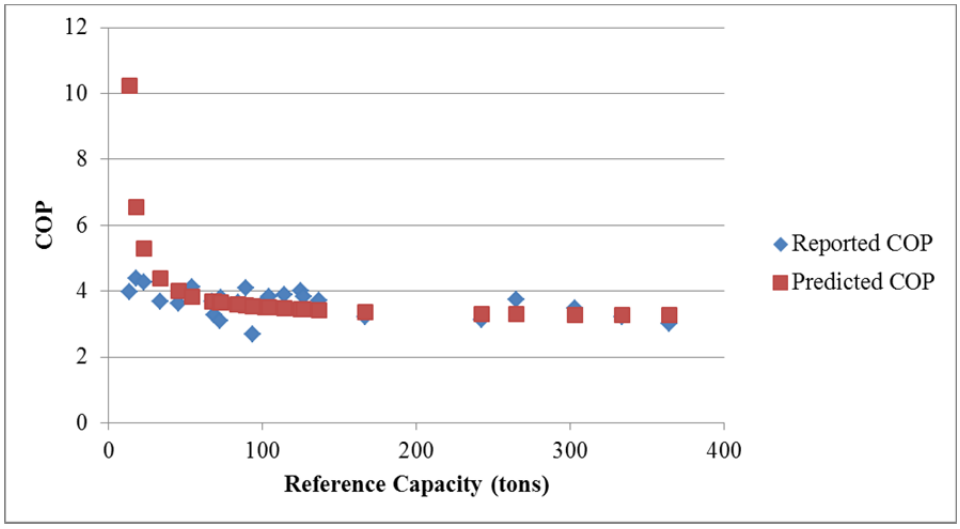

Figure 28. Plot of reported COP and predicted COP vs. reference capacity for Carrier and Trane reciprocating chillers.

Comparing the reported and predicted COP values for the restricted set of 25 chillers showed an average error of 9.49% with a standard deviation of 7.39%. These results indicate an improvement in the ability of the linear functions to predict chiller COP at full-load capacity.

Equations 44, 45, and 46 may thus be used to calculate A_0^*, A_1^*, and A_2^* for a given water-cooled reciprocating chiller reference capacity (independent of manufacturer) between 20 and 364 tons. Use of these constants, the cooling load, and evaporator and

condenser fluid temperatures in Equation 1 allows the chiller COP at full-load conditions to be predicted.

Considering that the majority of chiller operation occurs at part-load conditions, as presented in Section 2.4.2, it is necessary to be able to characterize chiller COP at part-load.

Due to the inability to obtain performance data for water-cooled reciprocating chillers, the three curves used to characterize reciprocating chiller performance by EnergyPlus were employed.

EnergyPlus makes use of a single set of three curves to model a generic reciprocating chiller. The EIRFPLR coefficients, EIRFT coefficients, and CAPFT coefficients were obtained from the EnergyPlus library. The EIRFPLR coefficients were used to calculate the actual EIR fraction ($EIR_{frac,PLR}$) when PLR varies from 100% to 20%. The EIRFT coefficients were used to calculate the actual EIR fraction ($EIR_{frac,T}$) for entering condenser water temperatures (T_{cond}^{in}) of 65°F, 73°F, 84°F, 93°F, and 102°F and exiting CHW temperatures (T_{evap}^{out}) of 40°F, 41°F, 43°F, 45°F, and 46°F, resulting in 25 data points. The selected temperature ranges were chosen based on standard water-cooled chiller rating conditions established by the AHRI (AHRI 2003). The CAPFT coefficients were used to calculate the actual fraction of reference capacity (CAP_{frac}) for the same water temperature conditions.

A generic reciprocating chiller with a 10 kW (2.83 ton) reference capacity and 3.67 reference COP was modeled for each of the 25 temperature conditions and at PLRs of 1, 0.8, 0.6, 0.4, and 0.2. A plot of the chiller COP for varying PLRs and entering condenser water temperatures (ECWTs) (with a constant leaving chiller water temperature (LCHWT) of 43°F) is shown in Figure 29.

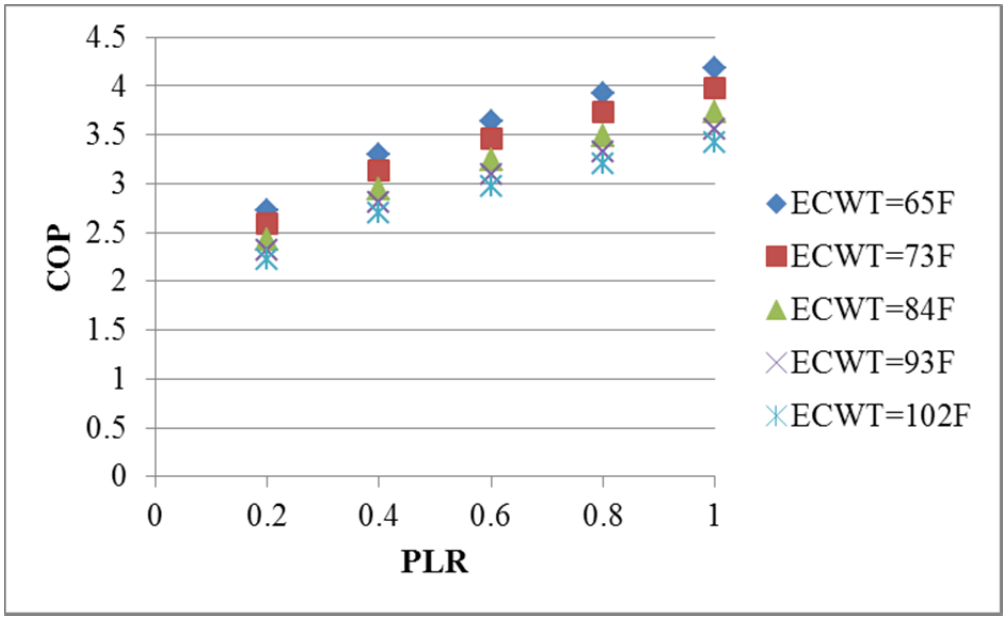

Figure 29. Plot of COP vs. PLR for a generic reciprocating chiller with varying ECWTs and constant LCHWT (43°F).

In order to normalize the behavior of COP as a function of PLR, the fraction of full-load COP (when PLR=1) was calculated for each temperature and PLR condition. Figure 30 shows that the fraction of full-load COP is strictly dependent on the PLR and independent of the fluid temperature conditions.

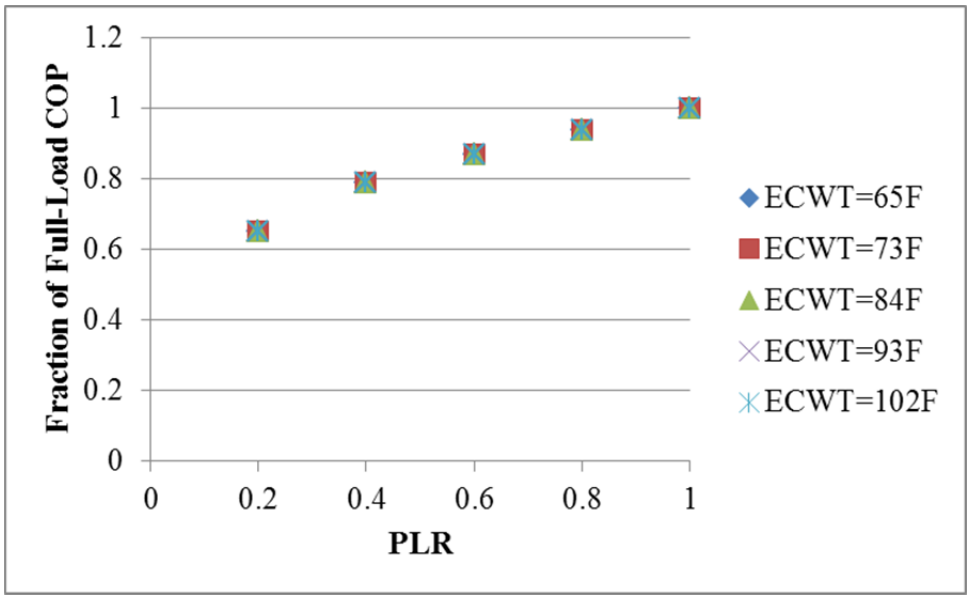

Figure 30. Plot of fraction of full-load COP vs. PLR for a generic reciprocating chiller with varying ECWTs and constant LCHWT (43°F).

A polynomial curve fit was found to best fit the data and resulted in the following equation relating the fraction of full-load COP ($COP_{FL,frac}$) to PLR,

$$COP_{FL,frac} = -0.289(PLR)^2 + 0.769(PLR) + 0.516 \quad (47)$$

Using the preceding equation, the fraction of full-load COP at varying PLR conditions was calculated and compared to the COP calculated from the EnergyPlus curves. The error obtained from this comparison is shown in Table 4, with the average error being 0.81% with a standard deviation of 0.42%.

Table 4. Error between predicted fraction of full-load COP and that calculated from EnergyPlus curves for different PLR values.

PLR	% Error
1	0.47109
0.8	0.91498
0.6	0.29232
0.4	1.51678
0.2	0.85214

Given the cooling load and the chiller reference capacity, the PLR may be calculated and used in Equation 47 to obtain the fraction of full-load COP. This value may then be multiplied by the predicted full-load chiller COP to obtain the actual chiller COP at current operating conditions with a total (combined full-load and part-load) average error of 10.30% and standard deviation of 7.81%. .

3.2.3 Screw Chillers

The quasi-steady-state method used thus far to model air-cooled scroll and screw chillers and water-cooled scroll and reciprocating chillers has utilized manufacturers' data. Since such data is no longer provided for water-cooled screw chillers, the performance curves used by the EnergyPlus building energy simulation program to predict chiller COP under varying conditions will be utilized.

From the EnergyPlus library, screw chillers from York and Carrier were selected to represent the range of reference capacities available for modeling. York model YS chillers with reference capacities of 221, 249, and 498 tons and Carrier model 23XL chillers with reference capacities of 194, 235, 244, 301, 314, and 339 tons were selected.

For each reference capacity, the EIRFPLR coefficients, EIRFT coefficients, and CAPFT coefficients were obtained from the EnergyPlus library. These coefficients have been compiled and are shown in Appendix H with their respective regression functions. The

EIRFPLR coefficients were used to calculate the actual EIR fraction ($EIR_{frac,PLR}$) when PLR varies from 100% to 20% for each reference capacity. The EIRFT coefficients were used to calculate the actual EIR fraction ($EIR_{frac,T}$) for entering condenser water temperatures (T_{cond}^{in}) of 65°F, 75°F, and 85°F and exiting CHW temperatures (T_{evap}^{out}) of 40°F, 43°F, 46°F, and 50°F, resulting in 12 values per reference capacity. The selected temperature ranges were chosen based on standard water-cooled chiller rating conditions established by the AHRI (AHRI 2003). The CAPFT coefficients were used to calculate the actual fraction of reference capacity (CAP_{frac}) for the same water temperature conditions.

The $EIR_{frac,PLR}$ values obtained for each reference capacity were then plotted vs. PLR, as shown in Figure 31.

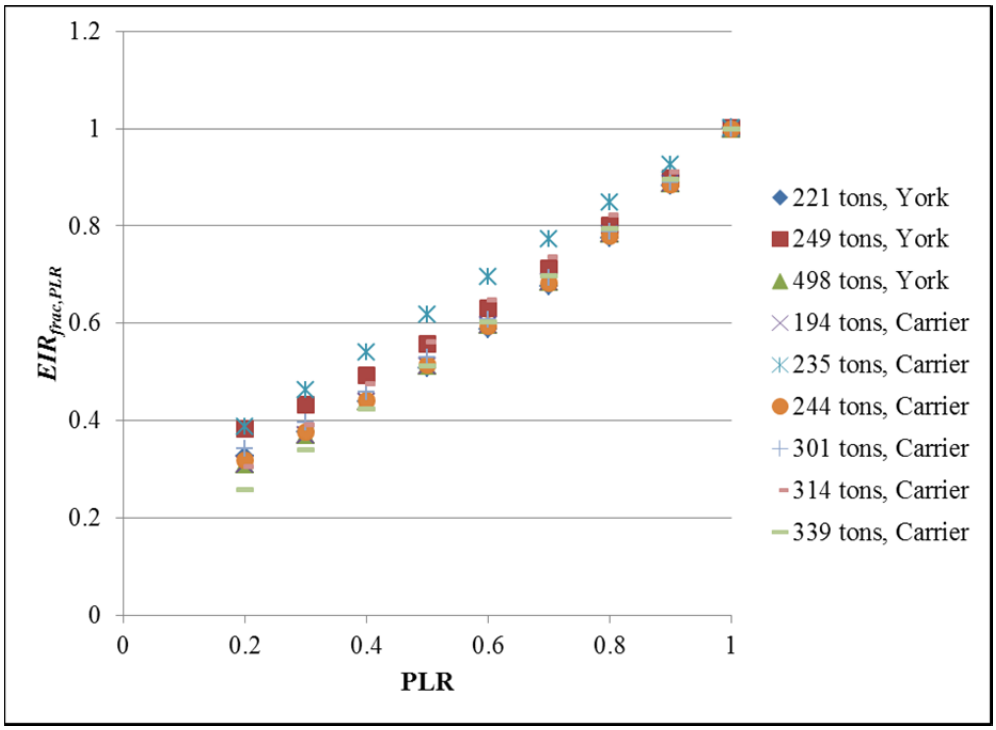

Figure 31. Plot of EIR fraction from EIRFPLR vs. PLR for York and Carrier screw chillers.

A polynomial curve was found to best fit the data shown in the preceding figure, and provided the following function relating $EIR_{frac,PLR}$ to PLR:

$$EIR_{frac,PLR} = 0.286(PLR)^2 + 0.488(PLR) + 0.227 \quad (48)$$

The $EIR_{frac,T}$ values obtained for each reference capacity were then plotted vs. the absolute temperature ratio $\left(T_{cond}^{in}/T_{evap}^{out}\right)$, as shown in Figure 32.

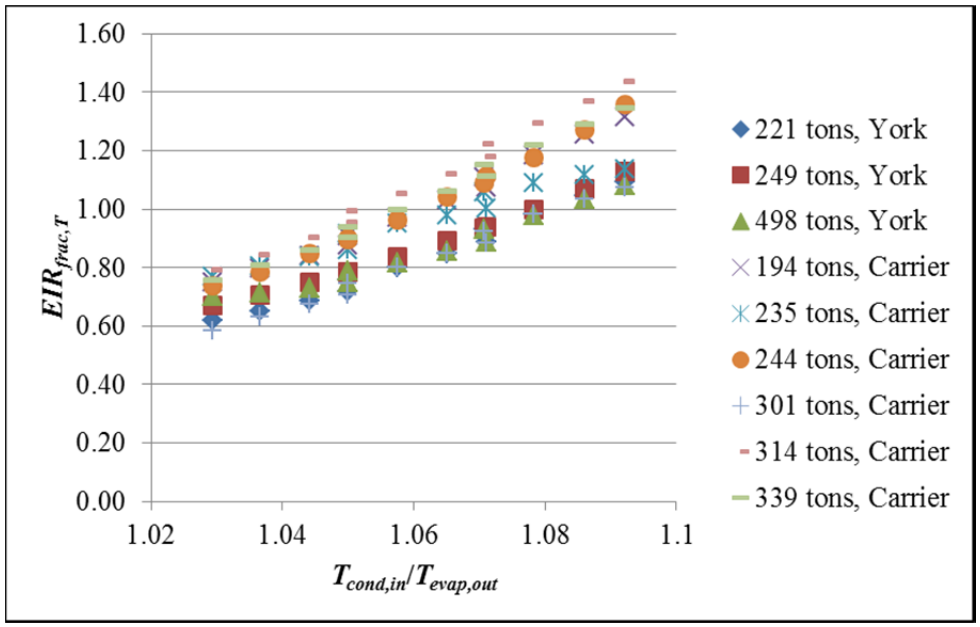

Figure 32. Plot of EIR fraction from EIRFT vs. absolute temperature ratio for York and Carrier screw chillers.

A straight line was found to best fit the data shown in the preceding figure, and provided the following function relating $EIR_{frac,T}$ to $T_{cond}^{in}/T_{evap}^{out}$:

$$EIR_{frac,T} = 8.377 * \frac{T_{cond}^{in}}{T_{evap}^{out}} - 7.942 \quad (49)$$

The CAP_{frac} values obtained for each reference capacity were then plotted vs. the absolute temperature ratio $\left(T_{cond}^{in}/T_{evap}^{out}\right)$, as shown in Figure 33.

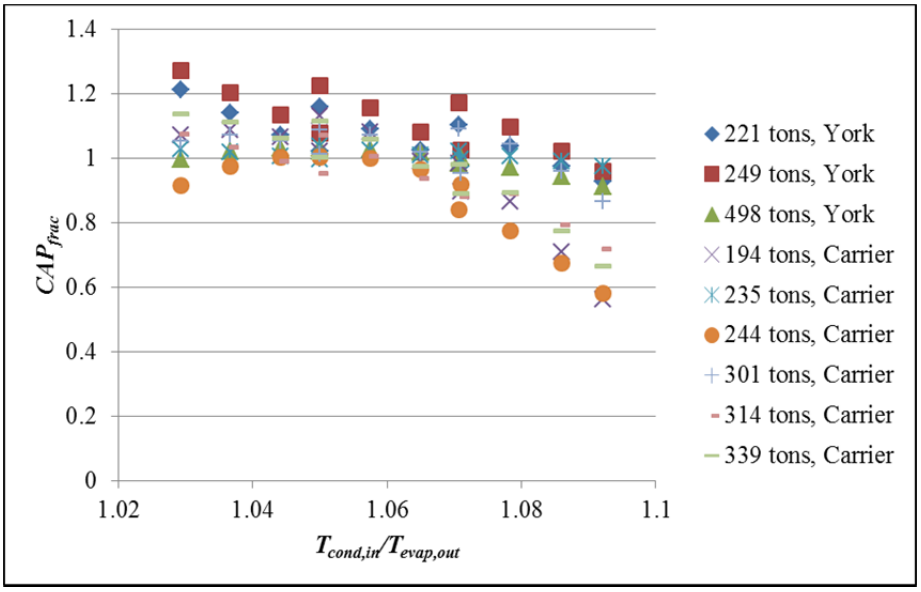

Figure 33. Plot of capacity fraction from CAPFT vs. absolute temperature ratio for York and Carrier screw chillers.

A polynomial curve was found to best fit the data shown in the preceding figure, and provided the following function relating CAP_{frac} to $T_{cond}^{in}/T_{evap}^{out}$:

$$CAP_{frac} = -90.418\left(\frac{T_{cond}^{in}}{T_{evap}^{out}}\right)^2 + 187.764\left(\frac{T_{cond}^{in}}{T_{evap}^{out}}\right) - 96.405 \quad (50)$$

Based on the description of how EnergyPlus uses the CAP_{frac}, $EIR_{frac,T}$, and $EIR_{frac,PLR}$ values to determine chiller performance, it was necessary to compare the actual CAP_{frac} values and total EIR fraction values ($EIR_{total} = EIR_{frac,T} * EIR_{frac,PLR}$) to those predicted by Equations 48, 49, and 50.

The actual CAP_{frac} values obtained for each reference capacity at 12 different water temperature conditions were multiplied by the chiller reference capacity to obtain the actual full-load capacity. Equation 50 was used with the same 12 water temperature conditions to calculate the predicted CAP_{frac} values for each reference capacity. The predicted CAP_{frac} values were multiplied by the chiller reference capacity to obtain the predicted full-load capacity. Comparing the actual and predicted full-load capacities for the 9 chillers under each temperature condition (108 data points) showed an average error of 7.42% with a standard deviation of 2.96%. These results indicate that Equation 50 may be used to calculate CAP_{frac} for water-cooled screw chillers (independent of manufacturer) as operating conditions change.

For each reference capacity, the actual $EIR_{frac,T}$ values obtained at 12 different water temperature conditions were multiplied by the actual $EIR_{frac,PLR}$ value obtained for the same reference capacity when PLR was set equal to 1. Multiplying the actual $EIR_{frac,T}$ and actual $EIR_{frac,PLR}$ values together provided the actual EIR_{total}. Equation 49 was used with the same 12 water temperature conditions to calculate the predicted $EIR_{frac,T}$ values for each reference capacity. Equation 48 was used to calculate the predicted $EIR_{frac,PLR}$ value for each reference capacity with PLR set equal to 1. Multiplying the predicted $EIR_{frac,T}$ and predicted $EIR_{frac,PLR}$ values together provided the predicted EIR_{total}. Comparing the actual and predicted EIR_{total} for the 9 chillers under each temperature condition (108 data points) showed an average error of 9.57% with a standard deviation of 3.63%.

The comparison of actual and predicted EIR_{total} values was repeated for PLR = 0.8, 0.6, 0.4, and 0.2. The error associated with each part-load operation is summarized in Table 5.

Table 5. Water-cooled screw chiller average error and standard deviation between actual and predicted total EIR fraction values for different PLR values.

PLR	Average Error (%)	Standard Deviation (%)
1	9.57	3.63
0.8	10.25	4.93
0.6	10.30	6.50
0.4	9.13	7.56
0.2	9.26	6.17

The average error for all load conditions is 9.70% with a standard deviation of 5.76%, indicating that Equations 48 and 49 may be used to calculate $EIR_{frac,PLR}$ and $EIR_{frac,T}$, respectively. The resulting values may then be multiplied to obtain the EIR_{total} value for water-cooled screw chillers (independent of manufacturer) as operating conditions change.

Equations 48, 49, and 50 provide a means for calculating chiller COP (independent of manufacturer) as operating conditions change for water-cooled screw chillers with reference capacities between 194 and 498 tons.

Further validation of the use of Equations 48, 49, and 50 for calculating chiller COP was provided by comparing the COP resulting from the EnergyPlus curves and the COP resulting from the correlations represented by Equation 48, 49, and 50. Chiller COP was calculated by both methods for each of the 9 chillers subject to the 12 temperature conditions and for PLRs of 1, 0.8, 0.6, 0.4, and 0.2. The error between the EnergyPlus

and predicted COP values for the 540 data points is summarized in Table 6. The average error for all load conditions is 9.87% with a standard deviation of 3.65%.

Table 6. Water-cooled screw chiller average error and standard deviation between actual and predicted COP values for different PLR values.

PLR	Average Error (%)	Standard Deviation (%)
1	7.89	1.56
0.8	9.11	1.96
0.6	10.25	3.27
0.4	10.58	5.00
0.2	11.54	6.45

An example of the COP comparison conducted is shown in Figure 34 for two water-cooled screw chillers. The COP curves resulting from EnergyPlus and the correlations are plotted for a constant leaving chilled water temperature (LCHWT) of 6°C and entering condenser water temperature (ECWT) of 24.15°C. The predicted COP at part-load is shown to closely match the COP resulting from the EnergyPlus curves.

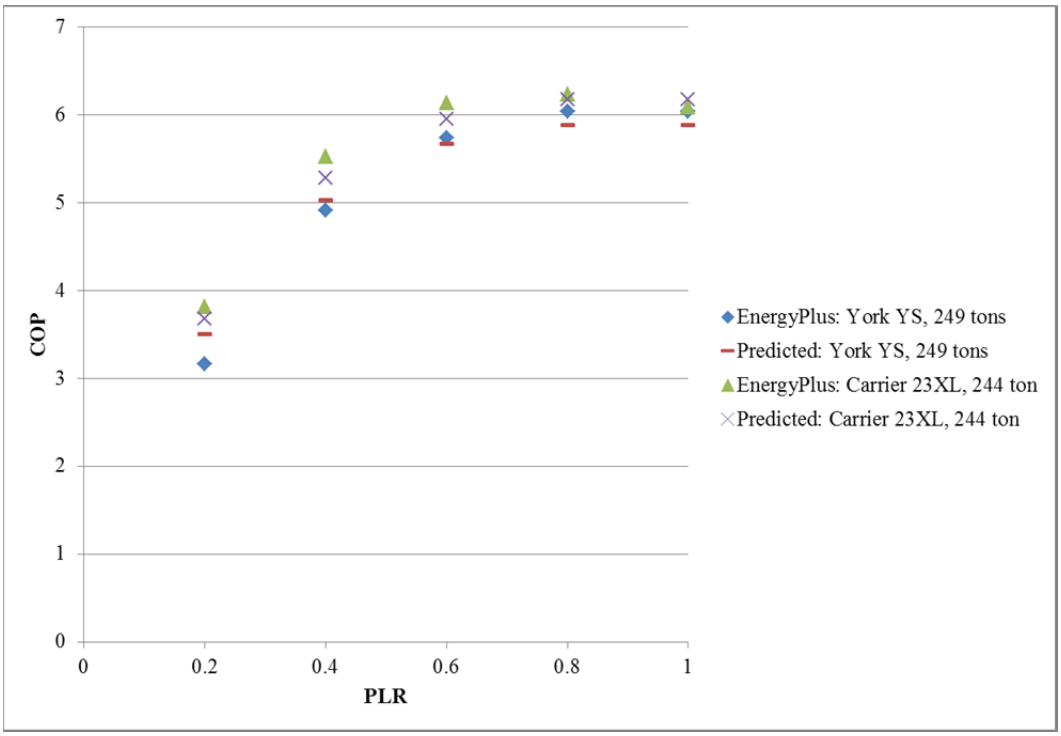

Figure 34. Plot of COP vs. PLR for two water-cooled screw chillers.

3.2.4 Centrifugal Chillers

Considering the lack of published manufacturers' data for water-cooled centrifugal chillers, the same approach as that taken for water-cooled screw chillers was taken. Specifically, the performance curves used by the EnergyPlus building energy simulation program to predict chiller COP under varying conditions were utilized.

From the EnergyPlus library, centrifugal chillers from York and Carrier were selected to represent the range of reference capacities available for modeling. The chillers were also selected to account for the type of capacity control employed: inlet guide vanes or variable-speed drive (VSD). For inlet guide vane capacity control, York model YT chillers with reference capacities of 272, 290, 297, 395, 498, and 597 tons and Carrier model 19XR chillers with reference capacities of 233, 339, 356, 463, and 677 tons were selected. For VSD capacity control, York model YT chillers with reference capacities of

254, 309, 387, 498, and 532 tons and Carrier model 19XR chillers with reference capacities of 210, 254, 324, 441, and 677 tons were selected. All York and Carrier chillers selected use a single-stage compressor (York 2001; Carrier 2010, Form 19XR-9PD).

Single-stage compressors served as the focus of this study because the majority of centrifugal chillers in the EnergyPlus library are single-stage and the reference capacities for which data is provided cover the range previously shown (233-677 tons). Trane CVHE is the only model available using a three-stage compressor (Trane 2005) and the reference capacities for which data is provided are only 320, 378, 390, and 422 tons. In addition, Trane CVHF and Carrier 19EX are the only models available using a two-stage compressor (Trane 2005; Carrier 1999, Form 19EX-3PD). Data for the Trane CVHF model is available for reference capacities of 478, 500, 506, 581, 621, 654, 659, 730, 796, and 1330 tons. Data for the Carrier 19EX model is available for reference capacities of 1327, 1421, 1464, and 1481 tons. A reliable model for two-stage and three-stage compressors could not be obtained due to the lack of data at similar reference capacities between multiple manufacturers. Unlike two-stage and three-stage compressors, the availability of data from multiple manufacturers at similar reference capacities for single-stage compressors allowed an accurate, justifiable model to be developed.

For each reference capacity, the EIRFPLR coefficients, EIRFT coefficients, and CAPFT coefficients were obtained from the EnergyPlus library. These coefficients have been compiled and are shown in Appendix I with their respective regression functions. The EIRFPLR coefficients were used to calculate the actual EIR fraction ($EIR_{frac,PLR}$) when PLR varies from 100% to 20% for each reference capacity. The EIRFT coefficients were used to calculate the actual EIR fraction ($EIR_{frac,T}$) for entering condenser water temperatures (T_{cond}^{in}) of 65°F, 75°F, and 85°F and exiting CHW temperatures (T_{evap}^{out}) of 40°F, 43°F, 46°F, and 50°F, resulting in 12 values per reference capacity. The selected

temperature ranges were chosen based on standard water-cooled chiller rating conditions established by the AHRI (AHRI 2003). The CAPFT coefficients were used to calculate the actual fraction of reference capacity (CAP_{frac}) for the same water temperature conditions.

The $EIR_{frac,PLR}$ values obtained for each reference capacity were then plotted vs. PLR, as shown in Figure 35.

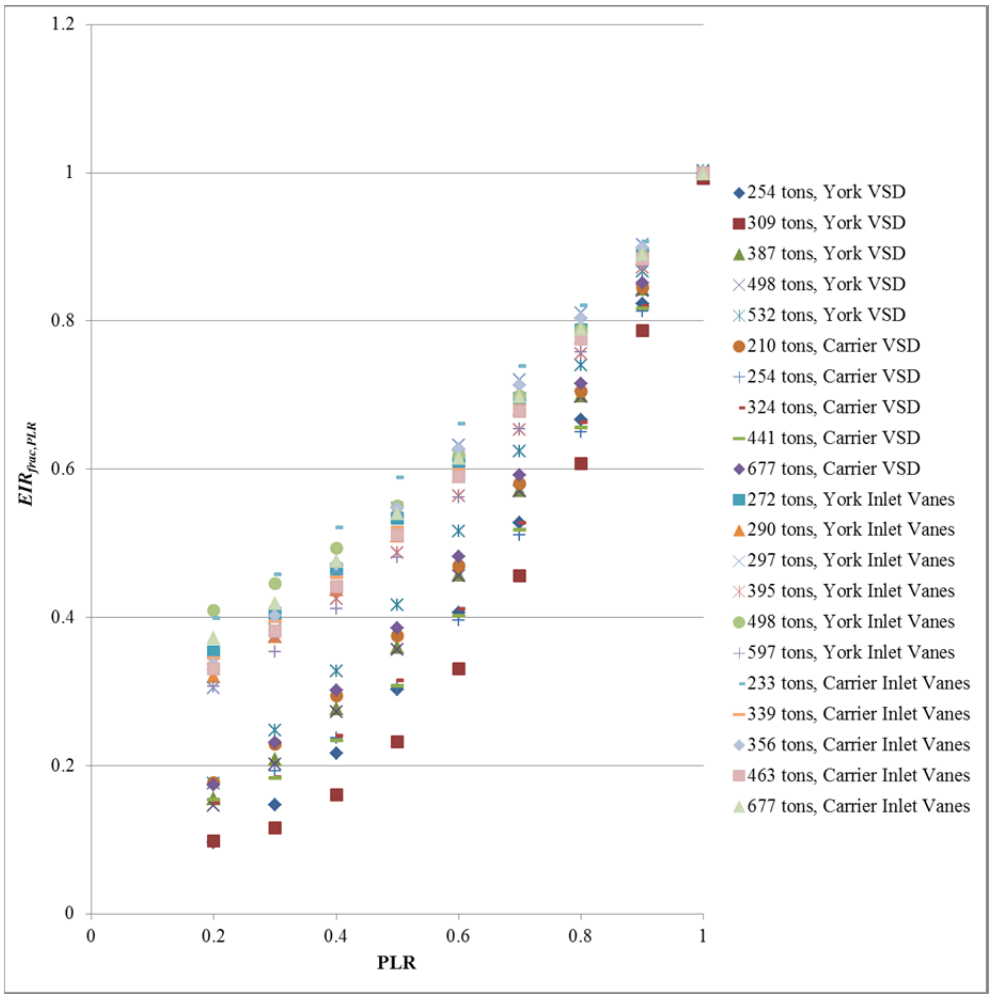

Figure 35. Plot of EIR fraction from EIRFPLR vs. PLR for York and Carrier centrifugal chillers with inlet guide vane and VSD capacity control.

Analysis of the preceding figure shows a distinct difference in behavior between the types of capacity control employed. This distinction is further revealed by the manufacturer-independent plot shown in Figure 36.

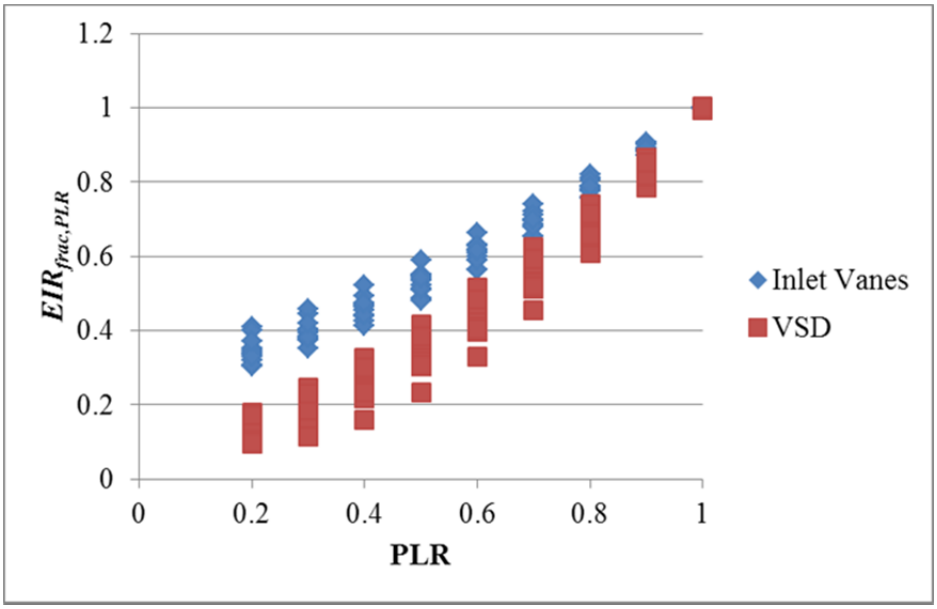

Figure 36. Plot of EIR fraction from EIRFPLR vs. PLR for centrifugal chillers with inlet guide vane and VSD capacity control.

Polynomial curves were found to best fit the data shown in the preceding figure, and provided the following functions relating $EIR_{frac,PLR}$ to PLR for inlet guide vane capacity control

$$EIR_{frac,PLR} = 0.417(PLR)^2 + 0.316(PLR) + 0.267 \quad (51)$$

and

$$EIR_{frac,PLR} = 0.884(PLR)^2 - 0.001(PLR) + 0.115 \quad (52)$$

for VSD capacity control.

The $EIR_{frac,T}$ values obtained for each reference capacity were then plotted vs. the absolute temperature ratio $\left(T_{cond}^{in}/T_{evap}^{out}\right)$, as shown in Figure 37.

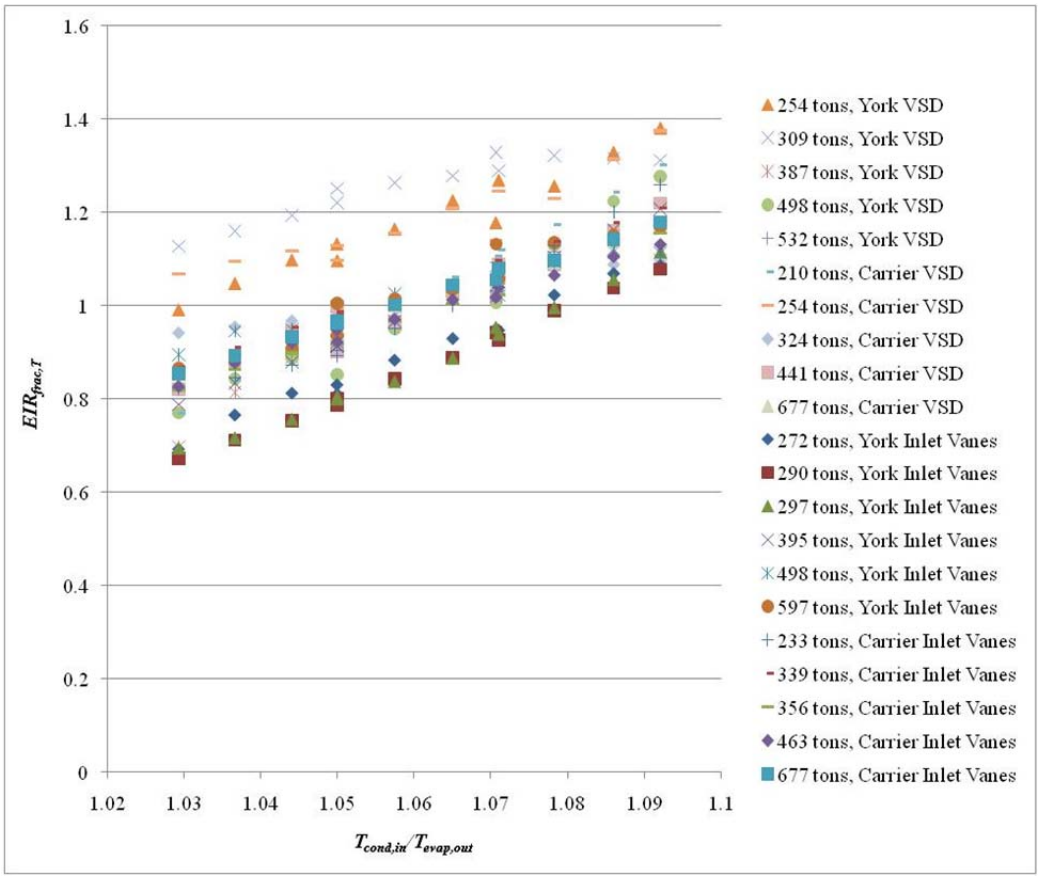

Figure 37. Plot of EIR fraction from EIRFT vs. absolute temperature ratio for York and Carrier centrifugal chillers with inlet guide vane and VSD capacity control.

Analysis of the preceding figure shows an offset between the linear behaviors of each type of capacity control employed. This distinction is better exposed by the manufacturer-independent plot shown in Figure 38.

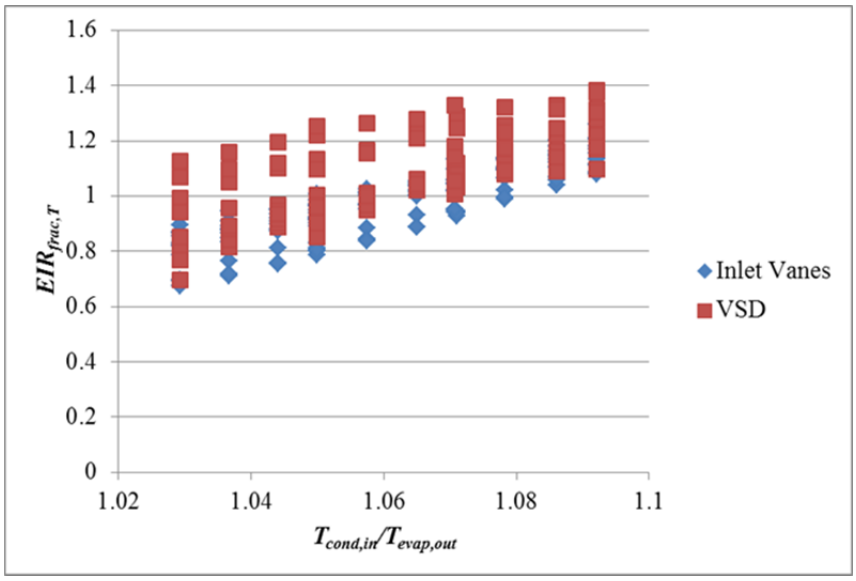

Figure 38. Plot of EIR fraction from EIRFT vs. absolute temperature ratio for centrifugal chillers with inlet guide vane and VSD capacity control.

Straight lines were found to best fit the data shown in the preceding figure and provided the following functions relating $EIR_{frac,T}$ to $T_{cond}^{in}/T_{evap}^{out}$ for inlet guide vane capacity control

$$EIR_{frac,T} = 5.721 * \frac{T_{cond}^{in}}{T_{evap}^{out}} - 5.097 \quad (53)$$

and

$$EIR_{frac,T} = 5.478 * \frac{T_{cond}^{in}}{T_{evap}^{out}} - 4.744 \quad (54)$$

for VSD capacity control.

The CAP_{frac} values obtained for each reference capacity were then plotted vs. the absolute temperature ratio $\left(T_{cond}^{in}/T_{evap}^{out}\right)$, as shown in Figure 39.

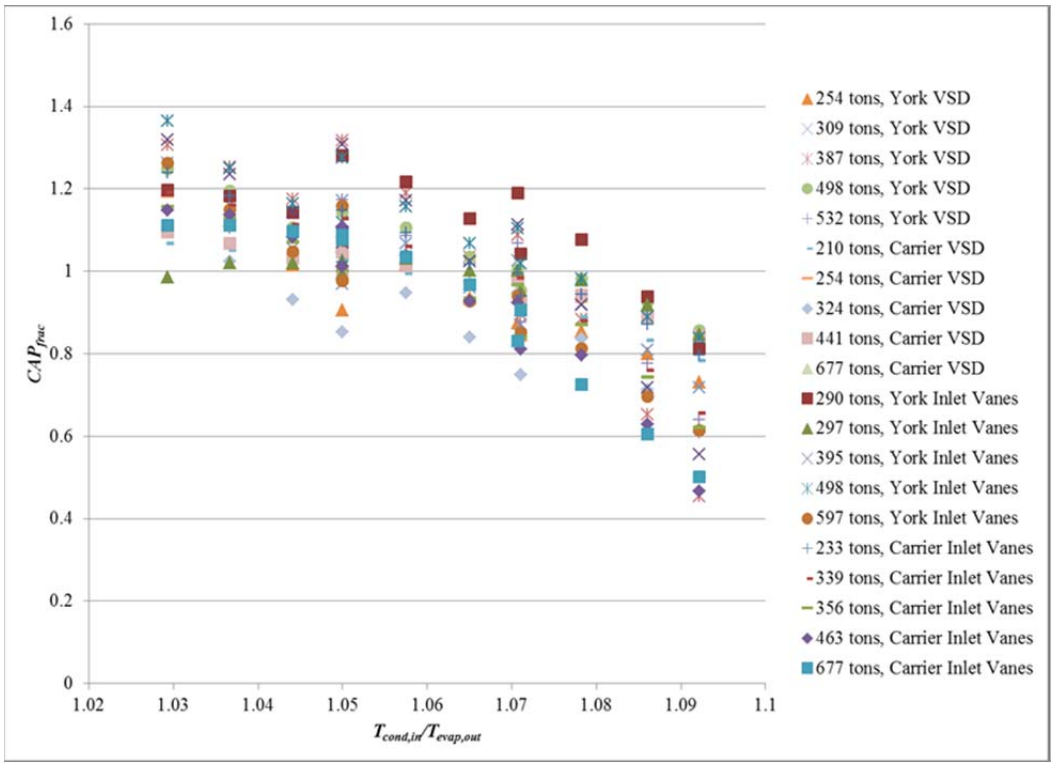

Figure 39. Plot of capacity fraction from CAPFT vs. absolute temperature ratio for York and Carrier centrifugal chillers with inlet guide vane and VSD capacity control.

Unlike the $EIR_{frac,PLR}$ and $EIR_{frac,T}$ curves, the preceding figure indicates that the CAP_{frac} vs. $\left(T_{cond}^{in}/T_{evap}^{out}\right)$ curves have similar behavior regardless of the capacity control type. A polynomial curve was found to best fit the data shown in the preceding figure, and provided the following function relating CAP_{frac} to $T_{cond}^{in}/T_{evap}^{out}$:

$$CAP_{frac} = -90.63\left(\frac{T_{cond}^{in}}{T_{evap}^{out}}\right)^2 + 185.06\left(\frac{T_{cond}^{in}}{T_{evap}^{out}}\right) - 93.306 \qquad (55)$$

Based on the description of how EnergyPlus uses the CAP_{frac}, $EIR_{frac,T}$, and $EIR_{frac,PLR}$ values to determine chiller performance, it was necessary to compare the

actual CAP_{frac} values and total EIR fraction values ($EIR_{total} = EIR_{frac,T} * EIR_{frac,PLR}$) to those predicted by Equations 51-55.

The actual CAP_{frac} values obtained for each reference capacity at 12 different water temperature conditions were multiplied by the chiller reference capacity to obtain the actual full-load capacity. Equation 55 was used with the same 12 water temperature conditions to calculate the predicted CAP_{frac} values for each reference capacity. The predicted CAP_{frac} values were multiplied by the chiller reference capacity to obtain the predicted full-load capacity. Comparing the actual and predicted full-load capacities for the 21 chillers under each temperature condition (252 data points) showed an average error of 8.53% with a standard deviation of 3.96%. These results indicate that Equation 55 may be used to calculate CAP_{frac} for water-cooled centrifugal chillers (independent of manufacturer) as operating conditions change.

For each reference capacity, the actual $EIR_{frac,T}$ values obtained at 12 different water temperature conditions were multiplied by the actual $EIR_{frac,PLR}$ value obtained for the same reference capacity when PLR was set equal to 1. Multiplying the actual $EIR_{frac,T}$ and actual $EIR_{frac,PLR}$ values together provided the actual EIR_{total}. Equations 53 and 54 were used with the same 12 water temperature conditions to calculate the predicted $EIR_{frac,T}$ values for each reference capacity. Equations 51 and 52 were used to calculate the predicted $EIR_{frac,PLR}$ value for each reference capacity with PLR set equal to 1. Multiplying the predicted $EIR_{frac,T}$ and predicted $EIR_{frac,PLR}$ values together provided the predicted EIR_{total}. Comparing the actual and predicted EIR_{total} for the 21 chillers under each temperature condition (252 data points) showed an average error of 6.77% with a standard deviation of 3.51%.

The comparison of actual and predicted EIR_{total} values was repeated for PLR = 0.8, 0.6, 0.4, and 0.2. The error associated with each part-load operation is summarized in Table 7.

Table 7. Water-cooled centrifugal chiller average error and standard deviation between actual and predicted total EIR fraction values for different PLR values.

PLR	Average Error (%)	Standard Deviation (%)
1	6.77	3.51
0.8	5.80	2.93
0.6	7.08	3.47
0.4	10.04	7.08
0.2	12.80	10.01

The average error for all load conditions is 8.50% with a standard deviation of 5.40%, indicating that Equations 51-54 may be used to calculate $EIR_{frac,PLR}$ and $EIR_{frac,T}$. The resulting values may then be multiplied to obtain the EIR_{total} value for water-cooled centrifugal chillers (independent of manufacturer) as operating conditions change.

Equations 51-55 provide a means for calculating chiller COP (independent of manufacturer) as operating conditions change for water-cooled centrifugal chillers with inlet guide vane capacity control and reference capacities between 233 and 677 tons and water-cooled centrifugal chillers with VSD capacity control and reference capacities between 210 and 677 tons.

Further validation of the use of Equations 51-55 for calculating chiller COP was provided by comparing the COP resulting from the EnergyPlus curves and the COP resulting from the correlations represented by Equation 51-55. Chiller COP was calculated by both methods for each of the 11 chillers with inlet guide vane capacity control and each of the 10 chillers with VSD capacity control. For all 21chillers, COP

was calculated for the 12 temperature conditions and for PLRs of 1, 0.8, 0.6, 0.4, and 0.2. The error between the EnergyPlus and predicted COP values for the 1260 data points is summarized in Tables 8 and 9. The average error for inlet guide vane capacity control under all load conditions is 12.07% with a standard deviation of 5.96%. The average error for VSD capacity control under all load conditions is 12.18% with a standard deviation of 4.61%.

Table 8. Water-cooled centrifugal chiller with inlet guide vane capacity control average error and standard deviation between actual and predicted COP values for different PLR values.

PLR	Average Error (%)	Standard Deviation (%)
1	10.57	4.51
0.8	10.70	4.53
0.6	11.34	5.11
0.4	12.65	6.48
0.2	15.09	9.19

Table 9. Water-cooled centrifugal chiller with VSD capacity control average error and standard deviation between actual and predicted COP values for different PLR values.

PLR	Average Error (%)	Standard Deviation (%)
1	11.56	3.05
0.8	9.51	2.59
0.6	10.10	3.70
0.4	13.71	5.57
0.2	16.04	8.13

An example of the COP comparison conducted is shown in Figure 40 for four water-cooled centrifugal chillers with inlet guide vane capacity control. The COP curves resulting from EnergyPlus and the correlations are plotted for a constant leaving chilled

water temperature (LCHWT) of 6°C and entering condenser water temperature (ECWT) of 24.15°C. The predicted COP at part-load is shown to closely match the COP resulting from the EnergyPlus curves.

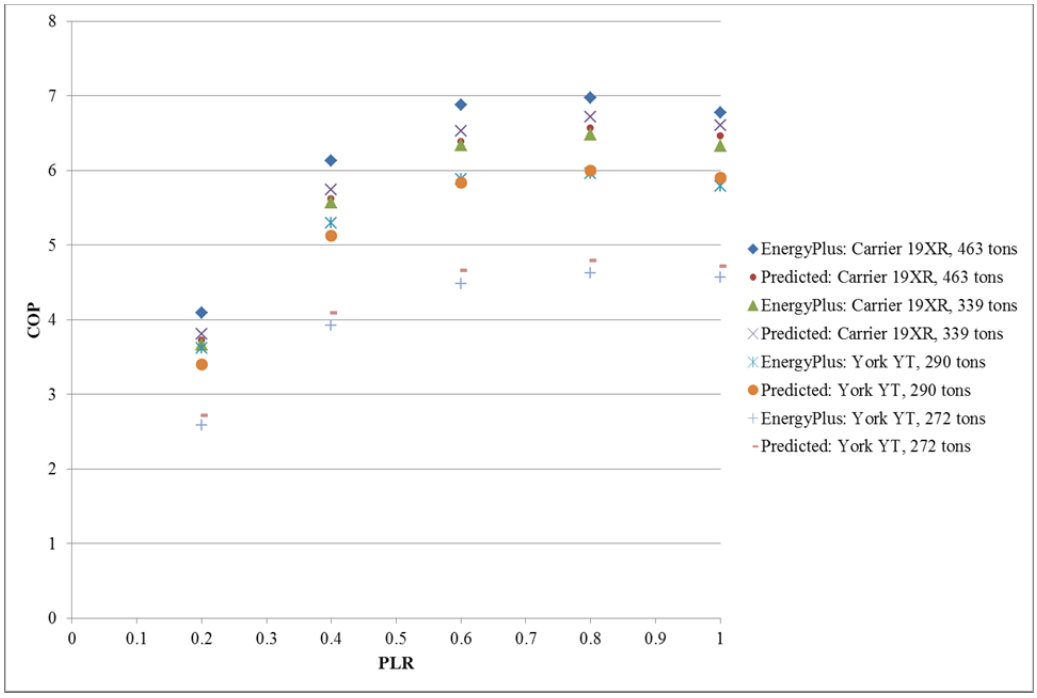

Figure 40. Plot of COP vs. PLR for four water-cooled centrifugal chillers with inlet guide vane capacity control.

Another example of the COP comparison conducted is shown in Figure 41 for four water-cooled centrifugal chillers with VSD capacity control. The COP curves resulting from EnergyPlus and the correlations are plotted for a constant leaving chilled water temperature (LCHWT) of 6°C and entering condenser water temperature (ECWT) of 24.15°C. The predicted COP at part-load is shown to closely match the COP resulting from the EnergyPlus curves.

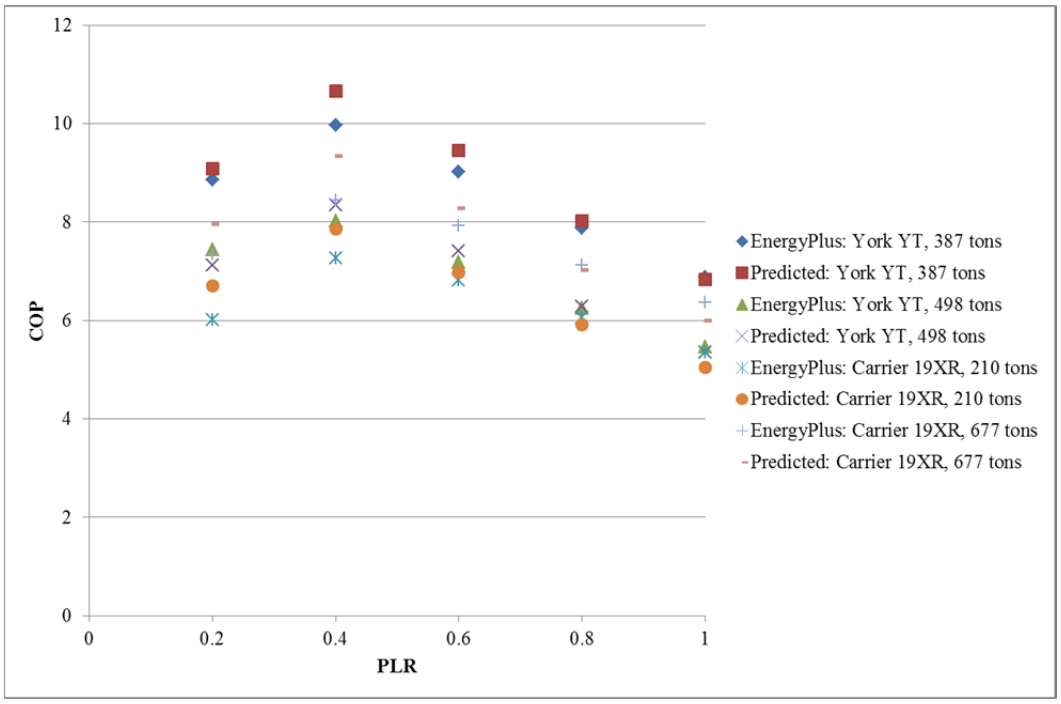

Figure 41. Plot of COP vs. PLR for four water-cooled centrifugal chillers with VSD capacity control.

4. COOLING TOWER MODEL DEVELOPMENT

The subsequent discussion is based upon the methods and assumptions presented in Section 2.5. Research of the underlying principles upon which EnergyPlus has been developed showed that the Merkel method is employed for cooling tower modeling (U.S. DOE 2010b). Considering the detailed nature of EnergyPlus as a building energy simulation program, utilization of the Merkel method for modeling cooling towers in WinAM is a viable approach. Two of the assumptions made by the Merkel method will be of fundamental importance for the cooling tower model developed for WinAM. These two assumptions are that the air exiting the cooling tower is saturated and the effects of water loss through evaporation are negligible (Kloppers et al. 2005).

The consequence of these assumptions is that accurate consideration of exiting air conditions is lost. However, it was shown that for an operating range of 10°F, evaporation losses are approximately 1.2% (Burger 2005) and drift losses are usually on the order of 0.02% of the CW (Burger 2005). An expected loss of 1.22% of the CW reinforces the validity of the two assumptions upon which the Merkel method is based.

Furthermore, it was shown that even without accurate consideration of exiting air conditions, the Merkel method predicts nearly the same CW temperature leaving the cooling tower as the Poppe method (Kloppers et al. 2005). The ability of the Merkel method to accurately predict CW temperature leaving the cooling tower lends itself for implementation in a cooling tower mass and energy balance.

4.1 Mass and Energy Balances

A schematic diagram of a cooling tower (the control volume) with water and air entering and exiting conditions is shown in Figure 42.

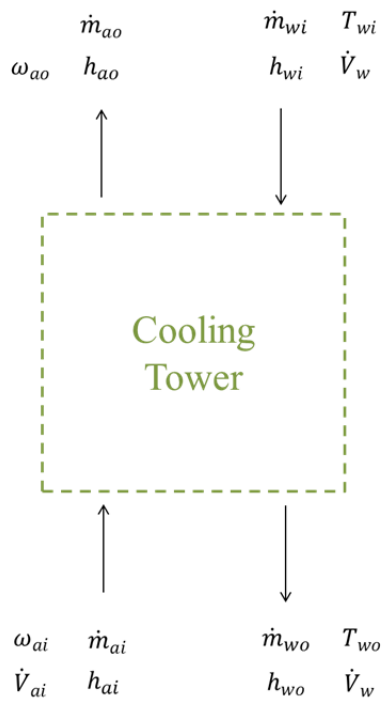

Figure 42. Diagram showing a cooling tower with water and air entering and exiting conditions.

Assuming steady-state operation, conservation of mass for the water and air flowing through the control volume requires that

$$\dot{m}_{ai} = \dot{m}_{ao} \tag{56}$$

$$\dot{m}_{wi} + \dot{m}_{ai}\omega_{ai} = \dot{m}_{wo} + \dot{m}_{ao}\omega_{ao} \tag{57}$$

where $\dot{m}$ designates mass flow rate, ω designates the humidity ratio, the w and a subscripts refer to the water and air, respectively, and the i and o subscripts refer to the conditions at the inlet and outlet of the control volume, respectively.

Substituting Equation 56 into Equation 57 and collecting like terms,

$$\dot{m}_{wi} + \dot{m}_{ai}(\omega_{ai} - \omega_{ao}) = \dot{m}_{wo} \tag{58}$$

Assuming steady-state operation, conservation of energy within the control volume requires that

$$0 = \Delta E_w + \Delta E_a \tag{59}$$

where ΔE is the change in energy between entering and exiting the control volume.

The change in energy of the water may be expressed as

$$\Delta E_w = \dot{m}_{wi} h_{wi} - \dot{m}_{wo} h_{wo} \tag{60}$$

where h designates enthalpy.

The change in energy of the air may similarly be expressed as

$$\Delta E_a = \dot{m}_{ai} h_{ai} - \dot{m}_{ao} h_{ao} \tag{61}$$

Equation 59 may thus be rewritten as

$$0 = (\dot{m}_{wi} h_{wi} - \dot{m}_{wo} h_{wo}) + (\dot{m}_{ai} h_{ai} - \dot{m}_{ao} h_{ao}) \tag{62}$$

Combining Equations 56, 58, and 62 and rearranging terms provides

$$\begin{aligned} 0 = \dot{m}_{wi}(h_{wi} - h_{wo}) + \dot{m}_{ai}(h_{ai} - h_{ao}) \\ - \dot{m}_{ai} h_{wo}(\omega_{ai} - \omega_{ao}) \end{aligned} \tag{63}$$

Writing the enthalpy of water in terms of its specific heat, c_{pw}, and temperature, T_w, one obtains

$$h_w = c_{pw} T_w \tag{64}$$

and Equation 63 may be rewritten as

$$\begin{aligned} 0 = \dot{m}_{wi} c_{pw}(T_{wi} - T_{wo}) + \dot{m}_{ai}(h_{ai} - h_{ao}) \\ - \dot{m}_{ai} c_{pw} T_{wo}(\omega_{ai} - \omega_{ao}) \end{aligned} \tag{65}$$

Considering that cooling towers consume energy by powering fans and pumping water (SPX 2009), the water and air mass flow rate terms are of interest. However, it was previously presented that water flow rates in cooling towers are specified to provide adequate water distribution and should not be varied (Kreider et al. 2002). Since the mass flow rate of water should not vary, the primary term of interest is the air mass flow rate. Equation 65 may be solved for the air mass flow rate and results in

$$\dot{m}_{ai} = \frac{-\dot{m}_{wi} c_{pw} (T_{wi} - T_{wo})}{(h_{ai} - h_{ao}) - c_{pw} T_{wo} (\omega_{ai} - \omega_{ao})} \tag{66}$$

The mass flow rate of a fluid may be expressed in terms of the fluids' density, ρ, and volumetric flow rate, $\dot{V}$, by

$$\dot{m} = \rho \dot{V} \tag{67}$$

Considering that water-cooled chiller manufacturers report performance for CW temperatures between 85°F and 105°F (York 2011a), the density of water over this range varies from 62.17 lb_m/ft^3 to 61.93 lb_m/ft^3 (Cengel et al. 2011). As this variation is small, the median value of 62.05 lb_m/ft^3 will serve as the approximate density of the water flowing through the cooling tower. Over this same CW temperature range, the specific heat of water is 0.999 Btu/lb_m-°F (Cengel et al. 2011).

The density of the air passing through the cooling tower will depend on ambient conditions. Using air properties at 1 atm pressure, air density varies from 0.08270 lb_m/ft^3 at 20°F to 0.06963 lb_m/ft^3 at 100°F. The median value of 0.076165 lb_m/ft^3 will serve as the approximate density of the air passing through the cooling tower.

Considering that a typical cooling tower is designed with a flow rate of 3 gpm per ton of nominal cooling capacity, $Q_{nominal}$, (U.S. DOE 2010b; ASHRAE 2008; Kreider et al. 2002), the volumetric flow rate of water may be expressed as

$$\dot{V}_w = \frac{3\ \text{gpm}}{\text{ton}} * Q_{nominal} \tag{68}$$

Introducing Equations 67, 68 and the approximations for water density, water specific heat, and air density, Equation 66 may be written as

$$\dot{V}_{ai} = \frac{-\left(62.05\frac{\text{lb}_\text{m}}{\text{ft}^3}\right)\left(\frac{3\ \text{gpm}}{\text{ton}}\right)Q_{nominal}\left(0.999\frac{\text{Btu}}{\text{lb}_\text{m}{}^\text{o}\text{F}}\right)(T_{wi}-T_{wo})}{\left(0.076165\frac{\text{lb}_\text{m}}{\text{ft}^3}\right)\left[(h_{ai}-h_{ao})-\left(0.999\frac{\text{Btu}}{\text{lb}_\text{m}{}^\text{o}\text{F}}\right)T_{wo}(\omega_{ai}-\omega_{ao})\right]} \tag{69}$$

In order to convert Equation 69 into units for direct implementation in WinAM, the conversion factor of 1 gallon = 0.134 ft^3 is applied to Equation 69, yielding

$$\dot{V}_{ai} = \frac{-\left(62.05\frac{\text{lb}_\text{m}}{\text{ft}^3}\right)\left(\frac{3\ \text{gpm}}{\text{ton}}\right)\left(\frac{0.134\ \text{ft}^3}{\text{gallon}}\right)Q_{nominal}\left(0.999\frac{\text{Btu}}{\text{lb}_\text{m}{}^\text{o}\text{F}}\right)(T_{wi}-T_{wo})}{\left(0.076165\frac{\text{lb}_\text{m}}{\text{ft}^3}\right)\left[(h_{ai}-h_{ao})-\left(0.999\frac{\text{Btu}}{\text{lb}_\text{m}{}^\text{o}\text{F}}\right)T_{wo}(\omega_{ai}-\omega_{ao})\right]} \tag{70}$$

Equation 70 can be further modified to directly account for the cooling load placed on the tower. Figure 43 shows a control volume taken about a chiller condenser and the relevant heat transfer terms.

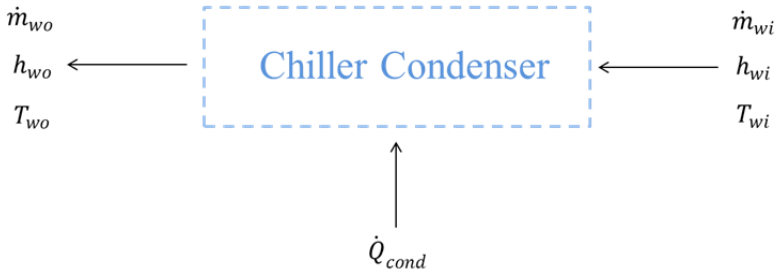

Figure 43. Diagram showing a chiller condenser with water entering and exiting conditions and cooling load.

Assuming steady-state operation, the mass and energy balances may be written respectively as

$$\dot{m}_{wi} = \dot{m}_{wo} \tag{71}$$

$$\Delta E_{cond} = \dot{Q}_{cond} = \dot{m}_{wi} h_{wi} - \dot{m}_{wo} h_{wo} \tag{72}$$

where $\dot{Q}_{cond}$ is the tower cooling load.

Inserting Equation 71 into Equation 72 and writing the enthalpy of water according to Equation 64, Equation 72 may be written as

$$\dot{Q}_{cond} = \dot{m}_w c_{pw} (T_{wi} - T_{wo}) \tag{73}$$

The CW temperature leaving the chiller may be calculated by

$$T_{wo} = T_{wi} + \frac{\dot{Q}_{cond}}{\dot{m}_w c_{pw}} \tag{74}$$

Employing Equations 67, 68 and the approximations for water density and specific heat, Equation 74 may be written as

$$T_{wo} = T_{wi} + \frac{\dot{Q}_{cond}}{\left(62.05 \frac{\text{lb}_\text{m}}{\text{ft}^3}\right)\left(\frac{3 \text{ gpm}}{\text{ton}}\right) Q_{nominal} \left(0.999 \frac{\text{Btu}}{\text{lb}_\text{m}{}^\text{o}\text{F}}\right)} \tag{75}$$

In order to convert Equation 75 into units for direct implementation in WinAM, the conversion factors of 1 gallon = 0.134 ft^3 and 1 hr = 60 min are applied to Equation 75, yielding

$$T_{wo} = T_{wi} + \frac{\dot{Q}_{cond} \left(\frac{1 \text{ hr}}{60 \text{ min}}\right)}{\left(62.05 \frac{\text{lb}_\text{m}}{\text{ft}^3}\right)\left(\frac{3 \text{ gpm}}{\text{ton}}\right)\left(\frac{0.134 \text{ ft}^3}{\text{gallon}}\right) Q_{nominal} \left(0.999 \frac{\text{Btu}}{\text{lb}_\text{m}{}^\text{o}\text{F}}\right)} \tag{76}$$

The term T_{wi} of Equation 70 is the temperature of the water entering the cooling tower, which is equivalent to the temperature of the water leaving the chiller condenser, term $T_{wo}$of Equation 76. Therefore, replacing T_{wi} of Equation 70 with T_{wo} of Equation 76 allows the required air volumetric flow rate to be directly calculated from the tower

cooling load. The tower cooling load was shown in Section 2.2 to be equivalent to the sum of the building cooling load and the power input to the chiller compressor.

Use of Equations 70 and 76 require specifying $Q_{nominal}$ as the cooling towers' nominal capacity in tons (specified by the user), $\dot{Q}_{cond}$ as the towers' cooling load in Btu/hr (calculated from the building cooling load and chiller compressor power), T_{wo} in °F (CW supply temperature reset schedule specified by the user), the air enthalpy in Btu/lb_{da}, and the air humidity ratio in lb_w/lb_{da}.

4.2 Psychrometric Calculations

Ambient air conditions are currently used in WinAM for the air-side modeling techniques employed. These conditions include the ambient air dry-bulb and wet-bulb temperatures, T_{adb} and T_{awb}, respectively. The following procedure may be used to derive the air enthalpy and humidity ratio values required by Equation 70.

First, T_{adb} and T_{awb} serve as the inlet air conditions, T_{adbi} and T_{awbi}, and are converted from °F to their absolute values (°R). Equation 11 is then used to calculate the K parameter for both T_{adbi} and T_{awbi}. The entering saturation pressure for both T_{adbi} and T_{awbi} is then calculated by Equation 10. Using the absolute T_{adbi} and T_{awbi}, Equation 12 is then used to calculate the entering air partial pressure. The relative humidity of the air entering the cooling tower is calculated by Equation 9, the entering air humidity ratio is calculated by Equation 8, and the entering air enthalpy is calculated by Equation 7.

Employing the assumption that the air exits the cooling tower as saturated, the relative humidity of the air leaving the cooling tower is equal to 1 and the dry-bulb temperature of the air exiting the cooling tower, T_{adbo}, is equal to the wet-bulb temperature of the air entering the cooling tower, T_{awbi}. Using the absolute T_{adbo}, the K parameter is calculated by Equation 11. The leaving saturation pressure for T_{adbo} is then calculated

by Equation 10. The humidity ratio of the leaving air is calculated by Equation 8 and the leaving air enthalpy is calculated by Equation 7.

Implementation of the preceding method provides h_{ai} and h_{ao} in Btu/lb_{da} and ω_{ai} and ω_{ao} in lb_w/lb_{da}, as required by Equation 70.

4.3 Fan Control

The methods described in Sections 4.1 and 4.2 allow the air volumetric flow rate required to meet the cooling tower load to be calculated. Determining the energy consumption of the cooling tower has been shown to depend on the fan operation. As such, determining cooling tower energy consumption reduces to determining fan energy consumption. The capacity control method employed by EnergyPlus will serve as the basis for quantifying fan energy consumption.

The user will specify the following parameters depending on cooling tower fan type:

- Single-Speed: W'_{rated}, V'_{rated}
- Two-Speed: $W'_{rated,high}$, $V'_{rated,high}$, $W'_{rated,low}$
- Variable-Speed with Modulating Outlet Dampers: W'_{rated}, V'_{rated}
- Variable-Speed with VFD: W'_{rated}, V'_{rated}

where W'_{rated} is the fan's rated power consumption, $W'_{rated,high}$ and $W'_{rated,low}$ are the fan's rated power consumption at high and low speed, respectively, V'_{rated} is the fan's rated volumetric flow rate, and $V'_{rated,high}$ is the fan's rated volumetric flow rate at high speed. Considering that CC® engineers will most likely not know the total fan efficiency, η_{fan}, the default value of 0.5 provided by EnergyPlus will be used (U.S. DOE 2010b).

If the fan is specified as single-speed, the required air volumetric flow rate, $\dot{V}_{ai}$, will be calculated by Equation 70. If $\dot{V}_{ai} = 0$, then the fan will be treated as off with no energy

consumed. If $\dot{V}_{ai} > 0$, then the fan will be treated as on and the power consumption calculated by

$$\dot{W} = \frac{\dot{W}_{rated}}{\eta_{fan}} \tag{77}$$

If the fan is specified as two-speed, the volumetric air flow rate provided by the fan at low speed, $\dot{V}_{low}$, is calculated by Equations 2 and 3. Specifically,

$$\dot{V}_{low} = \dot{V}_{rated,high} \left(\frac{\dot{W}_{rated,low}}{\dot{W}_{rated,high}} \right)^{1/3} \tag{78}$$

The required air volumetric flow rate, $\dot{V}_{ai}$, will then be calculated by Equation 70. If $\dot{V}_{ai} = 0$, then the fan will be treated as off with no energy consumed. If $0 < \dot{V}_{ai} < \dot{V}_{low}$, then the fan will be treated as running at low speed and the power consumption calculated by

$$\dot{W} = \frac{\dot{W}_{rated,low}}{\eta_{fan}} \tag{79}$$

If $\dot{V}_{low} < \dot{V}_{ai}$, then the fan will be treated as running at high speed and the power consumption calculated by

$$\dot{W} = \frac{\dot{W}_{rated,high}}{\eta_{fan}} \tag{80}$$

If the fan is specified as variable-speed, the required air volumetric flow rate, $\dot{V}_{ai}$, will be calculated by Equation 70. If $\dot{V}_{ai} = 0$, then the fan will be treated as off with no energy consumed. If $\dot{V}_{ai} > 0$, then the part load ratio, PLR, will be calculated by

$$PLR = \frac{\dot{V}_{ai}}{\dot{V}_{rated}} \tag{81}$$

and the power consumption, $\dot{W}$, calculated by Equation 4, if control is by modulating outlet dampers, or Equation 5, if control is by VFD.

5. WINAM IMPLEMENTATION

The primary objective of this research is provide additional functionality to WinAM such that the potential energy savings resulting from applying CC® measures to plant cooling equipment can be quantified. The procedure shown in Figure 44 will serve as a guide for how the models developed in Sections 3 and 4 can be implemented in WinAM.

1. User selects chiller type
    a. Air-cooled
        i. Scroll Compressor
            1. User inputs
                a. Chiller reference capacity between 15 and 168 tons
                b. CHW supply temperature (T_{evap}^{out}) reset schedule
            2. WinAM calculates chiller full-load COP from Equation 1
                a. WinAM uses Equations 19, 20, and 21 to calculate ${A_0}^*$, ${A_1}^*$, and ${A_2}^*$
                b. WinAM uses the simulated cooling load for Q_{evap}
                c. WinAM uses the user-specified T_{evap}^{out}
                d. WinAM uses the ambient air dry-bulb temperature for T_{cond}^{in}
            3. WinAM calculates the actual COP
                a. WinAM divides the simulated cooling load by the reference capacity to obtain the PLR
                b. WinAM uses the PLR in Equation 22 to calculate $COP_{FL,frac}$
                c. WinAM multiplies the chiller full-load COP by $COP_{FL,frac}$
            4. WinAM divides the simulated cooling load by the calculated actual COP to obtain the chiller energy consumption
        ii. Screw Compressor
            1. User inputs
                a. Chiller reference capacity between 69 and 513 tons
                b. CHW supply temperature (T_{evap}^{out}) reset schedule
            2. WinAM calculates chiller full-load COP from Equation 1

Figure 44. Procedure for implementation in WinAM.

a. WinAM uses Equations 29, 30, and 31 to calculate $A_0{}^*$, $A_1{}^*$, and $A_2{}^*$
b. WinAM uses the simulated cooling load for Q_{evap}
c. WinAM uses the user-specified T_{evap}^{out}
d. WinAM uses the ambient air dry-bulb temperature for T_{cond}^{in}

3. WinAM calculates the actual COP
   a. WinAM divides the simulated cooling load by the reference capacity to obtain the PLR
   b. WinAM uses the PLR to calculate $COP_{FL,frac}$
      i. Reference capacity ≤ 151 tons: Equation 32
      ii. Reference capacity > 151 tons: Equation 33
   c. WinAM multiplies the chiller full-load COP by $COP_{FL,frac}$
4. WinAM divides the simulated cooling load by the calculated actual COP to obtain the chiller energy consumption

b. Water-cooled
   i. Scroll Compressor
      1. User inputs
         a. Chiller reference capacity between 20 and 200 tons
         b. CHW supply temperature (T_{evap}^{out}) reset schedule
         c. Cooling tower outlet CW temperature (T_{cond}^{in}) reset schedule
      2. WinAM calculates chiller full-load COP from Equation 1
         a. WinAM uses Equations 40, 41, and 42 to calculate $A_0{}^*$, $A_1{}^*$, and $A_2{}^*$
         b. WinAM uses the simulated cooling load for Q_{evap}
         c. WinAM uses the user-specified T_{evap}^{out}
         d. WinAM uses the user-specified T_{cond}^{in}
      3. WinAM calculates the actual COP
         a. WinAM divides the simulated cooling load by the reference capacity to obtain the PLR
         b. WinAM uses the PLR in Equation 43 to calculate $COP_{FL,frac}$
         c. WinAM multiplies the chiller full-load COP by $COP_{FL,frac}$
      4. WinAM divides the simulated cooling load by the calculated actual COP to obtain the chiller energy consumption

Figure 44. Continued.

ii. Reciprocating Compressor
    1. User inputs
        a. Chiller reference capacity between 20 and 364 tons
        b. CHW supply temperature (T_{evap}^{out}) reset schedule
        c. Cooling tower outlet CW temperature (T_{cond}^{in}) reset schedule
    2. WinAM calculates chiller full-load COP from Equation 1
        a. WinAM uses Equations 44, 45, and 46 to calculate ${A_0}^*$, ${A_1}^*$, and ${A_2}^*$
        b. WinAM uses the simulated cooling load for Q_{evap}
        c. WinAM uses the user-specified T_{evap}^{out}
        d. WinAM uses the user-specified T_{cond}^{in}
    3. WinAM calculates the actual COP
        a. WinAM divides the simulated cooling load by the reference capacity to obtain the PLR
        b. WinAM uses the PLR in Equation 47 to calculate $COP_{FL,frac}$
        c. WinAM multiplies the chiller full-load COP by $COP_{FL,frac}$
    4. WinAM divides the simulated cooling load by the calculated actual COP to obtain the chiller energy consumption

iii. Screw Compressor
    1. User inputs
        a. Chiller reference capacity between 194 and 498 tons
        b. Chiller reference COP*
            i. From manufacturer's data when T_{cond}^{in} = 85°F and T_{evap}^{out} = 44°F
                1. These are conditions upon which EnergyPlus curves are based
        c. CHW supply temperature (T_{evap}^{out}) reset schedule
        d. Cooling tower outlet CW temperature (T_{cond}^{in}) reset schedule
    2. WinAM calculates full-load capacity
        a. WinAM uses Equation 50 to calculate CAP_{frac} from user-specified T_{cond}^{in} and T_{evap}^{out}
        b. WinAM multiplies CAP_{frac} by user-specified reference capacity

Figure 44. Continued.

3. WinAM calculates chiller EIR
    a. WinAM calculates PLR by dividing simulated cooling load by calculated full-load capacity
    b. WinAM uses Equation 48 to calculate $EIR_{frac,PLR}$ from calculated PLR
    c. WinAM uses Equation 49 to calculate $EIR_{frac,T}$ from user-specified T_{cond}^{in} and T_{evap}^{out}
    d. WinAM calculates EIR_{total} by multiplying the $EIR_{frac,PLR}$ and $EIR_{frac,T}$ values together
    e. WinAM calculates chiller EIR by multiplying EIR_{total} by the inverse of the reference COP
4. WinAM multiplies the simulated cooling load and the calculated EIR to obtain the chiller energy consumption

iv. Centrifugal Compressor
1. User inputs
    a. Capacity control type
        i. Inlet Guide Vanes
            1. Chiller reference capacity between 233 and 677 tons
        ii. VSD
            1. Chiller reference capacity between 210 and 677 tons
    b. Chiller reference COP*
        i. From manufacturer's data when T_{cond}^{in} = 85°F and T_{evap}^{out} = 44°F
            1. These are conditions upon which EnergyPlus curves are based
    c. CHW supply temperature (T_{evap}^{out}) reset schedule
    d. Cooling tower outlet CW temperature (T_{cond}^{in}) reset schedule
2. WinAM calculates full-load capacity
    a. WinAM uses Equation 55 to calculate CAP_{frac} from user-specified T_{cond}^{in} and T_{evap}^{out}
    b. WinAM multiplies CAP_{frac} by user-specified reference capacity
3. WinAM calculates chiller EIR
    a. WinAM calculates PLR by dividing simulated cooling load by calculated full-load capacity

Figure 44. Continued.

b. WinAM calculates $EIR_{frac,PLR}$ from calculated PLR
   i. Inlet Guide Vanes: Equation 51
   ii. VSD: Equation 52
c. WinAM calculates $EIR_{frac,T}$ from user-specified T_{cond}^{in} and T_{evap}^{out}
   i. Inlet Guide Vanes: Equation 53
   ii. VSD: Equation 54
d. WinAM calculates EIR_{total} by multiplying the $EIR_{frac,PLR}$ and $EIR_{frac,T}$ values together
e. WinAM calculates chiller EIR by multiplying EIR_{total} by the inverse of the reference COP

4. WinAM multiplies the simulated cooling load and the calculated EIR to obtain the chiller energy consumption

2. If chiller type selected is air-cooled, no cooling tower modeling is performed
3. If chiller type selected is water-cooled, cooling tower modeling is performed
   a. User inputs
      i. Fan motor type and rated values
         1. Single-speed
            a. W'_{rated}, V'_{rated}
         2. Two-speed
            a. $W'_{rated,high}$, $V'_{rated,high}$, $W'_{rated,low}$
         3. Variable-speed
            a. VFD
               i. W'_{rated}, V'_{rated}
            b. Modulating outlet dampers
               i. W'_{rated}, V'_{rated}
      ii. Cooling tower nominal capacity ($Q_{nominal}$) in tons
   b. WinAM calculates required air volumetric flow rate ($\dot{V}_{ai}$) by Equation 70
      i. WinAM uses the user-specified $Q_{nominal}$
      ii. T_{wi} of Equation 70 is obtained by the value calculated for T_{wo} from Equation 76
         1. To solve Equation 76
            a. T_{wi} is the cooling tower outlet CW temperature (T_{cond}^{in}) reset schedule
               i. Specified by the user for modeling the water-cooled chiller
            b. WinAM calculates the tower cooling load ($\dot{Q}_{cond}$) in Btu/hr

Figure 44. Continued.

i. Equal to the sum of the simulated building cooling load and chiller compressor energy consumption

iii. T_{wo} is the cooling tower outlet CW temperature (T_{cond}^{in}) reset schedule
1. Specified by the user for modeling the water-cooled chiller

iv. WinAM calculates h_{ai}, h_{ao}, ω_{ai}, ω_{ao}
1. T_{adbi} and T_{awbi} from weather data are converted from °F to absolute °R
2. Calculate K parameter for both T_{adbi} and T_{awbi} by Equation 11
3. Calculate p_{sat} for both T_{adbi} and T_{awbi} by Equation 10
4. Calculate p_m from the absolute T_{adbi} and T_{awbi} by Equation 12
5. Calculate ϕ for the air entering the cooling tower by Equation 9
6. Calculate ω_{ai} by Equation 8
7. Calculate h_{ai} by Equation 7
8. Let ϕ = 1 for the air leaving the cooling tower and T_{adbo} = T_{awbi}
9. Calculate K parameter from absolute T_{adbo} by Equation 11
10. Calculate p_{sat} for T_{adbo} by Equation 10
11. Calculate ω_{ao} by Equation 8
12. Calculate h_{ao} by Equation 7

c. WinAM calculates fan power consumption

i. Single-speed
1. If $\dot{V}_{ai}$ = 0, fan is off
2. If $\dot{V}_{ai}$ > 0, energy consumption calculated by Equation 77

ii. Two-speed
1. WinAM calculates $\dot{V}_{low}$ by Equation 78
2. If $\dot{V}_{ai}$ = 0, fan is off
3. If 0 < $\dot{V}_{ai}$ < $\dot{V}_{low}$, energy consumption calculated by Equation 79
4. If $\dot{V}_{low}$ < $\dot{V}_{ai}$, then energy consumption calculated by Equation 80

iii. Variable-speed
1. If $\dot{V}_{ai}$ = 0, fan is off
2. If $\dot{V}_{ai}$ > 0, then WinAM calculates PLR by Equation 81
a. Energy consumption calculated by
i. Modulating outlet dampers: Equation 4

Figure 44. Continued.

ii. VFD: Equation 5

Note: * this may be input as 1 when only concerned with relative savings between pre- and post-CC® measures. In this case, chiller percent savings will be calculated by the change in EIR_{total} summed over the period. Cooling tower modeling may not be used because added cooling load from the compressor is not calculated without the actual reference COP.

Figure 44. Continued.

6. CONCLUSIONS

WinAM is a tool that provides CC® engineers with an efficient way to identify energy saving measures in existing buildings. However, at this stage of its development, there remain many opportunities to improve its utility. This research has sought to provide WinAM users with the ability to not only estimate energy savings from air-side CC® measures, but to also estimate energy savings from CC® measures applied to plant cooling equipment.

Through the development of techniques for modeling water-cooled chillers, air-cooled chillers, and cooling towers, a means has been provided for CC® engineers to quantify the benefits of adjusting plant cooling equipment operation. Limiting the parameters required from WinAM users to model such cooling equipment served as a guiding principle, as added complexity would inhibit this research from being beneficial. The correlations developed to maintain a user-friendly modeling approach served to provide the chiller modeling capabilities shown in Figure 45.

- Air-cooled chillers
  - Scroll: 15-168 tons
    - Average error of 8.07% with standard deviation of 9.13%
  - Screw: 69-513 tons
    - Average error of 7.38% with standard deviation of 6.13%
- Water-cooled chillers
  - Scroll: 20-200 tons
    - Average error of 8.16% with standard deviation of 9.72%
  - Reciprocating: 20-364 tons
    - Average error of 10.30% with standard deviation of 7.81%

Figure 45. Chiller modeling capabilities.

- Screw: 194-498 tons
  - Average error of 9.87% with standard deviation of 3.65%
- Centrifugal
  - Inlet Guide Vanes: 233-677 tons

    Average error of 12.07% with standard deviation of 5.96%
  - VSD: 210-677 tons

    Average error of 12.18% with standard deviation of 4.61%

Figure 45. Continued.

The development of a cooling tower model to predict energy consumption under varying conditions utilized assumptions made by the Merkel method, as well as mass and energy balances. The model developed provides the following modeling capabilities dependent on cooling tower fan control:

- Single-speed
- Two-speed
- Variable-speed
  - Modulating outlet dampers
  - VFD

Two areas for further work have been identified and include verifying the energy savings predicted by the models and implementation of an iterative technique for modeling cooling tower performance. The assumptions made by the Merkel method provide an accurate means for estimating the CW temperatures needed for an energy balance. However, these assumptions prevent the model from predicting actual leaving air conditions.

Implementation of the step-by-step approach outlined in Section 5 will provide WinAM with additional functionality and ultimately aid CC® engineers in reducing existing building energy consumption.

REFERENCES

AHRI. 2003. Standard for performance rating of water-chilling packages using the vapor compression cycle. *AHRI Standard 550/590.* Arlington, VA: AHRI.

ASHRAE. 2008. Compressors. In *2008 ASHRAE Handbook on HVAC Systems and Equipment*, 37.1. IP Edition. Atlanta, GA: ASHRAE.

Burger, R. 2005. Cooling tower technology. *Ullmann's Encyclopedia of Industrial Chemistry*. Dallas, TX: Wiley-VCH.

Carrier. 1999. Form 19EX-3PD. *19EX Centrifugal Liquid Chiller*. Syracuse, NY: Carrier Corporation.

Carrier. 2005. Cat. No. 04-819192-25. *Evergreen™ Water-Cooled Chillers*. Farmington, CT: Carrier Corporation.

Carrier. 2010. Form 19XR-9PD. *Evergreen® 19XR, XRV High-Efficiency Hermetic Centrifugal Liquid Chiller*. Syracuse, NY: Carrier Corporation.

Cengel, Y. and A.J. Ghajar. 2011. *Heat and Mass Transfer: Fundamentals and Applications,* Fourth Edition*.* New York, NY: McGraw-Hill.

Drbal, L.F., and P.G. Boston. 1996. *Power Plant Engineering*. New York, NY: Springer Science+Business Media, Inc.

ESL. 2011. *WinAM Users Manual Version 4.1.* College Station, TX: The Texas Engineering Experiment Station.

Fisenko, S.P., A.I. Petruchik, and A.D. Solodukhin. 2002. Evaporative cooling of water in a natural draft cooling tower. *International Journal of Heat and Mass Transfer* 45:4683-4694.

Gordon, J.M. and K.C. Ng. 1994. Thermodynamic modeling of reciprocating chillers. *Journal of Applied Physics* 75(6):2769-2774.

Gordon, J.M., K.C. Ng, and H.T. Chua. 1995. Centrifugal chillers: Thermodynamic modeling and a diagnostic case study. *International Journal of Refrigeration* 18(4):253-257.

Graves, R.D. 2003. Thermodynamic modeling and optimization of a screw compressor chiller and cooling tower system. M.S. Thesis, Texas A&M University, College Station, Texas.

Henninger, R.H. and M.J. Witte. 2010. *EnergyPlus Testing with HVAC Equipment Component Tests*. Arlington Heights, IL: GARD Analytics.

Hydeman, M. and K.L. Gillespie Jr. 2002. Tools and techniques to calibrate electric chiller component models. *ASHRAE Transactions* 108(1):733-741.

Kelso, J. D. 2009. *2009 Buildings Energy Data Book*. Silver Spring, MD: D&R International, Ltd.

Kloppers, J.C. and D.G. Kroger. 2005. Cooling tower performance evaluation: Merkel, Poppe, and e-NTU methods of analysis. *Journal of Engineering for Gas Turbines and Power* 127:1-7.

Kreider, J.F., P.S. Curtiss, and A. Rabl. 2002. *Heating and Cooling of Buildings*. New York, NY: McGraw-Hill.

Leff, H.S. and W.D. Teeters. 1978. EER, COP, and the second law efficiency for air conditioners. *American Journal of Physics* 46(1):19-22.

Leverenz, D.J. and N.E. Bergan. 1983. Development and validation of a reciprocating chiller model for hourly energy analysis programs. *ASHRAE Transactions* 1983(1B):156-164.

Liu, M., D.E. Claridge, and W.D. Turner. 2002. *Continuous Commissioning*^{SM} *Guidebook: Maximizing Building Energy Efficiency and Comfort*. Washington, DC: U.S. Department of Energy Federal Energy Management Program, October.

Liu, M. 1999. Improving building energy system performance by continuous commissioning. *Energy Engineering* 96(5): 46-57.

Sheet Metal and Air Conditioning Contractor's National Association, Inc. (SMACNA) 1995. *HVAC Systems-Applications*, Fifth Edition. Chantilly, VA: SMACNA.

SPX Cooling Technologies. 2009. *Cooling Tower Fundamentals*. Overland Park, KS: SPX Cooling Technologies, Inc.

Trane. 1999. RLC-DS-2. *Series R® Rotary Liquid Chiller*. La Crosse, WI: The Trane Company.

Trane. 2002a. CG-PRC007-EN. *Air-Cooled Liquid Chillers*. La Crosse, WI: The Trane Company.

Trane. 2002b. CG-PRC011-EN. *Scroll Liquid Chillers*. La Crosse, WI: The Trane Company.

Trane. 2002c. RLC-PRC016-EN. *Air-Cooled Series R^{TM} Rotary Liquid Chiller*. La Crosse, WI: The Trane Company.

Trane. 2005. CVHE-SVU01E-EN. *Operation Maintenance*. La Cross, WI: The Trane Company.

Trane. 2006. PROD-SLB012-EN. *Central Plant Product Guide*. La Crosse, WI: The Trane Company.

U.S. DOE. 2010a. Getting started. *EnergyPlus Documentation*, version 6.0. Berkeley, CA: Lawrence Berkeley National Laboratory.

U.S. DOE. 2010b. Input-output reference. *EnergyPlus Documentation*, version 6.0. Berkeley, CA: Lawrence Berkeley National Laboratory.

York. 2001. Form 160.55-EG1 (901). *Centrifugal Liquid Chillers Model YT*. York, PA: York International Corporation.

York. 2010. PUBL-6374 (1010). *York Water-Cooled Chillers*. Milwaukee, WI: Johnson Controls, Inc.

York. 2011a. Form 150.26-EG1 (611). *Model YCWL Water-Cooled Scroll Liquid Chiller Style A*. Milwaukee, WI: Johnson Controls, Inc.

York. 2011b. Form 150.62-EG3 (409). *Model YLAA Air-Cooled Scroll Chillers Style A*. Milwaukee, WI: Johnson Controls, Inc.

York. 2011c. Form 150.67-EG1 (311). *Model YCAL Air-Cooled Scroll Compressor Liquid Chillers Style E*. Milwaukee, WI: Johnson Controls, Inc.

York. 2011d. Form 201.21-EG1 (209). *Model YCAV Air-Cooled Screw Compressor Liquid Chillers Style A*. Milwaukee, WI: Johnson Controls, Inc.

APPENDIX A

Collection of manufacturers' full-load data used to model air-cooled scroll chillers.

	Reference Capacity (tons)	Tevap,out (°F)	Tcond,in (°F)	Power in (kW)	Capacity (tons)	Capacity (kW)	COP
York	15.4	40	75	13.6	16.2	56.98	4.19
		42	75	13.7	16.7	58.73	4.29
		44	75	13.9	17.3	60.84	4.38
		45	75	13.9	17.6	61.90	4.45
		46	75	14	17.8	62.60	4.47
		48	75	14.1	18.4	64.71	4.59
		50	75	14.3	19	66.82	4.67
		40	80	14.4	15.8	55.57	3.86
		42	80	14.6	16.3	57.33	3.93
		44	80	14.7	16.8	59.09	4.02
		45	80	14.8	17.1	60.14	4.06
		46	80	14.8	17.4	61.20	4.13
		48	80	15	18	63.31	4.22
		50	80	15.1	18.5	65.06	4.31
		40	85	15.3	15.3	53.81	3.52
		42	85	15.5	15.9	55.92	3.61
		44	85	15.6	16.4	57.68	3.70
		45	85	15.7	16.7	58.73	3.74
		46	85	15.7	16.9	59.44	3.79
		48	85	15.9	17.5	61.55	3.87
		50	85	16	18	63.31	3.96
		40	90	16.3	14.9	52.40	3.21
		42	90	16.4	15.4	54.16	3.30
		44	90	16.6	15.9	55.92	3.37
		45	90	16.6	16.2	56.98	3.43
		46	90	16.7	16.5	58.03	3.47
		48	90	16.8	17	59.79	3.56
		50	90	17	17.5	61.55	3.62
		40	95	17.3	14.4	50.64	2.93
		42	95	17.4	14.9	52.40	3.01
		44	95	17.6	15.4	54.16	3.08
		45	95	17.6	15.7	55.22	3.14
		46	95	17.7	16	56.27	3.18

		48	95	17.9	16.5	58.03	3.24
		50	95	18	17	59.79	3.32
York	18.7	40	75	16.7	19.9	69.99	4.19
		42	75	16.8	20.6	72.45	4.31
		44	75	17	21.2	74.56	4.39
		45	75	17.1	21.6	75.97	4.44
		46	75	17.2	21.9	77.02	4.48
		48	75	17.4	22.6	79.48	4.57
		50	75	17.5	23.3	81.95	4.68
		40	80	17.6	19.4	68.23	3.88
		42	80	17.8	20	70.34	3.95
		44	80	18	20.7	72.80	4.04
		45	80	18.1	21	73.86	4.08
		46	80	18.2	21.3	74.91	4.12
		48	80	18.4	22	77.37	4.21
		50	80	18.6	22.7	79.84	4.29
		40	85	18.7	18.8	66.12	3.54
		42	85	18.9	19.4	68.23	3.61
		44	85	19.1	20	70.34	3.68
		45	85	19.2	20.4	71.75	3.74
		46	85	19.3	20.7	72.80	3.77
		48	85	19.4	21.4	75.26	3.88
		50	85	19.6	22	77.37	3.95
		40	90	19.9	18.1	63.66	3.20
		42	90	20	18.7	65.77	3.29
		44	90	20.2	19.4	68.23	3.38
		45	90	20.3	19.7	69.28	3.41
		46	90	20.4	20	70.34	3.45
		48	90	20.6	20.7	72.80	3.53
		50	90	20.8	21.3	74.91	3.60
		40	95	21.1	17.5	61.55	2.92
		42	95	21.3	18.1	63.66	2.99
		44	95	21.5	18.7	65.77	3.06
		45	95	21.6	19	66.82	3.09
		46	95	21.7	19.3	67.88	3.13
		48	95	21.9	20	70.34	3.21
		50	95	22.1	20.6	72.45	3.28
York	25.6	40	75	22	26.5	93.20	4.24
		42	75	22.2	27.4	96.37	4.34

		44	75	22.4	28.4	99.88	4.46
		45	75	22.5	28.8	101.29	4.50
		46	75	22.6	29.3	103.05	4.56
		48	75	22.8	30.3	106.57	4.67
		50	75	23.1	31.3	110.08	4.77
		40	80	23.1	25.9	91.09	3.94
		42	80	23.3	26.8	94.26	4.05
		44	80	23.5	27.7	97.42	4.15
		45	80	23.6	28.2	99.18	4.20
		46	80	23.7	28.6	100.59	4.24
		48	80	24	29.6	104.10	4.34
		50	80	24.2	30.5	107.27	4.43
		40	85	24.3	25.3	88.98	3.66
		42	85	24.5	26.1	91.79	3.75
		44	85	24.7	27	94.96	3.84
		45	85	24.9	27.5	96.72	3.88
		46	85	25	27.9	98.12	3.92
		48	85	25.2	28.8	101.29	4.02
		50	85	25.4	29.8	104.81	4.13
		40	90	25.6	24.6	86.52	3.38
		42	90	25.8	25.5	89.68	3.48
		44	90	26.1	26.3	92.50	3.54
		45	90	26.2	26.8	94.26	3.60
		46	90	26.3	27.2	95.66	3.64
		48	90	26.5	28.1	98.83	3.73
		50	90	26.8	29	101.99	3.81
		40	95	27.1	23.9	84.06	3.10
		42	95	27.3	24.7	86.87	3.18
		44	95	27.5	25.6	90.04	3.27
		45	95	27.6	26	91.44	3.31
		46	95	27.7	26.4	92.85	3.35
		48	95	27.9	27.3	96.01	3.44
		50	95	28.2	28.2	99.18	3.52
York	28.6	40	75	23.8	29.7	104.45	4.39
		42	75	24	30.7	107.97	4.50
		44	75	24.2	31.7	111.49	4.61
		45	75	24.4	32.2	113.25	4.64
		46	75	24.5	32.7	115.01	4.69
		48	75	24.8	33.7	118.52	4.78

		50	75	25.1	34.8	122.39	4.88
		40	80	25	29	101.99	4.08
		42	80	25.2	30	105.51	4.19
		44	80	25.4	31	109.03	4.29
		45	80	25.6	31.5	110.79	4.33
		46	80	25.7	32	112.54	4.38
		48	80	26	33	116.06	4.46
		50	80	26.3	34	119.58	4.55
		40	85	26.3	28.3	99.53	3.78
		42	85	26.5	29.2	102.70	3.88
		44	85	26.7	30.2	106.21	3.98
		45	85	26.9	30.7	107.97	4.01
		46	85	27	31.2	109.73	4.06
		48	85	27.3	32.2	113.25	4.15
		50	85	27.6	33.2	116.76	4.23
		40	90	27.7	27.5	96.72	3.49
		42	90	27.9	28.5	100.23	3.59
		44	90	28.1	29.4	103.40	3.68
		45	90	28.3	29.9	105.16	3.72
		46	90	28.4	30.4	106.92	3.76
		48	90	28.7	31.4	110.43	3.85
		50	90	29	32.3	113.60	3.92
		40	95	29.2	26.7	93.90	3.22
		42	95	29.4	27.6	97.07	3.30
		44	95	29.6	28.6	100.59	3.40
		45	95	29.8	29	101.99	3.42
		46	95	29.9	29.5	103.75	3.47
		48	95	30.2	30.5	107.27	3.55
		50	95	30.5	31.4	110.43	3.62
York	37.2	40	75	30.8	38.7	136.11	4.42
		42	75	31	40	140.68	4.54
		44	75	31.1	41.4	145.60	4.68
		45	75	31.2	42.1	148.07	4.75
		46	75	31.3	42.7	150.18	4.80
		48	75	31.5	44.1	155.10	4.92
		50	75	31.7	45.6	160.38	5.06
		40	80	32.3	37.8	132.94	4.12
		42	80	32.5	39.1	137.51	4.23
		44	80	32.7	40.5	142.44	4.36

		45	80	32.8	41.1	144.55	4.41
		46	80	32.9	41.8	147.01	4.47
		48	80	33.2	43.2	151.93	4.58
		50	80	33.4	44.7	157.21	4.71
		40	85	34.1	36.8	129.43	3.80
		42	85	34.3	38.1	134.00	3.91
		44	85	34.6	39.5	138.92	4.02
		45	85	34.7	40.1	141.03	4.06
		46	85	34.8	40.8	143.49	4.12
		48	85	35	42.2	148.42	4.24
		50	85	35.2	43.6	153.34	4.36
		40	90	36.2	35.7	125.56	3.47
		42	90	36.4	37.1	130.48	3.58
		44	90	36.6	38.4	135.05	3.69
		45	90	36.7	39.1	137.51	3.75
		46	90	36.8	39.7	139.62	3.79
		48	90	37	41.1	144.55	3.91
		50	90	37.3	42.5	149.47	4.01
		40	95	38.4	34.6	121.69	3.17
		42	95	38.6	35.9	126.26	3.27
		44	95	38.8	37.2	130.83	3.37
		45	95	38.9	37.9	133.29	3.43
		46	95	39	38.6	135.76	3.48
		48	95	39.3	39.9	140.33	3.57
		50	95	39.5	41.3	145.25	3.68
York	39.4	40	75	32.4	41	144.20	4.45
		42	75	32.6	42.5	149.47	4.59
		44	75	32.9	43.9	154.40	4.69
		45	75	33	44.7	157.21	4.76
		46	75	33.1	45.4	159.67	4.82
		48	75	33.4	46.9	164.95	4.94
		50	75	33.6	48.5	170.57	5.08
		40	80	34.2	40	140.68	4.11
		42	80	34.4	41.4	145.60	4.23
		44	80	34.6	42.9	150.88	4.36
		45	80	34.8	43.6	153.34	4.41
		46	80	34.9	44.4	156.15	4.47
		48	80	35.2	45.9	161.43	4.59
		50	80	35.4	47.4	166.71	4.71

		40	85	36.1	39	137.16	3.80
		42	85	36.3	40.4	142.09	3.91
		44	85	36.6	41.8	147.01	4.02
		45	85	36.7	42.5	149.47	4.07
		46	85	36.8	43.2	151.93	4.13
		48	85	37.1	44.7	157.21	4.24
		50	85	37.4	46.2	162.49	4.34
		40	90	38.2	37.9	133.29	3.49
		42	90	38.4	39.2	137.87	3.59
		44	90	38.7	40.6	142.79	3.69
		45	90	38.8	41.4	145.60	3.75
		46	90	39	42.1	148.07	3.80
		48	90	39.2	43.5	152.99	3.90
		50	90	39.5	45	158.26	4.01
		40	95	40.5	36.7	129.07	3.19
		42	95	40.8	38.1	134.00	3.28
		44	95	41	39.4	138.57	3.38
		45	95	41.1	40.1	141.03	3.43
		46	95	41.3	40.8	143.49	3.47
		48	95	41.5	42.3	148.77	3.58
		50	95	41.8	43.7	153.69	3.68
York	46.2	40	75	38	47.7	167.76	4.41
		42	75	38.3	49.4	173.74	4.54
		44	75	38.7	51.2	180.07	4.65
		45	75	38.9	52	182.88	4.70
		46	75	39	52.9	186.05	4.77
		48	75	39.4	54.8	192.73	4.89
		50	75	39.8	56.6	199.06	5.00
		40	80	40.1	46.6	163.89	4.09
		42	80	40.4	48.3	169.87	4.20
		44	80	40.8	50	175.85	4.31
		45	80	40.9	50.8	178.66	4.37
		46	80	41.1	51.7	181.83	4.42
		48	80	41.5	53.5	188.16	4.53
		50	80	41.9	55.3	194.49	4.64
		40	85	42.3	45.5	160.02	3.78
		42	85	42.6	47.1	165.65	3.89
		44	85	43	48.8	171.63	3.99
		45	85	43.2	49.6	174.44	4.04

		46	85	43.3	50.5	177.61	4.10
		48	85	43.7	52.2	183.59	4.20
		50	85	44.1	54	189.92	4.31
		40	90	44.7	44.3	155.80	3.49
		42	90	45	45.9	161.43	3.59
		44	90	45.4	47.5	167.06	3.68
		45	90	45.5	48.3	169.87	3.73
		46	90	45.7	49.2	173.04	3.79
		48	90	46.1	50.9	179.02	3.88
		50	90	46.5	52.6	184.99	3.98
		40	95	47.2	43.1	151.58	3.21
		42	95	47.6	44.7	157.21	3.30
		44	95	47.9	46.2	162.49	3.39
		45	95	48.1	47	165.30	3.44
		46	95	48.3	47.8	168.11	3.48
		48	95	48.6	49.5	174.09	3.58
		50	95	49	51.1	179.72	3.67
York	56.2	40	75	48.2	58.2	204.69	4.25
		42	75	48.7	60.2	211.72	4.35
		44	75	49.2	62.3	219.11	4.45
		45	75	49.5	63.3	222.63	4.50
		46	75	49.7	64.4	226.49	4.56
		48	75	50.3	66.5	233.88	4.65
		50	75	50.9	68.6	241.27	4.74
		40	80	50.7	56.9	200.12	3.95
		42	80	51.2	58.9	207.15	4.05
		44	80	51.7	60.9	214.19	4.14
		45	80	52	61.9	217.70	4.19
		46	80	52.2	62.9	221.22	4.24
		48	80	52.8	65	228.60	4.33
		50	80	53.4	67.1	235.99	4.42
		40	85	53.3	55.5	195.19	3.66
		42	85	53.8	57.5	202.23	3.76
		44	85	54.4	59.4	208.91	3.84
		45	85	54.6	60.4	212.43	3.89
		46	85	54.9	61.4	215.94	3.93
		48	85	55.5	63.5	223.33	4.02
		50	85	56.1	65.5	230.36	4.11
		40	90	56.2	54.1	190.27	3.39

		42	90	56.7	55.9	196.60	3.47
		44	90	57.2	57.9	203.63	3.56
		45	90	57.5	58.8	206.80	3.60
		46	90	57.8	59.8	210.32	3.64
		48	90	58.3	61.8	217.35	3.73
		50	90	58.9	63.8	224.38	3.81
		40	95	59.3	52.5	184.64	3.11
		42	95	59.8	54.3	190.97	3.19
		44	95	60.3	56.2	197.66	3.28
		45	95	60.6	57.2	201.17	3.32
		46	95	60.9	58.1	204.34	3.36
		48	95	61.4	60	211.02	3.44
		50	95	62	62	218.05	3.52
York	66.1	40	75	58	68.6	241.27	4.16
		42	75	58.6	71	249.71	4.26
		44	75	59.2	73.5	258.50	4.37
		45	75	59.6	74.7	262.72	4.41
		46	75	59.9	76	267.29	4.46
		48	75	60.6	78.6	276.44	4.56
		50	75	61.3	81.1	285.23	4.65
		40	80	60.8	67	235.64	3.88
		42	80	61.5	69.3	243.73	3.96
		44	80	62.1	71.7	252.17	4.06
		45	80	62.4	73	256.74	4.11
		46	80	62.8	74.2	260.96	4.16
		48	80	63.5	76.7	269.75	4.25
		50	80	64.2	79.2	278.55	4.34
		40	85	63.9	65.3	229.66	3.59
		42	85	64.5	67.6	237.75	3.69
		44	85	65.2	69.9	245.84	3.77
		45	85	65.6	71.1	250.06	3.81
		46	85	65.9	72.3	254.28	3.86
		48	85	66.6	74.8	263.07	3.95
		50	85	67.4	77.3	271.86	4.03
		40	90	67.2	63.5	223.33	3.32
		42	90	67.9	65.8	231.42	3.41
		44	90	68.5	68.1	239.51	3.50
		45	90	68.9	69.2	243.38	3.53
		46	90	69.2	70.4	247.60	3.58

		48	90	70	72.8	256.04	3.66
		50	90	70.8	75.2	264.48	3.74
		40	95	70.8	61.7	217.00	3.06
		42	95	71.4	63.9	224.74	3.15
		44	95	72.1	66.1	232.47	3.22
		45	95	72.5	67.3	236.69	3.26
		46	95	72.8	68.4	240.56	3.30
		48	95	73.6	70.8	249.00	3.38
		50	95	74.3	73.1	257.09	3.46
York	71.8	40	75	59.9	69.3	243.73	4.07
		42	75	60.5	71.6	251.82	4.16
		44	75	61.1	73.9	259.91	4.25
		45	75	61.4	75	263.77	4.30
		46	75	61.8	76.2	268.00	4.34
		48	75	62.4	78.6	276.44	4.43
		50	75	63	81.1	285.23	4.53
		40	80	63.2	67.6	237.75	3.76
		42	80	63.8	69.8	245.49	3.85
		44	80	64.4	72	253.22	3.93
		45	80	64.7	73.1	257.09	3.97
		46	80	65	74.3	261.31	4.02
		48	80	65.7	76.6	269.40	4.10
		50	80	66.3	79	277.84	4.19
		40	85	66.7	65.7	231.07	3.46
		42	85	67.3	67.9	238.80	3.55
		44	85	68	70.1	246.54	3.63
		45	85	68.3	71.2	250.41	3.67
		46	85	68.6	72.3	254.28	3.71
		48	85	69.2	74.5	262.02	3.79
		50	85	69.9	76.8	270.11	3.86
		40	90	70.5	63.9	224.74	3.19
		42	90	71.1	65.9	231.77	3.26
		44	90	71.7	68.1	239.51	3.34
		45	90	72.1	69.1	243.02	3.37
		46	90	72.4	70.2	246.89	3.41
		48	90	73	72.4	254.63	3.49
		50	90	73.7	74.6	262.37	3.56
		40	95	74.5	61.9	217.70	2.92
		42	95	75.1	63.9	224.74	2.99

		44	95	75.8	66	232.12	3.06
		45	95	76.1	67	235.64	3.10
		46	95	76.4	68.1	239.51	3.13
		48	95	77.1	70.2	246.89	3.20
		50	95	77.7	72.4	254.63	3.28
York	77.7	40	75	66.3	76.8	270.11	4.07
		42	75	67	79.3	278.90	4.16
		44	75	67.7	81.8	287.69	4.25
		45	75	68.1	83.1	292.26	4.29
		46	75	68.4	84.4	296.83	4.34
		48	75	69.2	87	305.98	4.42
		50	75	70	89.7	315.47	4.51
		40	80	70	74.7	262.72	3.75
		42	80	70.7	77.2	271.51	3.84
		44	80	71.4	79.6	279.95	3.92
		45	80	71.7	80.9	284.53	3.97
		46	80	72.1	82.2	289.10	4.01
		48	80	72.9	84.7	297.89	4.09
		50	80	73.7	87.3	307.03	4.17
		40	85	74	72.6	255.33	3.45
		42	85	74.6	75	263.77	3.54
		44	85	75.4	77.4	272.22	3.61
		45	85	75.7	78.7	276.79	3.66
		46	85	76.1	79.9	281.01	3.69
		48	85	76.9	82.4	289.80	3.77
		50	85	77.7	84.9	298.59	3.84
		40	90	78.2	70.5	247.95	3.17
		42	90	78.9	72.8	256.04	3.25
		44	90	79.6	75.1	264.13	3.32
		45	90	80	76.3	268.35	3.35
		46	90	80.4	77.5	272.57	3.39
		48	90	81.2	79.9	281.01	3.46
		50	90	81.9	82.4	289.80	3.54
		40	95	82.8	68.2	239.86	2.90
		42	95	83.5	70.5	247.95	2.97
		44	95	84.2	72.8	256.04	3.04
		45	95	84.6	73.9	259.91	3.07
		46	95	84.9	75.1	264.13	3.11
		48	95	85.7	77.5	272.57	3.18

		50	95	86.5	79.9	281.01	3.25
York	85.8	40	75	76.9	91	320.05	4.16
		42	75	77.8	94	330.60	4.25
		44	75	78.7	96.9	340.80	4.33
		45	75	79.2	98.4	346.07	4.37
		46	75	79.7	100	351.70	4.41
		48	75	80.7	103	362.25	4.49
		50	75	81.8	106.1	373.15	4.56
		40	80	81	88.5	311.25	3.84
		42	80	82	91.4	321.45	3.92
		44	80	82.9	94.3	331.65	4.00
		45	80	83.4	95.7	336.58	4.04
		46	80	83.9	97.2	341.85	4.07
		48	80	84.9	100.2	352.40	4.15
		50	80	86	103.2	362.95	4.22
		40	85	85.5	85.9	302.11	3.53
		42	85	86.5	88.7	311.96	3.61
		44	85	87.4	91.5	321.81	3.68
		45	85	87.9	92.9	326.73	3.72
		46	85	88.5	94.4	332.00	3.75
		48	85	89.5	97.3	342.20	3.82
		50	85	90.6	100.2	352.40	3.89
		40	90	90.3	83.2	292.61	3.24
		42	90	91.3	85.9	302.11	3.31
		44	90	92.2	88.7	311.96	3.38
		45	90	92.7	90.1	316.88	3.42
		46	90	93.2	91.5	321.81	3.45
		48	90	94.3	94.3	331.65	3.52
		50	90	95.4	97.2	341.85	3.58
		40	95	95.4	80.4	282.77	2.96
		42	95	96.4	83.1	292.26	3.03
		44	95	97.3	85.8	301.76	3.10
		45	95	97.8	87.2	306.68	3.14
		46	95	98.3	88.6	311.61	3.17
		48	95	99.4	91.4	321.45	3.23
		50	95	100.4	94.2	331.30	3.30
York	95.8	40	75	87.5	101	355.22	4.06
		42	75	88.4	104.3	366.82	4.15
		44	75	89.3	107.6	378.43	4.24

		45	75	89.8	109.3	384.41	4.28
		46	75	90.3	111	390.39	4.32
		48	75	91.4	114.4	402.34	4.40
		50	75	92.5	117.9	414.65	4.48
		40	80	92.2	98.3	345.72	3.75
		42	80	93.2	101.5	356.98	3.83
		44	80	94.2	104.7	368.23	3.91
		45	80	94.7	106.4	374.21	3.95
		46	80	95.2	108	379.84	3.99
		48	80	96.2	111.4	391.79	4.07
		50	80	97.3	114.8	403.75	4.15
		40	85	97.4	95.6	336.23	3.45
		42	85	98.3	98.7	347.13	3.53
		44	85	99.3	101.8	358.03	3.61
		45	85	99.8	103.4	363.66	3.64
		46	85	100.3	105.1	369.64	3.69
		48	85	101.3	108.3	380.89	3.76
		50	85	102.4	111.7	392.85	3.84
		40	90	102.9	92.7	326.03	3.17
		42	90	103.8	95.8	336.93	3.25
		44	90	104.8	98.9	347.83	3.32
		45	90	105.3	100.4	353.11	3.35
		46	90	105.8	102	358.73	3.39
		48	90	106.9	105.2	369.99	3.46
		50	90	108	108.4	381.24	3.53
		40	95	108.8	89.8	315.83	2.90
		42	95	109.7	92.8	326.38	2.98
		44	95	110.7	95.8	336.93	3.04
		45	95	111.2	97.3	342.20	3.08
		46	95	111.7	98.8	347.48	3.11
		48	95	112.8	101.9	358.38	3.18
		50	95	113.9	105.1	369.64	3.25
York	113.9	40	75	104.1	120.1	422.39	4.06
		42	75	105.3	123.9	435.76	4.14
		44	75	106.5	127.9	449.82	4.22
		45	75	107.1	129.9	456.86	4.27
		46	75	107.7	131.8	463.54	4.30
		48	75	108.9	135.9	477.96	4.39
		50	75	110.2	140	492.38	4.47

		40	80	109.6	117	411.49	3.75
		42	80	110.9	120.7	424.50	3.83
		44	80	112.1	124.5	437.87	3.91
		45	80	112.7	126.5	444.90	3.95
		46	80	113.3	128.4	451.58	3.99
		48	80	114.6	132.3	465.30	4.06
		50	80	115.9	136.3	479.37	4.14
		40	85	115.6	113.7	399.88	3.46
		42	85	116.8	117.4	412.90	3.54
		44	85	118	121.1	425.91	3.61
		45	85	118.6	123	432.59	3.65
		46	85	119.3	124.9	439.27	3.68
		48	85	120.5	128.7	452.64	3.76
		50	85	121.9	132.6	466.35	3.83
		40	90	122	110.4	388.28	3.18
		42	90	123.2	113.9	400.59	3.25
		44	90	124.4	117.6	413.60	3.32
		45	90	125	119.4	419.93	3.36
		46	90	125.7	121.2	426.26	3.39
		48	90	127	124.9	439.27	3.46
		50	90	128.3	128.7	452.64	3.53
		40	95	128.7	106.9	375.97	2.92
		42	95	129.9	110.4	388.28	2.99
		44	95	131.1	113.9	400.59	3.06
		45	95	131.8	115.7	406.92	3.09
		46	95	132.4	117.5	413.25	3.12
		48	95	133.7	121.1	425.91	3.19
		50	95	135.1	124.8	438.92	3.25
York	119.7	40	75	106.1	126.7	445.60	4.20
		42	75	107.3	130.8	460.02	4.29
		44	75	108.6	135	474.79	4.37
		45	75	109.3	137.1	482.18	4.41
		46	75	110	139.2	489.57	4.45
		48	75	111.3	143.4	504.34	4.53
		50	75	112.7	147.7	519.46	4.61
		40	80	111.7	123.2	433.29	3.88
		42	80	112.9	127.2	447.36	3.96
		44	80	114.2	131.3	461.78	4.04
		45	80	114.9	133.3	468.82	4.08

		46	80	115.6	135.4	476.20	4.12
		48	80	117	139.5	490.62	4.19
		50	80	118.4	143.7	505.39	4.27
		40	85	117.5	119.7	420.98	3.58
		42	85	118.8	123.6	434.70	3.66
		44	85	120.1	127.5	448.42	3.73
		45	85	120.8	129.5	455.45	3.77
		46	85	121.5	131.5	462.49	3.81
		48	85	122.9	135.6	476.91	3.88
		50	85	124.5	139.6	490.97	3.94
		40	90	123.9	116	407.97	3.29
		42	90	125.2	119.8	421.34	3.37
		44	90	126.5	123.6	434.70	3.44
		45	90	127.2	125.6	441.74	3.47
		46	90	127.9	127.5	448.42	3.51
		48	90	129.3	131.4	462.13	3.57
		50	90	130.8	135.4	476.20	3.64
		40	95	130.5	112.3	394.96	3.03
		42	95	131.9	115.9	407.62	3.09
		44	95	133.2	119.7	420.98	3.16
		45	95	133.9	121.5	427.32	3.19
		46	95	134.6	123.4	434.00	3.22
		48	95	136	127.3	447.71	3.29
		50	95	137.5	131.1	461.08	3.35
York	127.3	40	75	112.1	133.9	470.93	4.20
		42	75	113.3	138.2	486.05	4.29
		44	75	114.5	142.7	501.88	4.38
		45	75	115.1	144.9	509.61	4.43
		46	75	115.8	147.2	517.70	4.47
		48	75	117.1	151.8	533.88	4.56
		50	75	118.4	156.4	550.06	4.65
		40	80	118.1	130.4	458.62	3.88
		42	80	119.3	134.6	473.39	3.97
		44	80	120.5	139	488.86	4.06
		45	80	121.1	141.2	496.60	4.10
		46	80	121.8	143.4	504.34	4.14
		48	80	123.1	147.8	519.81	4.22
		50	80	124.5	152.4	535.99	4.31
		40	85	124.4	126.8	445.96	3.58

		42	85	125.6	131	460.73	3.67
		44	85	126.9	135.2	475.50	3.75
		45	85	127.5	137.3	482.88	3.79
		46	85	128.2	139.5	490.62	3.83
		48	85	129.5	143.9	506.10	3.91
		50	85	131	148.2	521.22	3.98
		40	90	131.3	123.1	432.94	3.30
		42	90	132.5	127.2	447.36	3.38
		44	90	133.8	131.3	461.78	3.45
		45	90	134.4	133.4	469.17	3.49
		46	90	135.1	135.5	476.55	3.53
		48	90	136.4	139.7	491.32	3.60
		50	90	137.8	144	506.45	3.68
		40	95	138.6	119.3	419.58	3.03
		42	95	139.8	123.2	433.29	3.10
		44	95	141.1	127.3	447.71	3.17
		45	95	141.7	129.3	454.75	3.21
		46	95	142.3	131.3	461.78	3.25
		48	95	143.7	135.5	476.55	3.32
		50	95	145.1	139.7	491.32	3.39
York	140.4	40	75	128.1	147.8	519.81	4.06
		42	75	129.5	152.6	536.69	4.14
		44	75	130.9	157.4	553.58	4.23
		45	75	131.6	159.9	562.37	4.27
		46	75	132.3	162.4	571.16	4.32
		48	75	133.8	167.3	588.39	4.40
		50	75	135.4	172.4	606.33	4.48
		40	80	135	144	506.45	3.75
		42	80	136.4	148.6	522.63	3.83
		44	80	137.8	153.3	539.16	3.91
		45	80	138.5	155.7	547.60	3.95
		46	80	139.3	158.1	556.04	3.99
		48	80	140.8	163	573.27	4.07
		50	80	142.4	167.9	590.50	4.15
		40	85	142.3	140	492.38	3.46
		42	85	143.7	144.6	508.56	3.54
		44	85	145.1	149.2	524.74	3.62
		45	85	145.9	151.5	532.83	3.65
		46	85	146.6	153.8	540.91	3.69

		48	85	148.2	158.5	557.44	3.76
		50	85	149.8	163.3	574.33	3.83
		40	90	150.1	135.9	477.96	3.18
		42	90	151.5	140.3	493.43	3.26
		44	90	153	144.8	509.26	3.33
		45	90	153.7	147.1	517.35	3.37
		46	90	154.5	149.4	525.44	3.40
		48	90	156	154	541.62	3.47
		50	90	157.7	158.6	557.80	3.54
		40	95	158.4	131.7	463.19	2.92
		42	95	159.8	136	478.31	2.99
		44	95	161.3	140.4	493.79	3.06
		45	95	162	142.6	501.52	3.10
		46	95	162.8	144.8	509.26	3.13
		48	95	164.4	149.2	524.74	3.19
		50	95	166	153.8	540.91	3.26
York	143.1	40	75	129.4	151.2	531.77	4.11
		42	75	130.8	156.1	549.00	4.20
		44	75	132.3	161.1	566.59	4.28
		45	75	133	163.6	575.38	4.33
		46	75	133.8	166.1	584.17	4.37
		48	75	135.3	171.2	602.11	4.45
		50	75	136	172.7	607.39	4.47
		40	80	136.2	147.2	517.70	3.80
		42	80	137.7	152	534.58	3.88
		44	80	139.2	156.8	551.47	3.96
		45	80	139.9	159.3	560.26	4.00
		46	80	140.7	161.7	568.70	4.04
		48	80	142.3	166.7	586.28	4.12
		50	80	143.9	171.7	603.87	4.20
		40	85	143.5	143.1	503.28	3.51
		42	85	144.9	147.7	519.46	3.58
		44	85	146.5	152.5	536.34	3.66
		45	85	147.2	154.8	544.43	3.70
		46	85	148	157.2	552.87	3.74
		48	85	149.7	162	569.75	3.81
		50	85	151.4	166.9	586.99	3.88
		40	90	151.3	138.8	488.16	3.23
		42	90	152.8	143.3	503.99	3.30

		44	90	154.3	147.9	520.16	3.37
		45	90	155.1	150.2	528.25	3.41
		46	90	155.9	152.6	536.69	3.44
		48	90	157.5	157.3	553.22	3.51
		50	90	159.2	162	569.75	3.58
		40	95	159.5	134.4	472.68	2.96
		42	95	161	138.8	488.16	3.03
		44	95	162.5	143.3	503.99	3.10
		45	95	163.3	145.5	511.72	3.13
		46	95	164.1	147.8	519.81	3.17
		48	95	165.8	152.4	535.99	3.23
		50	95	167.5	157	552.17	3.30
York	167.9	40	75	148.9	176.1	619.34	4.16
		42	75	150.5	181.8	639.39	4.25
		44	75	152.1	187.5	659.44	4.34
		45	75	152.9	190.5	669.99	4.38
		46	75	153.7	193.4	680.19	4.43
		48	75	155.3	199.3	700.94	4.51
		50	75	157	205.4	722.39	4.60
		40	80	157	171.7	603.87	3.85
		42	80	158.5	177.3	623.56	3.93
		44	80	160	182.9	643.26	4.02
		45	80	160.8	185.8	653.46	4.06
		46	80	161.7	188.7	663.66	4.10
		48	80	163.3	194.5	684.06	4.19
		50	80	165	200.4	704.81	4.27
		40	85	165.6	167.1	587.69	3.55
		42	85	167.1	172.6	607.03	3.63
		44	85	168.7	178.1	626.38	3.71
		45	85	169.5	180.9	636.23	3.75
		46	85	170.3	183.7	646.07	3.79
		48	85	172	189.3	665.77	3.87
		50	85	173.7	195.1	686.17	3.95
		40	90	174.7	162.4	571.16	3.27
		42	90	176.3	167.7	589.80	3.35
		44	90	177.9	173	608.44	3.42
		45	90	178.7	175.8	618.29	3.46
		46	90	179.6	178.5	627.78	3.50
		48	90	181.3	184	647.13	3.57

		50	90	183.1	189.6	666.82	3.64
		40	95	184.5	157.5	553.93	3.00
		42	95	186.1	162.6	571.86	3.07
		44	95	187.7	167.8	590.15	3.14
		45	95	188.6	170.5	599.65	3.18
		46	95	189.4	173.1	608.79	3.21
		48	95	191.2	178.5	627.78	3.28
		50	95	192.9	184	647.13	3.35
Trane	20	40	75	17.5	18	63.31	3.62
		42	75	17.7	18.7	65.77	3.72
		44	75	17.9	19.4	68.23	3.81
		45	75	18	19.7	69.28	3.85
		46	75	18.1	20.1	70.69	3.91
		48	75	18.2	20.8	73.15	4.02
		50	75	18.4	21.5	75.62	4.11
		40	85	19.3	17.2	60.49	3.13
		42	85	19.5	17.8	62.60	3.21
		44	85	19.6	18.5	65.06	3.32
		45	85	19.7	18.8	66.12	3.36
		46	85	19.8	19.1	67.17	3.39
		48	85	20.1	19.8	69.64	3.46
		50	85	20.3	20.5	72.10	3.55
		40	95	21.3	16.2	56.98	2.67
		42	95	21.5	16.9	59.44	2.76
		44	95	21.7	17.5	61.55	2.84
		45	95	21.8	17.8	62.60	2.87
		46	95	21.9	18.1	63.66	2.91
		48	95	22.1	18.7	65.77	2.98
		50	95	22.3	19.4	68.23	3.06
		40	105	23.6	15.3	53.81	2.28
		42	105	23.8	15.9	55.92	2.35
		44	105	24	16.4	57.68	2.40
		45	105	24.1	16.7	58.73	2.44
		46	105	24.2	17	59.79	2.47
		48	105	24.5	17.6	61.90	2.53
		50	105	24.7	18.3	64.36	2.61
		40	115	26.1	14.2	49.94	1.91
		42	115	26.4	14.8	52.05	1.97
		44	115	26.6	15.4	54.16	2.04

		45	115	26.7	15.6	54.87	2.05
		46	115	26.8	15.9	55.92	2.09
		48	115	27.1	16.5	58.03	2.14
		50	115	27.3	17.1	60.14	2.20
Trane	25	40	75	23.5	23.9	84.06	3.58
		42	75	23.8	24.8	87.22	3.66
		44	75	24	25.7	90.39	3.77
		45	75	24.1	26.2	92.15	3.82
		46	75	24.2	26.7	93.90	3.88
		48	75	24.5	27.6	97.07	3.96
		50	75	24.7	28.6	100.59	4.07
		40	85	25.7	22.8	80.19	3.12
		42	85	25.9	23.6	83.00	3.20
		44	85	26.2	24.5	86.17	3.29
		45	85	26.3	24.9	87.57	3.33
		46	85	26.4	25.4	89.33	3.38
		48	85	26.7	26.3	92.50	3.46
		50	85	27	27.2	95.66	3.54
		40	95	28.2	21.6	75.97	2.69
		42	95	28.4	22.4	78.78	2.77
		44	95	28.7	23.2	81.59	2.84
		45	95	28.8	23.6	83.00	2.88
		46	95	29	24.1	84.76	2.92
		48	95	29.2	24.9	87.57	3.00
		50	95	29.5	25.8	90.74	3.08
		40	105	31	20.3	71.40	2.30
		42	105	31.3	21.1	74.21	2.37
		44	105	31.5	21.9	77.02	2.45
		45	105	31.7	22.3	78.43	2.47
		46	105	31.8	22.7	79.84	2.51
		48	105	32.1	23.5	82.65	2.57
		50	105	32.4	24.4	85.81	2.65
		40	115	34.1	19	66.82	1.96
		42	115	34.4	19.8	69.64	2.02
		44	115	34.7	20.5	72.10	2.08
		45	115	34.9	20.9	73.51	2.11
		46	115	35	21.3	74.91	2.14
		48	115	35.3	22.1	77.73	2.20
		50	115	35.6	22.9	80.54	2.26

Trane	30	40	75	28.1	28.5	100.23	3.57
		42	75	28.3	29.6	104.10	3.68
		44	75	28.5	30.7	107.97	3.79
		45	75	28.6	31.2	109.73	3.84
		46	75	28.8	31.8	111.84	3.88
		48	75	29	32.9	115.71	3.99
		50	75	29.2	34	119.58	4.10
		40	85	30.7	27.1	95.31	3.10
		42	85	30.9	28.2	99.18	3.21
		44	85	31.2	29.2	102.70	3.29
		45	85	31.3	29.7	104.45	3.34
		46	85	31.4	30.3	106.57	3.39
		48	85	31.7	31.3	110.08	3.47
		50	85	31.9	32.4	113.95	3.57
		40	95	33.6	25.7	90.39	2.69
		42	95	33.9	26.7	93.90	2.77
		44	95	34.2	27.7	97.42	2.85
		45	95	34.3	28.2	99.18	2.89
		46	95	34.5	28.7	100.94	2.93
		48	95	34.7	29.7	104.45	3.01
		50	95	35	30.8	108.32	3.09
		40	105	37	24.2	85.11	2.30
		42	105	37.3	25.1	88.28	2.37
		44	105	37.6	26.1	91.79	2.44
		45	105	37.8	26.6	93.55	2.47
		46	105	37.9	27.1	95.31	2.51
		48	105	38.2	28	98.48	2.58
		50	105	38.5	29	101.99	2.65
		40	115	40.8	22.7	79.84	1.96
		42	115	41.1	23.6	83.00	2.02
		44	115	41.4	24.5	86.17	2.08
		45	115	41.6	24.9	87.57	2.11
		46	115	41.7	25.4	89.33	2.14
		48	115	42.1	26.3	92.50	2.20
		50	115	42.4	27.3	96.01	2.26
Trane	40	40	75	34.1	35.3	124.15	3.64
		42	75	34.4	36.6	128.72	3.74
		44	75	34.8	37.9	133.29	3.83
		45	75	35	38.5	135.40	3.87

		46	75	35.1	39.2	137.87	3.93
		48	75	35.5	40.6	142.79	4.02
		50	75	35.9	42	147.71	4.11
		40	85	37.5	33.5	117.82	3.14
		42	85	37.9	34.8	122.39	3.23
		44	85	38.3	36	126.61	3.31
		45	85	38.4	36.7	129.07	3.36
		46	85	38.6	37.3	131.18	3.40
		48	85	39	38.6	135.76	3.48
		50	85	39.4	39.9	140.33	3.56
		40	95	41.5	31.7	111.49	2.69
		42	95	41.9	32.9	115.71	2.76
		44	95	42.3	34.1	119.93	2.84
		45	95	42.5	34.7	122.04	2.87
		46	95	42.7	35.3	124.15	2.91
		48	95	43.1	36.6	128.72	2.99
		50	95	43.5	37.8	132.94	3.06
		40	105	46	29.8	104.81	2.28
		42	105	46.4	30.9	108.68	2.34
		44	105	46.8	32.1	112.90	2.41
		45	105	47	32.7	115.01	2.45
		46	105	47.2	33.2	116.76	2.47
		48	105	47.7	34.4	120.98	2.54
		50	105	48.1	35.6	125.21	2.60
		40	115	51	27.8	97.77	1.92
		42	115	51.5	28.9	101.64	1.97
		44	115	51.9	29.9	105.16	2.03
		45	115	52.1	30.5	107.27	2.06
		46	115	52.3	31	109.03	2.08
		48	115	52.8	32.1	112.90	2.14
		50	115	53.2	33.3	117.12	2.20
Trane	50	40	75	43.3	44.1	155.10	3.58
		42	75	43.7	45.7	160.73	3.68
		44	75	44.1	47.4	166.71	3.78
		45	75	44.3	48.3	169.87	3.83
		46	75	44.5	49.2	173.04	3.89
		48	75	44.9	50.9	179.02	3.99
		50	75	45.3	52.7	185.35	4.09
		40	85	47.3	41.9	147.36	3.12

		42	85	47.7	43.5	152.99	3.21
		44	85	48.1	45.1	158.62	3.30
		45	85	48.4	45.9	161.43	3.34
		46	85	48.6	46.8	164.60	3.39
		48	85	49	48.4	170.22	3.47
		50	85	49.5	50.1	176.20	3.56
		40	95	51.9	39.7	139.62	2.69
		42	95	52.4	41.2	144.90	2.77
		44	95	52.8	42.7	150.18	2.84
		45	95	53.1	43.5	152.99	2.88
		46	95	53.3	44.3	155.80	2.92
		48	95	53.8	45.9	161.43	3.00
		50	95	54.3	47.5	167.06	3.08
		40	105	57.1	37.4	131.54	2.30
		42	105	57.6	38.8	136.46	2.37
		44	105	58.1	40.3	141.74	2.44
		45	105	58.4	41	144.20	2.47
		46	105	58.6	41.8	147.01	2.51
		48	105	59.1	43.3	152.29	2.58
		50	105	59.7	44.9	157.91	2.65
		40	115	63	35	123.09	1.95
		42	115	63.5	36.4	128.02	2.02
		44	115	64	37.8	132.94	2.08
		45	115	64.3	38.5	135.40	2.11
		46	115	64.6	39.2	137.87	2.13
		48	115	65.1	40.6	142.79	2.19
		50	115	65.7	42.1	148.07	2.25
Trane	60	40	75	56.6	58.5	205.74	3.64
		42	75	57.2	60.5	212.78	3.72
		44	75	57.8	62.6	220.16	3.81
		45	75	58.1	63.7	224.03	3.86
		46	75	58.4	64.7	227.55	3.90
		48	75	59	66.9	235.29	3.99
		50	75	59.6	69.1	243.02	4.08
		40	85	62.2	55.6	195.55	3.14
		42	85	62.8	57.5	202.23	3.22
		44	85	63.4	59.5	209.26	3.30
		45	85	63.8	60.5	212.78	3.34
		46	85	64.1	61.6	216.65	3.38

48	85	64.8	63.6	223.68	3.45
50	85	65.4	65.7	231.07	3.53
40	95	68.5	52.6	184.99	2.70
42	95	69.1	54.4	191.32	2.77
44	95	69.8	56.4	198.36	2.84
45	95	70.2	57.3	201.52	2.87
46	95	70.5	58.3	205.04	2.91
48	95	71.3	60.3	212.08	2.97
50	95	72	62.3	219.11	3.04
40	105	75.5	49.5	174.09	2.31
42	105	76.3	51.2	180.07	2.36
44	105	77	53.1	186.75	2.43
45	105	77.4	54	189.92	2.45
46	105	77.8	54.9	193.08	2.48
48	105	78.6	56.8	199.77	2.54
50	105	79.3	58.7	206.45	2.60
40	115	83.4	46.2	162.49	1.95
42	115	84.2	48	168.82	2.00
44	115	85	49.7	174.79	2.06
45	115	85.4	50.6	177.96	2.08
46	115	85.8	51.4	180.77	2.11
48	115	86.6	53.2	187.10	2.16
50	115	87.5	55	193.43	2.21

APPENDIX B

Collection of manufacturers' part-load data used to model air-cooled scroll chillers.

Reference Capacity (tons)	Tcond,in (°F)	Tevap,out (°F)	PLR	EER	COP
15.4	70.2	44	1		4.36
	70.2	44	0.5	16	4.688
	70.2	44	0		0
18.7	72.1	44	1		4.20
	72.1	44	0.5	16.9	4.9517
	72.1	44	0		0
28.6	70	44	1		4.57
	70	44	0.5	15.7	4.6001
	70	44	0		0
37.2	55	44	1		6.08
	55	44	0.25	17.3	5.0689
	55	44	0		0
39.4	55	44	1		6.09
	55	44	0.25	17.5	5.1275
	55	44	0		0
46.2	55	44	1		5.94
	55	44	0.25	19.1	5.5963
	55	44	0		0
56.2	55	44	1		5.57
	55	44	0.25	18.1	5.3033
	55	44	0		0
66.1	82.6	44	1		3.70
	82.6	44	0.75	12.9	3.7797
	82.6	44	0		0
	69.3	44	1		4.36
	69.3	44	0.5	15.2	4.4536
	69.3	44	0		0
71.8	71.1	44	1		4.42
	71.1	44	0.5	15.6	4.5708
	71.1	44	0		0
77.7	71.1	44	1		4.35
	71.1	44	0.503	15.2	4.4536

	71.1	44	0		0
85.8	88.1	44	1		3.37
	88.1	44	0.836	11.5	3.3695
	88.1	44	0		0
	69.3	44	1		4.30
	69.3	44	0.493	16	4.688
	69.3	44	0		0
95.8	75.6	44	1		3.86
	75.6	44	0.57	14.4	4.2192
	75.6	44	0		0
	65.1	44	1		4.51
	65.1	44	0.43	14.5	4.2485
	65.1	44	0		0
113.9	84.3	44	1		3.46
	84.3	44	0.75	12	3.516
	84.3	44	0		0
	72	44	1		4.05
	72	44	0.5	15.3	4.4829
	72	44	0		0
	55	44	1		5.29
	55	44	0.25	16.3	4.7759
	55	44	0		0
119.7	83.9	44	1		3.59
	83.9	44	0.75	12.4	3.6332
	83.9	44	0		0
	70.8	44	1		4.24
	70.8	44	0.5	15.6	4.5708
	70.8	44	0		0
	55	44	1		5.44
	55	44	0.25	16.3	4.7759
	55	44	0		0
127.3	81.3	44	1		3.73
	81.3	44	0.75	13.2	3.8676
	81.3	44	0		0
	67.8	44	1		4.47
	67.8	44	0.5	16.3	4.7759
	67.8	44	0		0
140.4	87.7	44	1		3.33
	87.7	44	0.8	11.7	3.4281

	87.7	44	0		0
	77.1	44	1		3.79
	77.1	44	0.6	13.7	4.0141
	77.1	44	0		0
143.3	87.5	44	1		3.38
	87.5	44	0.8	11.9	3.4867
	87.5	44	0		0
	76.6	44	1		3.85
	76.6	44	0.6	13.8	4.0434
	76.6	44	0		0
167.8	71.3	44	1		4.22
	71.3	44	0.5	15.2	4.4536
	71.3	44	0		0

APPENDIX C

Collection of manufacturers' full-load data used to model air-cooled screw chillers.

	Reference Capacity (tons)	Tevap,out (°F)	Tcond,in (°F)	Power in (kW)	Capacity (tons)	Capacity (kW)	COP
Trane	69.2	40	75	58.6	72.5	254.98	4.35
		42	75	59.4	75	263.77	4.44
		44	75	60.2	77.5	272.57	4.53
		46	75	61.1	80.1	281.71	4.61
		48	75	61.9	82.7	290.86	4.70
		50	75	62.8	85.3	300.00	4.78
		55	75	64.9	92.1	323.92	4.99
		40	85	64.3	68.6	241.27	3.75
		42	85	65.1	71	249.71	3.84
		44	85	66	73.4	258.15	3.91
		46	85	66.8	75.9	266.94	4.00
		48	85	67.6	78.4	275.73	4.08
		50	85	68.5	81	284.88	4.16
		55	85	70.6	87.5	307.74	4.36
		40	95	70.8	64.6	227.20	3.21
		42	95	71.6	66.9	235.29	3.29
		44	95	72.4	69.2	243.38	3.36
		46	95	73.2	71.6	251.82	3.44
		48	95	74.1	74	260.26	3.51
		50	95	75	76.4	268.70	3.58
		55	95	77.2	82.7	290.86	3.77
		40	105	77.9	60.4	212.43	2.73
		42	105	78.8	62.6	220.16	2.79
		44	105	79.6	64.8	227.90	2.86
		46	105	80.5	67.1	235.99	2.93
		48	105	81.4	69.4	244.08	3.00
		50	105	82.3	71.7	252.17	3.06
		55	105	84.7	77.7	273.27	3.23
		40	115	85.8	56	196.95	2.30
		42	115	86.7	58.1	204.34	2.36
		44	115	87.6	60.3	212.08	2.42
		46	115	88.5	62.5	219.81	2.48
		48	115	89.5	64.7	227.55	2.54

		50	115	90.5	66.9	235.29	2.60
		55	115	91.5	69.1	243.02	2.66
Trane	79.7	40	75	68.9	82.9	291.56	4.23
		42	75	70.1	85.9	302.11	4.31
		44	75	71.3	88.9	312.66	4.39
		46	75	72.5	91.9	323.21	4.46
		48	75	73.8	95	334.11	4.53
		50	75	75	98.2	345.37	4.60
		55	75	78.3	106.3	373.86	4.77
		40	85	75.6	78.7	276.79	3.66
		42	85	76.8	81.5	286.64	3.73
		44	85	77.9	84.4	296.83	3.81
		46	85	79.2	87.3	307.03	3.88
		48	85	80.4	90.3	317.58	3.95
		50	85	81.7	93.3	328.14	4.02
		55	85	84.9	101.1	355.57	4.19
		40	95	83.1	74.3	261.31	3.14
		42	95	84.2	77	270.81	3.22
		44	95	85.4	79.7	280.30	3.28
		46	95	86.6	82.5	290.15	3.35
		48	95	87.9	85.3	300.00	3.41
		50	95	89.1	88.2	310.20	3.48
		55	95	92.4	95.6	336.23	3.64
		40	105	91.3	69.7	245.13	2.68
		42	105	92.5	72.2	253.93	2.75
		44	105	93.7	74.8	263.07	2.81
		46	105	94.9	77.5	272.57	2.87
		48	105	96.2	80.1	281.71	2.93
		50	105	97.4	82.9	291.56	2.99
		55	105	100.7	89.9	316.18	3.14
		40	115	100.4	64.9	228.25	2.27
		42	115	101.6	67.3	236.69	2.33
		44	115	102.8	69.8	245.49	2.39
		46	115	104	72.3	254.28	2.44
		48	115	105.3	74.8	263.07	2.50
		50	115	106.6	77.4	272.22	2.55
		55	115	109.9	84	295.43	2.69
Trane	90.6	40	75	81.8	94.5	332.36	4.06
		42	75	83.2	97.8	343.96	4.13

		44	75	84.7	101.1	355.57	4.20
		46	75	86.1	104.4	367.17	4.26
		48	75	87.6	107.9	379.48	4.33
		50	75	89.2	111.3	391.44	4.39
		55	75	93.1	120.3	423.09	4.54
		40	85	88.9	89.8	315.83	3.55
		42	85	90.3	92.8	326.38	3.61
		44	85	91.7	96	337.63	3.68
		46	85	93.1	99.2	348.89	3.75
		48	85	94.6	102.5	360.49	3.81
		50	85	96.1	105.8	372.10	3.87
		55	85	100	114.3	401.99	4.02
		40	95	97	84.7	297.89	3.07
		42	95	98.3	87.6	308.09	3.13
		44	95	99.7	90.6	318.64	3.20
		46	95	101.2	93.6	329.19	3.25
		48	95	102.7	96.7	340.09	3.31
		50	95	104.2	99.9	351.35	3.37
		55	95	108	108	379.84	3.52
		40	105	106.1	79.3	278.90	2.63
		42	105	107.5	82.1	288.75	2.69
		44	105	108.9	85	298.94	2.75
		46	105	110.3	87.8	308.79	2.80
		48	105	111.8	90.8	319.34	2.86
		50	105	113.3	93.7	329.54	2.91
		55	105	117.2	101.4	356.62	3.04
		40	115	116.4	73.8	259.55	2.23
		42	115	117.7	76.4	268.70	2.28
		44	115	119.2	79.1	278.19	2.33
		46	115	120.6	81.8	287.69	2.39
		48	115	122.1	84.5	297.19	2.43
		50	115	123.6	87.3	307.03	2.48
		55	115	124	91.8	322.86	2.60
Trane	100.6	40	75	94.3	105.1	369.64	3.92
		42	75	95.9	108.6	381.95	3.98
		44	75	97.6	112.2	394.61	4.04
		46	75	99.3	115.9	407.62	4.10
		48	75	101	119.6	420.63	4.16
		50	75	102.8	123.4	434.00	4.22

		55	75	107.5	133.1	468.11	4.35
		40	85	101.8	99.9	351.35	3.45
		42	85	103.4	103.2	362.95	3.51
		44	85	105	106.6	374.91	3.57
		46	85	106.6	110.1	387.22	3.63
		48	85	108.3	113.6	399.53	3.69
		50	85	110.1	117.2	412.19	3.74
		55	85	114.7	126.4	444.55	3.88
		40	95	110.5	94.2	331.30	3.00
		42	95	112.1	97.4	342.56	3.06
		44	95	113.7	100.6	353.81	3.11
		46	95	115.3	103.9	365.42	3.17
		48	95	117	107.2	377.02	3.22
		50	95	118.7	110.6	388.98	3.28
		55	95	123.2	119.4	419.93	3.41
		40	105	120.6	88.2	310.20	2.57
		42	105	122.1	91.2	320.75	2.63
		44	105	123.7	94.3	331.65	2.68
		46	105	125.3	97.4	342.56	2.73
		48	105	127	100.5	353.46	2.78
		50	105	128.7	103.7	364.71	2.83
		55	105	133.1	111.9	393.55	2.96
		40	115	131.9	81.9	288.04	2.18
		42	115	133.5	84.7	297.89	2.23
		44	115	135.1	87.6	308.09	2.28
		46	115	136.8	90.5	318.29	2.33
		48	115	138.4	93.5	328.84	2.38
		50	115	140.1	96.5	339.39	2.42
		55	115	138	99	348.18	2.52
Trane	108.3	40	75	102.5	113.2	398.12	3.88
		42	75	104.2	116.9	411.14	3.95
		44	75	106	120.7	424.50	4.00
		46	75	107.9	124.6	438.22	4.06
		48	75	109.7	128.6	452.29	4.12
		50	75	111.7	132.6	466.35	4.18
		55	75	116.7	142.9	502.58	4.31
		40	85	110.7	107.6	378.43	3.42
		42	85	112.4	111.1	390.74	3.48
		44	85	114.1	114.7	403.40	3.54

		46	85	115.9	118.4	416.41	3.59
		48	85	117.8	122.2	429.78	3.65
		50	85	119.7	126	443.14	3.70
		55	85	124.6	135.9	477.96	3.84
		40	95	120.2	101.5	356.98	2.97
		42	95	121.9	104.9	368.93	3.03
		44	95	123.7	108.3	380.89	3.08
		46	95	125.4	111.9	393.55	3.14
		48	95	127.3	115.4	405.86	3.19
		50	95	129.2	119.1	418.87	3.24
		55	95	134	128.4	451.58	3.37
		40	105	131.2	95.1	334.47	2.55
		42	105	132.9	98.3	345.72	2.60
		44	105	134.6	101.6	357.33	2.65
		46	105	136.4	104.9	368.93	2.70
		48	105	138.2	108.3	380.89	2.76
		50	105	140.1	111.7	392.85	2.80
		55	105	144.9	120.4	423.45	2.92
		40	115	143.6	88.3	310.55	2.16
		42	115	145.3	91.3	321.10	2.21
		44	115	147.1	94.4	332.00	2.26
		46	115	148.9	97.6	343.26	2.31
		48	115	150.5	100.5	353.46	2.35
		50	115	150.3	102.3	359.79	2.39
		55	115	147.4	105	369.28	2.51
Trane	119.6	40	75	113	125.2	440.33	3.90
		42	75	115	129.4	455.10	3.96
		44	75	117.1	133.6	469.87	4.01
		46	75	119.1	138	485.35	4.08
		48	75	121.3	142.4	500.82	4.13
		50	75	123.5	146.8	516.30	4.18
		55	75	129.2	158.4	557.09	4.31
		40	85	121.9	118.9	418.17	3.43
		42	85	123.8	122.8	431.89	3.49
		44	85	125.8	126.8	445.96	3.54
		46	85	127.9	130.9	460.38	3.60
		48	85	130	135.1	475.15	3.65
		50	85	132.1	139.4	490.27	3.71
		55	85	137.8	150.3	528.60	3.84

		40	95	132.2	112	393.90	2.98
		42	95	134.1	115.8	407.27	3.04
		44	95	136.1	119.6	420.63	3.09
		46	95	138.1	123.5	434.35	3.15
		48	95	140.2	127.5	448.42	3.20
		50	95	142.4	131.5	462.49	3.25
		55	95	147.9	141.7	498.36	3.37
		40	105	144	104.8	368.58	2.56
		42	105	145.9	108.4	381.24	2.61
		44	105	147.9	112	393.90	2.66
		46	105	150	115.6	406.57	2.71
		48	105	152	119.4	419.93	2.76
		50	105	154.2	123.1	432.94	2.81
		55	105	159.6	132.7	466.71	2.92
		40	115	157.4	97.2	341.85	2.17
		42	115	159.4	100.5	353.46	2.22
		44	115	161.4	103.9	365.42	2.26
		46	115	162	106.3	373.86	2.31
		48	115	160.6	107.1	376.67	2.35
		50	115	158.4	107.6	378.43	2.39
		55	115	152.6	109.4	384.76	2.52
Trane	132.2	40	75	122.5	138.3	486.40	3.97
		42	75	124.5	143.2	503.63	4.05
		44	75	126.6	148.2	521.22	4.12
		46	75	128.8	153.2	538.80	4.18
		48	75	131	158.4	557.09	4.25
		50	75	133.3	163.6	575.38	4.32
		55	75	139.3	177.1	622.86	4.47
		40	85	135	131	460.73	3.41
		42	85	137.2	135.6	476.91	3.48
		44	85	139.4	140.4	493.79	3.54
		46	85	141.6	145.2	510.67	3.61
		48	85	143.9	150.1	527.90	3.67
		50	85	146.3	155.1	545.49	3.73
		55	85	152.5	168	590.86	3.87
		40	95	149.6	123.3	433.65	2.90
		42	95	151.8	127.7	449.12	2.96
		44	95	154	132.2	464.95	3.02
		46	95	156.4	136.7	480.77	3.07

		48	95	158.8	141.4	497.30	3.13
		50	95	161.2	146.1	513.83	3.19
		55	95	167.7	158.3	556.74	3.32
		40	105	166.1	115.3	405.51	2.44
		42	105	168.4	119.4	419.93	2.49
		44	105	170.7	123.6	434.70	2.55
		46	105	173.1	127.9	449.82	2.60
		48	105	175.6	132.3	465.30	2.65
		50	105	178.1	136.7	480.77	2.70
		55	105	184.8	148.1	520.87	2.82
		40	115	184.7	107	376.32	2.04
		42	115	187	110.8	389.68	2.08
		44	115	189.4	114.7	403.40	2.13
		46	115	191.9	118.7	417.47	2.18
		48	115	194.4	122.7	431.54	2.22
		50	115	193.5	125.2	440.33	2.28
		55	115	183.9	127.8	449.47	2.44
Trane	142.6	40	75	132.4	149.6	526.14	3.97
		42	75	134.6	154.8	544.43	4.04
		44	75	137	160.1	563.07	4.11
		46	75	139.4	165.5	582.06	4.18
		48	75	141.8	171	601.41	4.24
		50	75	144.4	176.6	621.10	4.30
		55	75	151	191	671.75	4.45
		40	85	146	141.5	497.66	3.41
		42	85	148.4	146.5	515.24	3.47
		44	85	150.8	151.5	532.83	3.53
		46	85	153.3	156.7	551.11	3.60
		48	85	155.8	161.9	569.40	3.65
		50	85	158.5	167.2	588.04	3.71
		55	85	165.4	180.9	636.23	3.85
		40	95	161.7	133.1	468.11	2.89
		42	95	164.2	137.8	484.64	2.95
		44	95	166.7	142.6	501.52	3.01
		46	95	169.3	147.4	518.41	3.06
		48	95	171.9	152.3	535.64	3.12
		50	95	174.6	157.4	553.58	3.17
		55	95	181.8	170.2	598.59	3.29
		40	105	179.5	124.4	437.51	2.44

		42	105	182.1	128.7	452.64	2.49
		44	105	184.7	133.2	468.46	2.54
		46	105	187.3	137.7	484.29	2.59
		48	105	190.1	142.3	500.47	2.63
		50	105	192.9	147	517.00	2.68
		55	105	200.3	159.1	559.55	2.79
		40	115	199.5	115.3	405.51	2.03
		42	115	202.1	119.3	419.58	2.08
		44	115	201.1	121.8	428.37	2.13
		46	115	200	124.2	436.81	2.18
		48	115	195	124.9	439.27	2.25
		50	115	190.3	125.6	441.74	2.32
		55	115	181.4	128.8	452.99	2.50
Trane	151	40	75	141.1	156.7	551.11	3.91
		42	75	143.5	162.6	571.86	3.99
		44	75	146	168.5	592.61	4.06
		46	75	148.5	174.5	613.72	4.13
		48	75	151.1	180.7	635.52	4.21
		50	75	153.8	186.9	657.33	4.27
		55	75	160.7	203	713.95	4.44
		40	85	155.9	148.8	523.33	3.36
		42	85	158.4	154.5	543.38	3.43
		44	85	161	160	562.72	3.50
		46	85	163.6	165.8	583.12	3.56
		48	85	166.3	171.6	603.52	3.63
		50	85	169.1	177.6	624.62	3.69
		55	85	176.3	192.9	678.43	3.85
		40	95	172.7	140.5	494.14	2.86
		42	95	175.3	145.7	512.43	2.92
		44	95	178	151	531.07	2.98
		46	95	180.7	156.5	550.41	3.05
		48	95	183.5	162	569.75	3.10
		50	95	186.4	167.7	589.80	3.16
		55	95	193.9	182.1	640.45	3.30
		40	105	191.6	131.7	463.19	2.42
		42	105	194.2	136.6	480.42	2.47
		44	105	197	141.6	498.01	2.53
		46	105	199.8	146.7	515.94	2.58
		48	105	202.7	151.9	534.23	2.64

		50	105	205.6	157.2	552.87	2.69
		55	105	213.4	170.7	600.35	2.81
		40	115	212.5	122.6	431.18	2.03
		42	115	215.2	127.1	447.01	2.08
		44	115	218	131.8	463.54	2.13
		46	115	213.3	132.9	467.41	2.19
		48	115	210.4	134.7	473.74	2.25
		50	115	205.6	135.6	476.91	2.32
		55	115	196.5	139.1	489.21	2.49
Trane	166.1	40	75	160.2	172.9	608.09	3.80
		42	75	163.1	178.9	629.19	3.86
		44	75	166.1	185	650.64	3.92
		46	75	169.2	191.2	672.45	3.97
		48	75	172.4	197.6	694.96	4.03
		50	75	175.6	204	717.47	4.09
		55	75	184	220.5	775.50	4.21
		40	85	175.9	164.1	577.14	3.28
		42	85	178.9	169.8	597.19	3.34
		44	85	182	175.6	617.58	3.39
		46	85	185.2	181.6	638.69	3.45
		48	85	188.4	187.6	659.79	3.50
		50	85	191.8	193.7	681.24	3.55
		55	85	200.4	209.5	736.81	3.68
		40	95	193.9	155.1	545.49	2.81
		42	95	197	160.5	564.48	2.87
		44	95	200.2	166.1	584.17	2.92
		46	95	203.5	171.7	603.87	2.97
		48	95	206.9	177.4	623.92	3.02
		50	95	210.3	183.3	644.67	3.07
		55	95	219.3	198.2	697.07	3.18
		40	105	214.3	145.9	513.13	2.39
		42	105	217.5	151.1	531.42	2.44
		44	105	220.9	156.3	549.71	2.49
		46	105	224.3	161.6	568.35	2.53
		48	105	227.7	167	587.34	2.58
		50	105	231.3	172.5	606.68	2.62
		55	105	240.6	186.7	656.62	2.73
		40	115	226.5	131.2	461.43	2.04
		42	115	225.3	133.8	470.57	2.09

		44	115	224	136.2	479.02	2.14
		46	115	218.8	137	481.83	2.20
		48	115	215.7	138.9	488.51	2.26
		50	115	212	140.4	493.79	2.33
		55	115	201.7	143.7	505.39	2.51
Trane	174.9	40	75	169.3	180.5	634.82	3.75
		42	75	172.4	187.1	658.03	3.82
		44	75	175.6	193.8	681.59	3.88
		46	75	178.8	200.6	705.51	3.95
		48	75	182.1	207.5	729.78	4.01
		50	75	185.5	214.6	754.75	4.07
		55	75	194.2	232.6	818.05	4.21
		40	85	186.2	171.8	604.22	3.25
		42	85	189.4	178.1	626.38	3.31
		44	85	192.7	184.5	648.89	3.37
		46	85	196	191	671.75	3.43
		48	85	199.4	197.6	694.96	3.49
		50	85	202.9	204.3	718.52	3.54
		55	85	211.9	221.6	779.37	3.68
		40	95	205.3	162.9	572.92	2.79
		42	95	208.6	168.8	593.67	2.85
		44	95	212	174.9	615.12	2.90
		46	95	215.4	181.1	636.93	2.96
		48	95	219	187.4	659.09	3.01
		50	95	222.6	193.8	681.59	3.06
		55	95	231.9	210.2	739.27	3.19
		40	105	226.8	153.7	540.56	2.38
		42	105	230.2	159.3	560.26	2.43
		44	105	233.7	165	580.30	2.48
		46	105	237.2	170.9	601.06	2.53
		48	105	240.9	176.8	621.81	2.58
		50	105	244.6	182.8	642.91	2.63
		55	105	254.3	198.4	697.77	2.74
		40	115	235.7	136.8	481.13	2.04
		42	115	236.6	140.8	495.19	2.09
		44	115	235.3	143.8	505.74	2.15
		46	115	234	146.7	515.94	2.20
		48	115	229.6	148.2	521.22	2.27
		50	115	226.4	150.3	528.60	2.33

		55	115	214.9	153.6	540.21	2.51
Trane	190.1	40	75	188.3	196.8	692.15	3.68
		42	75	191.8	203.6	716.06	3.73
		44	75	195.5	210.5	740.33	3.79
		46	75	199.2	217.5	764.95	3.84
		48	75	203.1	224.7	790.27	3.89
		50	75	207	231.9	815.59	3.94
		55	75	217.2	250.5	881.01	4.06
		40	85	205.9	187.2	658.38	3.20
		42	85	209.6	193.7	681.24	3.25
		44	85	213.4	200.3	704.45	3.30
		46	85	217.2	207	728.02	3.35
		48	85	221.2	213.8	751.93	3.40
		50	85	225.2	220.7	776.20	3.45
		55	85	235.6	238.5	838.80	3.56
		40	95	226.3	177.6	624.62	2.76
		42	95	230.1	183.8	646.42	2.81
		44	95	233.9	190.1	668.58	2.86
		46	95	237.9	196.5	691.09	2.90
		48	95	242	203	713.95	2.95
		50	95	246.1	209.6	737.16	3.00
		55	95	256.9	226.6	796.95	3.10
		40	105	249.3	168	590.86	2.37
		42	105	253.2	173.9	611.61	2.42
		44	105	257.3	179.8	632.36	2.46
		46	105	261.4	185.9	653.81	2.50
		48	105	265.6	192.1	675.62	2.54
		50	105	269.9	198.4	697.77	2.59
		55	105	281	214.7	755.10	2.69
		40	115	253.8	147.7	519.46	2.05
		42	115	248.8	148.7	522.98	2.10
		44	115	243.5	149.6	526.14	2.16
		46	115	242.4	152.6	536.69	2.21
		48	115	236.6	153.3	539.16	2.28
		50	115	230.4	153.9	541.27	2.35
		55	115	218.5	157.4	553.58	2.53
Trane	195.2	40	75	191.3	202.5	712.19	3.72
		42	75	194.9	209.5	736.81	3.78
		44	75	198.7	216.6	761.78	3.83

		46	75	202.6	223.8	787.10	3.89
		48	75	206.5	231.1	812.78	3.94
		50	75	210.6	238.5	838.80	3.98
		55	75	221	257.4	905.28	4.10
		40	85	208.9	192.5	677.02	3.24
		42	85	212.7	199.1	700.23	3.29
		44	85	216.6	205.9	724.15	3.34
		46	85	220.5	212.8	748.42	3.39
		48	85	224.6	219.7	772.68	3.44
		50	85	228.7	226.8	797.66	3.49
		55	85	239.4	245	861.66	3.60
		40	95	229.2	182.5	641.85	2.80
		42	95	233.1	188.8	664.01	2.85
		44	95	237.1	195.2	686.52	2.90
		46	95	241.2	201.8	709.73	2.94
		48	95	245.4	208.4	732.94	2.99
		50	95	249.6	215.2	756.86	3.03
		55	95	260.7	232.6	818.05	3.14
		40	105	252.3	172.4	606.33	2.40
		42	105	256.3	178.4	627.43	2.45
		44	105	260.5	184.5	648.89	2.49
		46	105	264.7	190.8	671.04	2.54
		48	105	269	197.1	693.20	2.58
		50	105	273.4	203.6	716.06	2.62
		55	105	284.8	220.2	774.44	2.72
		40	115	252.1	149.3	525.09	2.08
		42	115	246.9	150.2	528.25	2.14
		44	115	241.4	151	531.07	2.20
		46	115	240.1	154.1	541.97	2.26
		48	115	234.1	154.7	544.08	2.32
		50	115	227.8	155.2	545.84	2.40
		55	115	215.5	158.6	557.80	2.59
Trane	235.4	40	75	221	244.8	860.96	3.90
		42	75	224.9	253.4	891.21	3.96
		44	75	228.9	262.2	922.16	4.03
		46	75	233	271.2	953.81	4.09
		48	75	237.2	280.3	985.81	4.16
		50	75	241.6	289.5	1018.17	4.21
		55	75	252.9	313.3	1101.88	4.36

		40	85	243.5	232.4	817.35	3.36
		42	85	247.5	240.7	846.54	3.42
		44	85	251.6	249	875.73	3.48
		46	85	255.9	257.6	905.98	3.54
		48	85	260.2	266.2	936.23	3.60
		50	85	264.7	275.1	967.53	3.66
		55	85	276.4	297.8	1047.36	3.79
		40	95	269.3	219.7	772.68	2.87
		42	95	273.5	227.5	800.12	2.93
		44	95	277.8	235.4	827.90	2.98
		46	95	282.2	243.5	856.39	3.03
		48	95	286.7	251.8	885.58	3.09
		50	95	291.3	260.1	914.77	3.14
		55	95	303.4	281.7	990.74	3.27
		40	105	298.6	206.6	726.61	2.43
		42	105	303	213.9	752.29	2.48
		44	105	307.4	221.4	778.66	2.53
		46	105	311.9	229	805.39	2.58
		48	105	316.6	236.8	832.83	2.63
		50	105	321.4	244.7	860.61	2.68
		55	105	334	265.1	932.36	2.79
		40	115	325.3	189.9	667.88	2.05
		42	115	325.4	194.5	684.06	2.10
		44	115	325.4	199.2	700.59	2.15
		46	115	325.3	203.9	717.12	2.20
		48	115	317.8	205.1	721.34	2.27
		50	115	313.8	208	731.54	2.33
		55	115	295.8	211.5	743.85	2.51
Trane	261.6	40	75	249.2	271.1	953.46	3.83
		42	75	253.7	281.6	990.39	3.90
		44	75	258.4	290.2	1020.63	3.95
		46	75	263.2	300.1	1055.45	4.01
		48	75	268.1	310.1	1090.62	4.07
		50	75	273.1	320.2	1126.14	4.12
		55	75	286.2	346.3	1217.94	4.26
		40	85	273.6	257.8	906.68	3.31
		42	85	278.3	266.8	938.34	3.37
		44	85	283.1	276	970.69	3.43
		46	85	288.1	285.4	1003.75	3.48

		48	85	293.1	294.9	1037.16	3.54
		50	85	298.3	304.6	1071.28	3.59
		55	85	311.8	329.5	1158.85	3.72
		40	95	301.8	244.2	858.85	2.85
		42	95	306.6	252.8	889.10	2.90
		44	95	311.6	261.6	920.05	2.95
		46	95	316.7	270.5	951.35	3.00
		48	95	321.9	279.5	983.00	3.05
		50	95	327.3	288.8	1015.71	3.10
		55	95	341.2	312.5	1099.06	3.22
		40	105	333.7	230.4	810.32	2.43
		42	105	338.7	238.6	839.16	2.48
		44	105	343.9	246.9	868.35	2.52
		46	105	349.1	255.3	897.89	2.57
		48	105	354.6	263.9	928.14	2.62
		50	105	360.1	272.6	958.73	2.66
		55	105	374.6	295.2	1038.22	2.77
		40	115	361	212.1	745.96	2.07
		42	115	357.9	215.6	758.26	2.12
		44	115	350.7	217.1	763.54	2.18
		46	115	345.4	219.7	772.68	2.24
		48	115	341.5	222.9	783.94	2.30
		50	115	333.4	224.1	788.16	2.36
		55	115	318.1	229.8	808.21	2.54
Trane	287.4	40	75	278	297	1044.55	3.76
		42	75	283.2	307.3	1080.77	3.82
		44	75	288.6	317.8	1117.70	3.87
		46	75	294	328.5	1155.33	3.93
		48	75	299.7	339.3	1193.32	3.98
		50	75	305.4	350.3	1232.00	4.03
		55	75	320.4	378.6	1331.54	4.16
		40	85	304.5	282.8	994.61	3.27
		42	85	309.9	292.6	1029.07	3.32
		44	85	315.4	302.6	1064.24	3.37
		46	85	321	312.8	1100.12	3.43
		48	85	326.8	323.2	1136.69	3.48
		50	85	332.7	333.7	1173.62	3.53
		55	85	348.1	360.7	1268.58	3.64
		40	95	334.9	268.5	944.31	2.82

		42	95	340.5	277.9	977.37	2.87
		44	95	346.2	287.4	1010.79	2.92
		46	95	352	297.1	1044.90	2.97
		48	95	358	307	1079.72	3.02
		50	95	364.1	317	1114.89	3.06
		55	95	380	342.9	1205.98	3.17
		40	105	369.4	254.1	893.67	2.42
		42	105	375.2	263	924.97	2.47
		44	105	381.1	272.1	956.98	2.51
		46	105	387.2	281.3	989.33	2.56
		48	105	393.4	290.7	1022.39	2.60
		50	105	399.8	300.3	1056.15	2.64
		55	105	416.2	325	1143.02	2.75
		40	115	387.3	229.1	805.74	2.08
		42	115	380.1	230.8	811.72	2.14
		44	115	372.6	232.4	817.35	2.19
		46	115	364.6	233.8	822.27	2.26
		48	115	358.5	236.3	831.07	2.32
		50	115	349.6	237.4	834.94	2.39
		55	115	332.5	243	854.63	2.57
Trane	333.4	40	75	314.3	345.9	1216.53	3.87
		42	75	319.9	358.1	1259.44	3.94
		44	75	325.7	370.5	1303.05	4.00
		46	75	331.7	383.1	1347.36	4.06
		48	75	337.8	396	1392.73	4.12
		50	75	344.1	409	1438.45	4.18
		55	75	360.4	442.6	1556.62	4.32
		40	85	345.6	328.7	1156.04	3.35
		42	85	351.4	340.4	1197.19	3.41
		44	85	357.4	352.2	1238.69	3.47
		46	85	363.5	364.2	1280.89	3.52
		48	85	369.9	376.5	1324.15	3.58
		50	85	376.3	389	1368.11	3.64
		55	85	393.2	421	1480.66	3.77
		40	95	381.5	311.2	1094.49	2.87
		42	95	387.6	322.2	1133.18	2.92
		44	95	393.8	333.4	1172.57	2.98
		46	95	400.1	344.9	1213.01	3.03
		48	95	406.7	356.5	1253.81	3.08

		50	95	413.4	368.4	1295.66	3.13
		55	95	430.8	398.9	1402.93	3.26
		40	105	422.3	293.2	1031.18	2.44
		42	105	428.6	303.6	1067.76	2.49
		44	105	435	314.2	1105.04	2.54
		46	105	441.6	325	1143.02	2.59
		48	105	448.4	336.1	1182.06	2.64
		50	105	455.3	347.3	1221.45	2.68
		55	105	473.4	376.2	1323.09	2.79
		40	115	455.7	268.5	944.31	2.07
		42	115	453.5	273.8	962.95	2.12
		44	115	451.1	279.2	981.95	2.18
		46	115	448.5	284.4	1000.23	2.23
		48	115	438.2	286.1	1006.21	2.30
		50	115	427.6	287.6	1011.49	2.37
		55	115	407.6	295	1037.51	2.55
Trane	359.7	40	75	342.5	372.3	1309.38	3.82
		42	75	348.8	385.4	1355.45	3.89
		44	75	355.3	398.6	1401.88	3.95
		46	75	361.9	412.1	1449.36	4.00
		48	75	368.7	425.9	1497.89	4.06
		50	75	375.7	439.8	1546.78	4.12
		55	75	393.9	475.7	1673.04	4.25
		40	85	375.8	354.2	1245.72	3.31
		42	85	382.3	366.6	1289.33	3.37
		44	85	389	379.3	1334.00	3.43
		46	85	395.8	392.2	1379.37	3.49
		48	85	402.8	405.3	1425.44	3.54
		50	85	410	418.6	1472.22	3.59
		55	85	428.7	452.9	1592.85	3.72
		40	95	414.1	335.8	1181.01	2.85
		42	95	420.8	347.7	1222.86	2.91
		44	95	427.7	359.7	1265.06	2.96
		46	95	434.8	372	1308.32	3.01
		48	95	442	384.5	1352.29	3.06
		50	95	449.4	397.2	1396.95	3.11
		55	95	468.8	429.9	1511.96	3.23
		40	105	457.5	317.2	1115.59	2.44
		42	105	464.4	328.4	1154.98	2.49

		44	105	471.6	339.8	1195.08	2.53
		46	105	479	351.5	1236.23	2.58
		48	105	486.5	363.6	1278.78	2.63
		50	105	494.2	375.4	1320.28	2.67
		55	105	514.2	406.5	1429.66	2.78
		40	115	489.5	289.9	1019.58	2.08
		42	115	484.1	294	1034.00	2.14
		44	115	478.6	298.3	1049.12	2.19
		46	115	468.5	300.2	1055.80	2.25
		48	115	457.8	302	1062.13	2.32
		50	115	446.7	303.5	1067.41	2.39
		55	115	425.5	311.1	1094.14	2.57
Trane	385.7	40	75	371.4	398.3	1400.82	3.77
		42	75	378.4	412.2	1449.71	3.83
		44	75	385.6	426.3	1499.30	3.89
		46	75	392.9	440.7	1549.94	3.94
		48	75	400.4	455.3	1601.29	4.00
		50	75	408.1	470.1	1653.34	4.05
		55	75	428.2	508.1	1786.99	4.17
		40	85	406.8	379.3	1334.00	3.28
		42	85	413.9	392.5	1380.42	3.34
		44	85	421.3	406	1427.90	3.39
		46	85	428.9	419.7	1476.08	3.44
		48	85	436.6	433.7	1525.32	3.49
		50	85	444.5	447.9	1575.26	3.54
		55	85	465.1	484.3	1703.28	3.66
		40	95	447.3	360.2	1266.82	2.83
		42	95	454.8	372.8	1311.14	2.88
		44	95	462.4	385.7	1356.51	2.93
		46	95	470.2	398.8	1402.58	2.98
		48	95	478.2	412.1	1449.36	3.03
		50	95	486.4	425.6	1496.83	3.08
		55	95	507.6	460.5	1619.58	3.19
		40	105	493.3	341	1199.30	2.43
		42	105	501	353	1241.50	2.48
		44	105	509	365.2	1284.41	2.52
		46	105	517.1	377.7	1328.37	2.57
		48	105	525.4	390.3	1372.68	2.61
		50	105	533.9	403.3	1418.41	2.66

		55	105	555.9	436.6	1535.52	2.76
		40	115	511.6	304.8	1071.98	2.10
		42	115	502	307.1	1080.07	2.15
		44	115	491.9	309.1	1087.10	2.21
		46	115	489.9	315.6	1109.96	2.27
		48	115	478.7	317.3	1115.94	2.33
		50	115	466.9	318.8	1121.22	2.40
		55	115	444.1	326.5	1148.30	2.59
York	152.6	40	75	131.5	149.1	524.38	3.99
		42	75	132.5	153.7	540.56	4.08
		44	75	133.5	158.3	556.74	4.17
		45	75	134	160.7	565.18	4.22
		46	75	134.6	163.1	573.62	4.26
		48	75	135.7	167.9	590.50	4.35
		50	75	137	172.8	607.74	4.44
		40	80	141.8	148	520.52	3.67
		42	80	142.6	152.5	536.34	3.76
		44	80	143.6	157.1	552.52	3.85
		45	80	144.1	159.4	560.61	3.89
		46	80	144.6	161.8	569.05	3.94
		48	80	145.7	166.6	585.93	4.02
		50	80	146.9	171.4	602.81	4.10
		40	85	152.6	146.7	515.94	3.38
		42	85	153.5	151.2	531.77	3.46
		44	85	154.4	155.7	547.60	3.55
		45	85	154.9	158.1	556.04	3.59
		46	85	155.4	160.4	564.13	3.63
		48	85	156.5	165.1	580.66	3.71
		50	85	157.7	169.9	597.54	3.79
		40	90	164.1	145.4	511.37	3.12
		42	90	165	149.8	526.85	3.19
		44	90	165.9	154.3	542.67	3.27
		45	90	166.4	156.5	550.41	3.31
		46	90	166.9	158.8	558.50	3.35
		48	90	167.9	163.5	575.03	3.42
		50	90	169	168.2	591.56	3.50
		40	95	176	143.9	506.10	2.88
		42	95	177	148.2	521.22	2.94
		44	95	177.9	152.6	536.69	3.02

		45	95	178.4	154.9	544.78	3.05
		46	95	178.9	157.1	552.52	3.09
		48	95	180	161.7	568.70	3.16
		50	95	181.1	166.4	585.23	3.23
York	168.4	40	75	144.7	165.7	582.77	4.03
		42	75	145.7	170.9	601.06	4.13
		44	75	146.8	176.1	619.34	4.22
		45	75	147.5	178.8	628.84	4.26
		46	75	148.2	181.5	638.34	4.31
		48	75	149.5	186.9	657.33	4.40
		50	75	151	192.4	676.67	4.48
		40	80	156.2	164.2	577.49	3.70
		42	80	157.3	169.3	595.43	3.79
		44	80	158.3	174.6	614.07	3.88
		45	80	158.9	177.2	623.21	3.92
		46	80	159.5	179.9	632.71	3.97
		48	80	160.8	185.4	652.05	4.06
		50	80	162.2	190.8	671.04	4.14
		40	85	168.5	162.4	571.16	3.39
		42	85	169.5	167.5	589.10	3.48
		44	85	170.6	172.8	607.74	3.56
		45	85	171.1	175.4	616.88	3.61
		46	85	171.7	178.1	626.38	3.65
		48	85	173	183.5	645.37	3.73
		50	85	174.3	189	664.71	3.81
		40	90	181.2	160.5	564.48	3.12
		42	90	182.3	165.5	582.06	3.19
		44	90	183.5	170.7	600.35	3.27
		45	90	184	173.3	609.50	3.31
		46	90	184.6	175.9	618.64	3.35
		48	90	185.9	181.3	637.63	3.43
		50	90	187.2	186.7	656.62	3.51
		40	95	194.4	158.4	557.09	2.87
		42	95	195.6	163.3	574.33	2.94
		44	95	196.8	168.4	592.26	3.01
		45	95	197.5	171	601.41	3.05
		46	95	197.8	173.5	610.20	3.08
		48	95	198.3	178.4	627.43	3.16
		50	95	198.8	183.4	645.02	3.24

York	184.2	40	75	156.2	180.3	634.11	4.06
		42	75	157.4	185.9	653.81	4.15
		44	75	158.8	191.7	674.21	4.25
		45	75	159.6	194.6	684.41	4.29
		46	75	160.4	197.5	694.61	4.33
		48	75	162.1	203.5	715.71	4.42
		50	75	163.8	209.5	736.81	4.50
		40	80	168.2	178.8	628.84	3.74
		42	80	169.4	184.4	648.53	3.83
		44	80	170.7	190	668.23	3.91
		45	80	171.4	192.9	678.43	3.96
		46	80	172.1	195.8	688.63	4.00
		48	80	173.7	201.7	709.38	4.08
		50	80	175.3	207.7	730.48	4.17
		40	85	181.1	177.1	622.86	3.44
		42	85	182.3	182.6	642.20	3.52
		44	85	183.5	188.2	661.90	3.61
		45	85	184.2	191.1	672.10	3.65
		46	85	184.9	193.9	681.95	3.69
		48	85	186.3	199.8	702.70	3.77
		50	85	187.8	205.7	723.45	3.85
		40	90	194.7	175.3	616.53	3.17
		42	90	195.8	180.7	635.52	3.25
		44	90	197.1	186.3	655.22	3.32
		45	90	197.7	189.1	665.06	3.36
		46	90	198.4	191.9	674.91	3.40
		48	90	199.8	197.6	694.96	3.48
		50	90	201.3	203.5	715.71	3.56
		40	95	208.9	173.4	609.85	2.92
		42	95	210.1	178.7	628.49	2.99
		44	95	211.3	184.2	647.83	3.07
		45	95	212	186.9	657.33	3.10
		46	95	212.7	189.7	667.17	3.14
		48	95	214.1	195.3	686.87	3.21
		50	95	215.5	201.1	707.27	3.28
York	197.6	40	75	168.3	194.8	685.11	4.07
		42	75	169.6	200.9	706.57	4.17
		44	75	171.2	207.2	728.72	4.26
		45	75	172	210.4	739.98	4.30

		46	75	173	213.6	751.23	4.34
		48	75	175.1	220.2	774.44	4.42
		50	75	177.4	226.9	798.01	4.50
		40	80	182.2	192.9	678.43	3.72
		42	80	183.3	199	699.88	3.82
		44	80	184.5	205.2	721.69	3.91
		45	80	185.2	208.3	732.59	3.96
		46	80	185.9	211.5	743.85	4.00
		48	80	187.6	218	766.71	4.09
		50	80	189.6	224.5	789.57	4.16
		40	85	197.4	190.9	671.40	3.40
		42	85	198.2	196.8	692.15	3.49
		44	85	199.3	202.9	713.60	3.58
		45	85	199.8	206	724.50	3.63
		46	85	200.4	209.1	735.40	3.67
		48	85	201.8	215.5	757.91	3.76
		50	85	203.5	222	780.77	3.84
		40	90	213.5	188.7	663.66	3.11
		42	90	214.3	194.6	684.41	3.19
		44	90	215.2	200.5	705.16	3.28
		45	90	215.7	203.6	716.06	3.32
		46	90	216.3	206.6	726.61	3.36
		48	90	217.5	212.9	748.77	3.44
		50	90	218.9	219.2	770.93	3.52
		40	95	230.3	186.4	655.57	2.85
		42	95	231.2	192.1	675.62	2.92
		44	95	231.3	197.6	694.96	3.00
		45	95	231.4	200.4	704.81	3.05
		46	95	231.5	203.2	714.65	3.09
		48	95	231.7	208.9	734.70	3.17
		50	95	232.1	214.8	755.45	3.25
York	215.3	40	75	180.4	211.3	743.14	4.12
		42	75	182	218	766.71	4.21
		44	75	183.7	224.9	790.97	4.31
		45	75	184.7	228.3	802.93	4.35
		46	75	185.7	231.8	815.24	4.39
		48	75	187.8	238.9	840.21	4.47
		50	75	190.1	246.2	865.89	4.55
		40	80	194.3	209.4	736.46	3.79

		42	80	195.7	216	759.67	3.88
		44	80	197.3	222.7	783.24	3.97
		45	80	198.2	226.2	795.55	4.01
		46	80	199.1	229.6	807.50	4.06
		48	80	201.1	236.7	832.47	4.14
		50	80	203.1	243.8	857.44	4.22
		40	85	209.2	207.3	729.07	3.49
		42	85	210.5	213.8	751.93	3.57
		44	85	212	220.4	775.15	3.66
		45	85	212.8	223.8	787.10	3.70
		46	85	213.7	227.2	799.06	3.74
		48	85	215.4	234.2	823.68	3.82
		50	85	217.4	241.2	848.30	3.90
		40	90	224.8	205.1	721.34	3.21
		42	90	226.2	211.4	743.49	3.29
		44	90	227.7	218	766.71	3.37
		45	90	228.5	221.3	778.31	3.41
		46	90	229.3	224.6	789.92	3.44
		48	90	231	231.4	813.83	3.52
		50	90	232.8	238.4	838.45	3.60
		40	95	241.3	202.7	712.90	2.95
		42	95	242.7	208.9	734.70	3.03
		44	95	244.2	215.3	757.21	3.10
		45	95	245.1	218.5	768.46	3.14
		46	95	245.9	221.8	780.07	3.17
		48	95	247.5	228.5	803.63	3.25
		50	95	249.2	235.3	827.55	3.32
York	236.4	40	75	198.8	231.8	815.24	4.10
		42	75	200.6	239.1	840.91	4.19
		44	75	202.6	246.5	866.94	4.28
		45	75	203.7	250.2	879.95	4.32
		46	75	204.8	254	893.32	4.36
		48	75	207.1	261.7	920.40	4.44
		50	75	209.5	269.6	948.18	4.53
		40	80	213.8	229.8	808.21	3.78
		42	80	215.6	236.9	833.18	3.86
		44	80	217.4	244.3	859.20	3.95
		45	80	218.4	248	872.22	3.99
		46	80	219.4	251.7	885.23	4.03

		48	80	221.6	259.4	912.31	4.12
		50	80	223.9	267.1	939.39	4.20
		40	85	229.8	227.6	800.47	3.48
		42	85	231.5	234.6	825.09	3.56
		44	85	233.3	241.9	850.76	3.65
		45	85	234.3	245.5	863.42	3.69
		46	85	235.2	249.2	876.44	3.73
		48	85	237.3	256.7	902.81	3.80
		50	85	239.5	264.4	929.89	3.88
		40	90	246.7	225.2	792.03	3.21
		42	90	248.4	232.1	816.30	3.29
		44	90	250.2	239.2	841.27	3.36
		45	90	251.2	242.8	853.93	3.40
		46	90	252.1	246.5	866.94	3.44
		48	90	254.1	253.9	892.97	3.51
		50	90	256.2	261.4	919.34	3.59
		40	95	264.4	222.7	783.24	2.96
		42	95	266.1	229.5	807.15	3.03
		44	95	268	236.4	831.42	3.10
		45	95	268.9	239.9	843.73	3.14
		46	95	269.9	243.5	856.39	3.17
		48	95	271.9	250.8	882.06	3.24
		50	95	274	258.2	908.09	3.31
York	257.6	40	75	217	252.3	887.34	4.09
		42	75	219	260.2	915.12	4.18
		44	75	221.2	268.2	943.26	4.26
		45	75	222.5	272.2	957.33	4.30
		46	75	223.6	276.3	971.75	4.35
		48	75	226.1	284.6	1000.94	4.43
		50	75	228.7	293.1	1030.83	4.51
		40	80	233.1	250.2	879.95	3.78
		42	80	235.2	258	907.39	3.86
		44	80	237.3	265.9	935.17	3.94
		45	80	238.4	269.9	949.24	3.98
		46	80	239.5	273.9	963.31	4.02
		48	80	242	282.1	992.15	4.10
		50	80	244.5	290.5	1021.69	4.18
		40	85	250.3	247.9	871.86	3.48
		42	85	252.2	255.6	898.94	3.56

		44	85	254.3	263.3	926.03	3.64
		45	85	255.5	267.3	940.09	3.68
		46	85	256.6	271.3	954.16	3.72
		48	85	258.9	279.4	982.65	3.80
		50	85	261.3	287.7	1011.84	3.87
		40	90	268.3	245.4	863.07	3.22
		42	90	270.4	252.9	889.45	3.29
		44	90	272.4	260.6	916.53	3.36
		45	90	273.6	264.5	930.25	3.40
		46	90	274.7	268.4	943.96	3.44
		48	90	276.9	276.4	972.10	3.51
		50	90	279.3	284.6	1000.94	3.58
		40	95	287.2	242.7	853.58	2.97
		42	95	289.2	250.1	879.60	3.04
		44	95	291.5	257.6	905.98	3.11
		45	95	292.5	261.4	919.34	3.14
		46	95	293.6	265.3	933.06	3.18
		48	95	296	273.1	960.49	3.24
		50	95	298.4	281.1	988.63	3.31
York	272.7	40	75	228	268.2	943.26	4.14
		42	75	229.7	276.6	972.80	4.24
		44	75	231.6	285.2	1003.05	4.33
		45	75	232.6	289.6	1018.52	4.38
		46	75	233.7	294	1034.00	4.42
		48	75	236.1	303	1065.65	4.51
		50	75	238.8	312.1	1097.66	4.60
		40	80	246.5	265.7	934.47	3.79
		42	80	248	274.1	964.01	3.89
		44	80	249.6	282.6	993.90	3.98
		45	80	250.5	286.9	1009.03	4.03
		46	80	251.4	291.3	1024.50	4.08
		48	80	253.5	300.2	1055.80	4.16
		50	80	255.8	309.3	1087.81	4.25
		40	85	266.4	262.9	924.62	3.47
		42	85	267.7	271.2	953.81	3.56
		44	85	269.2	279.6	983.35	3.65
		45	85	270	283.9	998.48	3.70
		46	85	270.8	288.3	1013.95	3.74
		48	85	272.7	297.1	1044.90	3.83

		50	85	274.7	306	1076.20	3.92
		40	90	287.2	259.9	914.07	3.18
		42	90	288.6	268	942.56	3.27
		44	90	290	276.3	971.75	3.35
		45	90	290.8	280.6	986.87	3.39
		46	90	291.6	284.9	1001.99	3.44
		48	90	293.3	293.5	1032.24	3.52
		50	90	295.2	302.4	1063.54	3.60
		40	95	308.8	256.7	902.81	2.92
		42	95	310.3	264.6	930.60	3.00
		44	95	311.7	272.7	959.09	3.08
		45	95	312.1	276.7	973.15	3.12
		46	95	312.5	280.7	987.22	3.16
		48	95	313.4	288.9	1016.06	3.24
		50	95	314.4	297.2	1045.25	3.32
York	302.9	40	75	251.5	298	1048.07	4.17
		42	75	253.3	307.4	1081.13	4.27
		44	75	255.6	317	1114.89	4.36
		45	75	256.9	321.9	1132.12	4.41
		46	75	258.2	326.9	1149.71	4.45
		48	75	261.3	336.9	1184.88	4.53
		50	75	264.7	347.2	1221.10	4.61
		40	80	272.2	295.2	1038.22	3.81
		42	80	273.7	304.5	1070.93	3.91
		44	80	275.5	314	1104.34	4.01
		45	80	276.5	318.8	1121.22	4.06
		46	80	277.6	323.7	1138.45	4.10
		48	80	280	333.6	1173.27	4.19
		50	80	282.9	343.7	1208.79	4.27
		40	85	294.8	292.2	1027.67	3.49
		42	85	296	301.3	1059.67	3.58
		44	85	297.5	310.6	1092.38	3.67
		45	85	298.3	315.4	1109.26	3.72
		46	85	299.2	320.2	1126.14	3.76
		48	85	301.2	329.9	1160.26	3.85
		50	85	303.5	339.9	1195.43	3.94
		40	90	318.9	289	1016.41	3.19
		42	90	320	297.9	1047.71	3.27
		44	90	321.3	307.1	1080.07	3.36

		45	90	322	311.7	1096.25	3.40
		46	90	322.7	316.4	1112.78	3.45
		48	90	324.5	326	1146.54	3.53
		50	90	326.6	335.8	1181.01	3.62
		40	95	344	285.6	1004.45	2.92
		42	95	345.1	294.3	1035.05	3.00
		44	95	345.6	302.9	1065.30	3.08
		45	95	345.8	307.3	1080.77	3.13
		46	95	346.1	311.7	1096.25	3.17
		48	95	346.9	320.6	1127.55	3.25
		50	95	347.7	329.8	1159.91	3.34
York	342.9	40	75	288	336.3	1182.77	4.11
		42	75	290.6	346.9	1220.05	4.20
		44	75	293.3	357.7	1258.03	4.29
		45	75	294.8	363.2	1277.37	4.33
		46	75	296.5	368.8	1297.07	4.37
		48	75	299.7	380.1	1336.81	4.46
		50	75	303.2	391.6	1377.26	4.54
		40	80	309.9	333.4	1172.57	3.78
		42	80	312.4	343.8	1209.14	3.87
		44	80	315	354.5	1246.78	3.96
		45	80	316.4	359.9	1265.77	4.00
		46	80	317.8	365.4	1285.11	4.04
		48	80	320.9	376.6	1324.50	4.13
		50	80	324.2	387.9	1364.24	4.21
		40	85	333.5	330.1	1160.96	3.48
		42	85	335.8	340.4	1197.19	3.57
		44	85	338.3	350.9	1234.11	3.65
		45	85	339.6	356.3	1253.11	3.69
		46	85	341	361.7	1272.10	3.73
		48	85	343.8	372.7	1310.79	3.81
		50	85	347	383.9	1350.18	3.89
		40	90	358.2	326.6	1148.65	3.21
		42	90	360.5	336.7	1184.17	3.28
		44	90	363.1	347.1	1220.75	3.36
		45	90	364.3	352.3	1239.04	3.40
		46	90	365.7	357.6	1257.68	3.44
		48	90	368.5	368.5	1296.01	3.52
		50	90	371.4	379.5	1334.70	3.59

		40	95	384.1	322.9	1135.64	2.96
		42	95	386.5	332.8	1170.46	3.03
		44	95	389	342.9	1205.98	3.10
		45	95	390.4	348.1	1224.27	3.14
		46	95	391.7	353.3	1242.56	3.17
		48	95	394.5	363.9	1279.84	3.24
		50	95	397.4	374.8	1318.17	3.32
York	385.3	40	75	324.5	377.3	1326.96	4.09
		42	75	327.5	389.1	1368.46	4.18
		44	75	330.7	401.2	1411.02	4.27
		45	75	332.4	407.4	1432.83	4.31
		46	75	334.3	413.5	1454.28	4.35
		48	75	337.9	426.1	1498.59	4.44
		50	75	341.8	439	1543.96	4.52
		40	80	348.7	374.2	1316.06	3.77
		42	80	351.6	385.8	1356.86	3.86
		44	80	354.8	397.8	1399.06	3.94
		45	80	356.4	403.8	1420.16	3.98
		46	80	358.1	410	1441.97	4.03
		48	80	361.6	422.4	1485.58	4.11
		50	80	365.5	435.1	1530.25	4.19
		40	85	374.4	370.7	1303.75	3.48
		42	85	377.3	382.2	1344.20	3.56
		44	85	380.3	394	1385.70	3.64
		45	85	382.1	399.9	1406.45	3.68
		46	85	383.7	406	1427.90	3.72
		48	85	387.1	418.2	1470.81	3.80
		50	85	390.7	430.8	1515.12	3.88
		40	90	401.4	366.9	1290.39	3.21
		42	90	404.5	378.2	1330.13	3.29
		44	90	407.5	389.8	1370.93	3.36
		45	90	409.1	395.7	1391.68	3.40
		46	90	410.9	401.6	1412.43	3.44
		48	90	414.2	413.7	1454.98	3.51
		50	90	417.8	426	1498.24	3.59
		40	95	429.8	362.9	1276.32	2.97
		42	95	432.8	374	1315.36	3.04
		44	95	436	385.3	1355.10	3.11
		45	95	437.7	391	1375.15	3.14

		46	95	439.3	396.9	1395.90	3.18
		48	95	442.9	408.7	1437.40	3.25
		50	95	446.4	420.9	1480.30	3.32
York	409.9	40	75	344	401.1	1410.67	4.10
		42	75	346.5	413.4	1453.93	4.20
		44	75	349.2	425.9	1497.89	4.29
		45	75	350.6	432.3	1520.40	4.34
		46	75	352.2	438.7	1542.91	4.38
		48	75	355.6	451.7	1588.63	4.47
		50	75	359.5	464.9	1635.05	4.55
		40	80	371.8	397.9	1399.41	3.76
		42	80	373.8	410	1441.97	3.86
		44	80	376.3	422.4	1485.58	3.95
		45	80	377.6	428.6	1507.39	3.99
		46	80	378.9	435	1529.89	4.04
		48	80	381.8	447.8	1574.91	4.12
		50	80	385	460.9	1620.98	4.21
		40	85	401.8	394.4	1387.10	3.45
		42	85	403.6	406.3	1428.96	3.54
		44	85	405.8	418.5	1471.86	3.63
		45	85	406.9	424.7	1493.67	3.67
		46	85	408.1	430.9	1515.47	3.71
		48	85	410.6	443.6	1560.14	3.80
		50	85	413.5	456.5	1605.51	3.88
		40	90	433.6	390.6	1373.74	3.17
		42	90	435.3	402.4	1415.24	3.25
		44	90	437.2	414.3	1457.09	3.33
		45	90	438.3	420.4	1478.55	3.37
		46	90	439.3	426.6	1500.35	3.42
		48	90	441.8	439	1543.96	3.49
		50	90	444.4	451.7	1588.63	3.57
		40	95	466.6	386.5	1359.32	2.91
		42	95	468.5	398.1	1400.12	2.99
		44	95	470.5	409.9	1441.62	3.06
		45	95	471.5	415.9	1462.72	3.10
		46	95	472.6	421.9	1483.82	3.14
		48	95	475	434.1	1526.73	3.21
		50	95	477.4	446.6	1570.69	3.29
York	439.3	40	75	377	429.2	1509.50	4.00

		42	75	380.2	442.4	1555.92	4.09
		44	75	383.7	455.8	1603.05	4.18
		45	75	385.5	462.5	1626.61	4.22
		46	75	387.3	469.4	1650.88	4.26
		48	75	391.4	483.2	1699.41	4.34
		50	75	395.7	497.2	1748.65	4.42
		40	80	406	425.5	1496.48	3.69
		42	80	408.9	438.5	1542.20	3.77
		44	80	412.2	451.8	1588.98	3.85
		45	80	413.9	458.5	1612.54	3.90
		46	80	415.6	465.3	1636.46	3.94
		48	80	419.4	479	1684.64	4.02
		50	80	423.4	492.9	1733.53	4.09
		40	85	436.7	421.4	1482.06	3.39
		42	85	439.6	434.3	1527.43	3.47
		44	85	442.7	447.4	1573.51	3.55
		45	85	444.3	454	1596.72	3.59
		46	85	446.1	460.7	1620.28	3.63
		48	85	449.6	474.3	1668.11	3.71
		50	85	453.4	488.1	1716.65	3.79
		40	90	469.3	416.9	1466.24	3.12
		42	90	472.2	429.7	1511.25	3.20
		44	90	475.2	442.6	1556.62	3.28
		45	90	476.8	449.1	1579.48	3.31
		46	90	478.5	455.7	1602.70	3.35
		48	90	481.9	469.1	1649.82	3.42
		50	90	485.6	482.7	1697.66	3.50
		40	95	503.3	412.1	1449.36	2.88
		42	95	506.3	424.7	1493.67	2.95
		44	95	509.4	437.4	1538.34	3.02
		45	95	510.9	443.9	1561.20	3.06
		46	95	512.6	450.4	1584.06	3.09
		48	95	516.1	463.5	1630.13	3.16
		50	95	519.1	476.7	1676.55	3.23
York	471	40	75	396.3	461.7	1623.80	4.10
		42	75	399.8	476.2	1674.79	4.19
		44	75	403.6	491	1726.85	4.28
		45	75	405.7	498.6	1753.58	4.32
		46	75	408	506.2	1780.30	4.36

		48	75	412.4	521.7	1834.82	4.45
		50	75	417.1	537.3	1889.68	4.53
		40	80	426.2	457.7	1609.73	3.78
		42	80	429.7	472	1660.02	3.86
		44	80	433.4	486.7	1711.72	3.95
		45	80	435.3	494.1	1737.75	3.99
		46	80	437.3	501.7	1764.48	4.03
		48	80	441.5	517	1818.29	4.12
		50	80	446.1	532.4	1872.45	4.20
		40	85	458.5	453.3	1594.26	3.48
		42	85	461.7	467.4	1643.85	3.56
		44	85	465.2	481.9	1694.84	3.64
		45	85	467	489.2	1720.52	3.68
		46	85	469	496.6	1746.54	3.72
		48	85	473	511.7	1799.65	3.80
		50	85	477.3	527.1	1853.81	3.88
		40	90	492.1	448.6	1577.73	3.21
		42	90	495.5	462.5	1626.61	3.28
		44	90	499.1	476.6	1676.20	3.36
		45	90	500.8	483.9	1701.88	3.40
		46	90	502.8	491.1	1727.20	3.44
		48	90	506.7	506	1779.60	3.51
		50	90	510.8	521.2	1833.06	3.59
		40	95	527.5	443.5	1559.79	2.96
		42	95	530.9	457.1	1607.62	3.03
		44	95	534.5	471	1656.51	3.10
		45	95	536.4	478.1	1681.48	3.13
		46	95	538.3	485.3	1706.80	3.17
		48	95	542.3	499.8	1757.80	3.24
		50	95	546.3	514.7	1810.20	3.31
York	492.1	40	75	414.4	482	1695.19	4.09
		42	75	418.2	497.2	1748.65	4.18
		44	75	422.2	512.7	1803.17	4.27
		45	75	424.4	520.5	1830.60	4.31
		46	75	426.8	528.5	1858.73	4.36
		48	75	431.5	544.6	1915.36	4.44
		50	75	436.3	560.7	1971.98	4.52
		40	80	445.5	478	1681.13	3.77
		42	80	449.2	492.9	1733.53	3.86

		44	80	453.2	508.2	1787.34	3.94
		45	80	455.2	516	1814.77	3.99
		46	80	457.3	523.8	1842.20	4.03
		48	80	461.8	539.8	1898.48	4.11
		50	80	466.6	555.8	1954.75	4.19
		40	85	478.8	473.5	1665.30	3.48
		42	85	482.4	488.2	1717.00	3.56
		44	85	486.1	503.3	1770.11	3.64
		45	85	488.1	510.9	1796.83	3.68
		46	85	490.3	518.6	1823.92	3.72
		48	85	494.5	534.4	1879.48	3.80
		50	85	499.1	550.4	1935.76	3.88
		40	90	513.7	468.6	1648.07	3.21
		42	90	517.4	483.1	1699.06	3.28
		44	90	521.1	497.9	1751.11	3.36
		45	90	523.1	505.4	1777.49	3.40
		46	90	525.3	513	1804.22	3.43
		48	90	529.5	528.5	1858.73	3.51
		50	90	533.9	544.3	1914.30	3.59
		40	95	550.3	463.4	1629.78	2.96
		42	95	553.9	477.6	1679.72	3.03
		44	95	558	492.1	1730.72	3.10
		45	95	560	499.5	1756.74	3.14
		46	95	562	507	1783.12	3.17
		48	95	566.4	522.1	1836.23	3.24
		50	95	570.8	537.7	1891.09	3.31
York	513.2	40	75	432.5	502.5	1767.29	4.09
		42	75	436.5	518.2	1822.51	4.18
		44	75	440.8	534.3	1879.13	4.26
		45	75	443	542.5	1907.97	4.31
		46	75	445.5	550.8	1937.16	4.35
		48	75	450.4	567.6	1996.25	4.43
		50	75	455.4	584.2	2054.63	4.51
		40	80	464.7	498.3	1752.52	3.77
		42	80	468.6	513.9	1807.39	3.86
		44	80	472.9	529.8	1863.31	3.94
		45	80	475.1	537.8	1891.44	3.98
		46	80	477.3	546	1920.28	4.02
		48	80	482	562.6	1978.66	4.11

50	80	487	579.2	2037.05	4.18
40	85	499.1	493.7	1736.34	3.48
42	85	502.9	509	1790.15	3.56
44	85	507	524.7	1845.37	3.64
45	85	509.1	532.7	1873.51	3.68
46	85	511.5	540.7	1901.64	3.72
48	85	516	557.1	1959.32	3.80
50	85	520.8	573.8	2018.05	3.87
40	90	535.1	488.7	1718.76	3.21
42	90	539.2	503.7	1771.51	3.29
44	90	543.2	519.2	1826.03	3.36
45	90	545.3	527	1853.46	3.40
46	90	547.7	534.9	1881.24	3.43
48	90	552.2	551	1937.87	3.51
50	90	556.9	567.5	1995.90	3.58
40	95	572.9	483.3	1699.77	2.97
42	95	576.9	498.1	1751.82	3.04
44	95	581.3	513.2	1804.92	3.10
45	95	583.4	520.9	1832.00	3.14
46	95	585.6	528.7	1859.44	3.18
48	95	590.3	544.5	1915.01	3.24
50	95	595	560.7	1971.98	3.31

APPENDIX D

Collection of manufacturers' part-load data used to model air-cooled screw chillers.

Reference Capacity (tons)	Tcond,in (°F)	Tevap,out (°F)	PLR	EER	COP
69.2	80	44	1		3.95
	80	44	0.75	12	3.516
	80	44	0		0
	65	44	1		4.93
	65	44	0.5	14.6	4.2778
	65	44	0		0
100.6	80	44	1		3.56
	80	44	0.75	11	3.223
	80	44	0		0
	65	44	1		4.27
	65	44	0.5	13.5	3.9555
	65	44	0		0
108.3	80	44	1		3.52
	80	44	0.75	11	3.223
	80	44	0		0
	65	44	1		4.22
	65	44	0.5	13.7	4.0141
	65	44	0		0
132.2	80	44	1		3.56
	80	44	0.75	11.9	3.4867
	80	44	0		0
	65	44	1		4.47
	65	44	0.5	14.3	4.1899
	65	44	0		0
142.6	80	44	1		3.51
	80	44	0.75	12.1	3.5453
	80	44	0		0
	65	44	1		4.33
	65	44	0.5	14.5	4.2485
	65	44	0		0
151	80	44	1		3.49
	80	44	0.75	11.8	3.4574

	80	44	0		0
	65	44	1		4.30
	65	44	0.5	13.5	3.9555
	65	44	0		0
166.1	80	44	1		3.35
	80	44	0.75	12.2	3.5746
	80	44	0		0
	65	44	1		3.95
	65	44	0.5	14.4	4.2192
	65	44	0		0
174.9	80	44	1		3.33
	80	44	0.75	12	3.516
	80	44	0		0
	65	44	1		3.93
	65	44	0.5	14	4.102
	65	44	0		0
190.1	80	44	1		3.24
	80	44	0.75	12.3	3.6039
	80	44	0		0
	65	44	1		3.71
	65	44	0.5	13.7	4.0141
	65	44	0		0
195.2	80	44	1		3.27
	80	44	0.75	12.5	3.6625
	80	44	0		0
	65	44	1		3.72
	65	44	0.5	13.9	4.0727
	65	44	0		0
235.4	80	44	1		3.46
	80	44	0.75	12.3	3.6039
	80	44	0		0
	65	44	1		4.19
	65	44	0.5	15.2	4.4536
	65	44	0		0
261.6	80	44	1		3.39
	80	44	0.75	12.3	3.6039
	80	44	0		0
	65	44	1		4.03
	65	44	0.5	15.8	4.6294

	65	44	0		0
287.4	80	44	1		3.32
	80	44	0.75	11.9	3.4867
	80	44	0		0
	65	44	1		3.85
	65	44	0.5	15.6	4.5708
	65	44	0		0
333.4	80	44	1		3.44
	80	44	0.75	12.3	3.6039
	80	44	0		0
	65	44	1		4.11
	65	44	0.5	15.4	4.5122
	65	44	0		0
359.7	80	44	1		3.39
	80	44	0.75	12.1	3.5453
	80	44	0		0
	65	44	1		3.99
	65	44	0.5	15.5	4.5415
	65	44	0		0
385.7	80	44	1		3.34
	80	44	0.75	12.1	3.5453
	80	44	0		0
	65	44	1		3.86
	65	44	0.5	15.2	4.4536
	65	44	0		0

APPENDIX E

Collection of manufacturers' full-load data used to model water-cooled scroll chillers.

	Reference Capacity (tons)	Tevap,out (°F)	Tcond,in (°F)	Power in (kW)	Capacity (tons)	Capacity (kW)	COP
York	52.4	40	85	35.3	51.3	180.42	5.11
		42	85	35.5	53.2	187.10	5.27
		44	85	35.8	55.1	193.79	5.41
		46	85	36.2	57	200.47	5.54
		48	85	36.5	59	207.50	5.69
		50	85	36.9	61.1	214.89	5.82
		40	95	38.8	48.8	171.63	4.42
		42	95	39	50.6	177.96	4.56
		44	95	39.2	52.4	184.29	4.70
		46	95	39.4	54.3	190.97	4.85
		48	95	39.7	56.2	197.66	4.98
		50	95	39.9	58.1	204.34	5.12
		40	105	43.2	46.1	162.13	3.75
		42	105	43.3	47.8	168.11	3.88
		44	105	43.5	49.6	174.44	4.01
		46	105	43.6	51.4	180.77	4.15
		48	105	43.8	53.2	187.10	4.27
		50	105	44	55.1	193.79	4.40
York	59.9	40	85	41.1	58.7	206.45	5.02
		42	85	41.4	60.8	213.83	5.17
		44	85	41.8	62.9	221.22	5.29
		46	85	42.1	65.1	228.96	5.44
		48	85	42.5	67.4	237.05	5.58
		50	85	43	69.7	245.13	5.70
		40	95	45.3	55.8	196.25	4.33
		42	95	45.5	57.8	203.28	4.47
		44	95	45.7	59.9	210.67	4.61
		46	95	46	62	218.05	4.74
		48	95	46.3	64.2	225.79	4.88
		50	95	46.6	66.4	233.53	5.01
		40	105	50.6	52.8	185.70	3.67
		42	105	50.7	54.8	192.73	3.80
		44	105	50.8	56.7	199.41	3.93

		46	105	51	58.8	206.80	4.05
		48	105	51.2	60.8	213.83	4.18
		50	105	51.4	63	221.57	4.31
York	67.8	40	85	48.3	66.6	234.23	4.85
		42	85	48.6	69	242.67	4.99
		44	85	48.9	71.4	251.11	5.14
		46	85	49.2	73.9	259.91	5.28
		48	85	49.5	76.5	269.05	5.44
		50	85	49.9	79.1	278.19	5.58
		40	95	53.1	63.2	222.27	4.19
		42	95	53.3	65.5	230.36	4.32
		44	95	53.6	67.8	238.45	4.45
		46	95	53.9	70.2	246.89	4.58
		48	95	54.2	72.7	255.69	4.72
		50	95	54.5	75.2	264.48	4.85
		40	105	58.8	59.6	209.61	3.56
		42	105	59	61.8	217.35	3.68
		44	105	59.3	64.1	225.44	3.80
		46	105	59.5	66.4	233.53	3.92
		48	105	59.8	68.8	241.97	4.05
		50	105	60.1	71.2	250.41	4.17
York	76.6	40	85	52.6	75.2	264.48	5.03
		42	85	52.8	78	274.33	5.20
		44	85	53	80.8	284.17	5.36
		46	85	53.2	83.7	294.37	5.53
		48	85	53.4	86.6	304.57	5.70
		50	85	53.6	89.6	315.12	5.88
		40	95	57.8	71.3	250.76	4.34
		42	95	58.1	73.9	259.91	4.47
		44	95	58.3	76.6	269.40	4.62
		46	95	58.6	79.3	278.90	4.76
		48	95	58.8	82.1	288.75	4.91
		50	95	59.1	85	298.94	5.06
		40	105	63.7	67.2	236.34	3.71
		42	105	64	69.7	245.13	3.83
		44	105	64.3	72.3	254.28	3.95
		46	105	64.6	74.9	263.42	4.08
		48	105	64.9	77.6	272.92	4.21
		50	105	65.2	80.4	282.77	4.34

York	85.8	40	85	57.3	84.3	296.48	5.17
		42	85	57.6	87.3	307.03	5.33
		44	85	57.9	90.4	317.94	5.49
		46	85	58.2	93.5	328.84	5.65
		48	85	58.5	96.8	340.45	5.82
		50	85	58.8	100.1	352.05	5.99
		40	95	63.2	80	281.36	4.45
		42	95	63.5	82.9	291.56	4.59
		44	95	63.8	85.9	302.11	4.74
		46	95	64.1	88.9	312.66	4.88
		48	95	64.4	92	323.56	5.02
		50	95	64.7	95.2	334.82	5.17
		40	105	70	75.6	265.89	3.80
		42	105	70.3	78.4	275.73	3.92
		44	105	70.6	81.2	285.58	4.05
		46	105	70.9	84.1	295.78	4.17
		48	105	71.2	87.1	306.33	4.30
		50	105	71.5	90.2	317.23	4.44
York	92.7	40	85	61.8	90.9	319.70	5.17
		42	85	62.2	94.1	330.95	5.32
		44	85	62.6	97.4	342.56	5.47
		46	85	63	100.8	354.51	5.63
		48	85	63.4	104.2	366.47	5.78
		50	85	63.9	107.8	379.13	5.93
		40	95	68.3	86.6	304.57	4.46
		42	95	68.6	89.7	315.47	4.60
		44	95	68.9	92.8	326.38	4.74
		46	95	69.3	96.1	337.98	4.88
		48	95	69.7	99.4	349.59	5.02
		50	95	70.1	102.8	361.55	5.16
		40	105	75.8	82.1	288.75	3.81
		42	105	76.1	85.1	299.30	3.93
		44	105	76.4	88.1	309.85	4.06
		46	105	76.7	91.2	320.75	4.18
		48	105	77.1	94.3	331.65	4.30
		50	105	77.4	97.6	343.26	4.43
York	110.4	40	85	74	108.7	382.30	5.17
		42	85	73.8	112.5	395.66	5.36
		44	85	73.6	116.4	409.38	5.56

		46	85	73.5	120.3	423.09	5.76
		48	85	73.3	124.4	437.51	5.97
		50	85	73.2	128.5	451.93	6.17
		40	95	85.3	103.2	362.95	4.26
		42	95	85.1	106.8	375.62	4.41
		44	95	84.9	110.5	388.63	4.58
		46	95	84.7	114.2	401.64	4.74
		48	95	84.5	118.1	415.36	4.92
		50	95	84.3	122.1	429.43	5.09
		40	105	98.3	97.3	342.20	3.48
		42	105	98.1	100.7	354.16	3.61
		44	105	97.9	104.3	366.82	3.75
		46	105	97.6	107.9	379.48	3.89
		48	105	97.4	111.6	392.50	4.03
		50	105	97.2	115.3	405.51	4.17
York	127.4	40	85	82.5	125.4	441.03	5.35
		42	85	82.4	129.7	456.15	5.54
		44	85	82.3	134.2	471.98	5.73
		46	85	82.2	138.8	488.16	5.94
		48	85	82.1	143.6	505.04	6.15
		50	85	82	148.4	521.92	6.36
		40	95	95	118.9	418.17	4.40
		42	95	94.8	123.1	432.94	4.57
		44	95	94.7	127.4	448.07	4.73
		46	95	94.5	131.8	463.54	4.91
		48	95	94.3	136.3	479.37	5.08
		50	95	94.2	140.9	495.55	5.26
		40	105	109.4	112.1	394.26	3.60
		42	105	109.2	116.1	408.32	3.74
		44	105	109	120.1	422.39	3.88
		46	105	108.8	124.3	437.16	4.02
		48	105	108.5	128.6	452.29	4.17
		50	105	108.3	133	467.76	4.32
York	140.5	40	85	93.9	137.7	484.29	5.16
		42	85	94.5	142.6	501.52	5.31
		44	85	95	147.7	519.46	5.47
		46	85	95.7	152.8	537.40	5.62
		48	85	96.3	158.1	556.04	5.77
		50	85	97	163.5	575.03	5.93

		40	95	103.7	131.2	461.43	4.45
		42	95	104.2	135.9	477.96	4.59
		44	95	104.7	140.7	494.84	4.73
		46	95	105.2	145.6	512.08	4.87
		48	95	105.8	150.7	530.01	5.01
		50	95	106.4	155.9	548.30	5.15
		40	105	115.1	124.3	437.16	3.80
		42	105	115.5	128.8	452.99	3.92
		44	105	116	133.4	469.17	4.04
		46	105	116.4	138.2	486.05	4.18
		48	105	116.9	143	502.93	4.30
		50	105	117.5	148	520.52	4.43
York	144	40	85	91.7	141.9	499.06	5.44
		42	85	91.5	147	517.00	5.65
		44	85	91.4	152.2	535.29	5.86
		46	85	91.3	157.6	554.28	6.07
		48	85	91.1	163.1	573.62	6.30
		50	85	91	168.7	593.32	6.52
		40	95	105.1	134.1	471.63	4.49
		42	95	104.9	139	488.86	4.66
		44	95	104.7	144	506.45	4.84
		46	95	104.5	149.1	524.38	5.02
		48	95	104.3	154.3	542.67	5.20
		50	95	104.1	159.7	561.66	5.40
		40	105	120.5	126.1	443.49	3.68
		42	105	120.2	130.8	460.02	3.83
		44	105	120	135.5	476.55	3.97
		46	105	119.7	140.4	493.79	4.13
		48	105	119.4	145.3	511.02	4.28
		50	105	119.1	150.4	528.96	4.44
York	167.7	40	85	104.6	163.9	576.44	5.51
		42	85	103.6	170.1	598.24	5.77
		44	85	102.5	176.5	620.75	6.06
		46	85	101.4	183	643.61	6.35
		48	85	100.3	189.8	667.53	6.66
		50	85	99.1	196.7	691.79	6.98
		40	95	119.5	156	548.65	4.59
		42	95	118.8	161.8	569.05	4.79
		44	95	118	167.7	589.80	5.00

		46	95	117.3	173.8	611.25	5.21
		48	95	116.5	180.2	633.76	5.44
		50	95	115.6	186.7	656.62	5.68
		40	105	137.4	147.1	517.35	3.77
		42	105	136.9	152.5	536.34	3.92
		44	105	136.4	158.1	556.04	4.08
		46	105	135.8	163.8	576.08	4.24
		48	105	135.3	169.7	596.83	4.41
		50	105	134.6	175.8	618.29	4.59
York	199.6	40	85	127.1	195.1	686.17	5.40
		42	85	125.9	202.4	711.84	5.65
		44	85	124.7	209.8	737.87	5.92
		46	85	123.5	217.5	764.95	6.19
		48	85	122.2	225.4	792.73	6.49
		50	85	120.8	233.5	821.22	6.80
		40	95	144.9	185.8	653.46	4.51
		42	95	144.1	192.6	677.37	4.70
		44	95	143.3	199.6	701.99	4.90
		46	95	142.4	206.8	727.32	5.11
		48	95	141.5	214.2	753.34	5.32
		50	95	140.6	221.8	780.07	5.55
		40	105	166.4	175.4	616.88	3.71
		42	105	165.9	181.8	639.39	3.85
		44	105	165.3	188.4	662.60	4.01
		46	105	164.7	195.1	686.17	4.17
		48	105	164	202	710.43	4.33
		50	105	163.4	209.2	735.76	4.50
Trane	19.9	40	75	13.8	19.2	67.53	4.89
		42	75	13.9	20	70.34	5.06
		44	75	13.9	20.8	73.15	5.26
		46	75	14	21.5	75.62	5.40
		48	75	14	22.4	78.78	5.63
		50	75	14.1	23.2	81.59	5.79
		40	80	14.5	19	66.82	4.61
		42	80	14.6	19.8	69.64	4.77
		44	80	14.7	20.5	72.10	4.90
		46	80	14.7	21.3	74.91	5.10
		48	80	14.8	22.1	77.73	5.25
		50	80	14.8	22.9	80.54	5.44

		40	85	15.4	18.6	65.42	4.25
		42	85	15.4	19.3	67.88	4.41
		44	85	15.4	19.9	69.99	4.54
		46	85	15.5	20.9	73.51	4.74
		48	85	15.6	21.6	75.97	4.87
		50	85	15.6	22.4	78.78	5.05
		40	90	16.1	18.1	63.66	3.95
		42	90	16.2	18.9	66.47	4.10
		44	90	16.3	19.6	68.93	4.23
		46	90	16.3	20.4	71.75	4.40
		48	90	16.4	21.1	74.21	4.52
		50	90	16.5	21.9	77.02	4.67
		40	95	17.1	17.7	62.25	3.64
		42	95	17.1	18.4	64.71	3.78
		44	95	17.2	19.1	67.17	3.91
		46	95	17.3	19.9	69.99	4.05
		48	95	17.3	20.6	72.45	4.19
		50	95	17.4	21.4	75.26	4.33
Trane	24.5	40	75	17.2	23.8	83.70	4.87
		42	75	17.3	24.7	86.87	5.02
		44	75	17.4	25.7	90.39	5.19
		46	75	17.4	26.6	93.55	5.38
		48	75	17.5	27.6	97.07	5.55
		50	75	17.6	28.7	100.94	5.74
		40	80	18.1	23.2	81.59	4.51
		42	80	18.2	24.2	85.11	4.68
		44	80	18.3	25.1	88.28	4.82
		46	80	18.3	26.1	91.79	5.02
		48	80	18.4	27	94.96	5.16
		50	80	18.5	28	98.48	5.32
		40	85	19.1	22.7	79.84	4.18
		42	85	19.2	23.6	83.00	4.32
		44	85	19.1	24.5	86.17	4.51
		46	85	19.3	25.5	89.68	4.65
		48	85	19.4	26.4	92.85	4.79
		50	85	19.4	27.4	96.37	4.97
		40	90	20.1	22.1	77.73	3.87
		42	90	20.2	23	80.89	4.00
		44	90	20.3	23.9	84.06	4.14

		46	90	20.3	24.9	87.57	4.31
		48	90	20.4	25.8	90.74	4.45
		50	90	20.5	26.8	94.26	4.60
		40	95	21.2	21.6	75.97	3.58
		42	95	21.3	22.4	78.78	3.70
		44	95	21.4	23.3	81.95	3.83
		46	95	21.5	24.2	85.11	3.96
		48	95	21.6	25.2	88.63	4.10
		50	95	21.6	26.1	91.79	4.25
Trane	29.2	40	75	20.7	28.3	99.53	4.81
		42	75	20.8	29.4	103.40	4.97
		44	75	20.8	30.6	107.62	5.17
		46	75	20.9	31.7	111.49	5.33
		48	75	21	32.9	115.71	5.51
		50	75	21.1	34.1	119.93	5.68
		40	80	21.7	27.6	97.07	4.47
		42	80	21.8	28.7	100.94	4.63
		44	80	21.9	29.9	105.16	4.80
		46	80	22	31	109.03	4.96
		48	80	22.1	32.2	113.25	5.12
		50	80	22.1	33.4	117.47	5.32
		40	85	22.9	27	94.96	4.15
		42	85	23	28	98.48	4.28
		44	85	22.9	29.2	102.70	4.48
		46	85	23.1	30.3	106.57	4.61
		48	85	23.2	31.4	110.43	4.76
		50	85	23.3	32.6	114.65	4.92
		40	90	24.1	26.3	92.50	3.84
		42	90	24.2	27.3	96.01	3.97
		44	90	24.3	28.4	99.88	4.11
		46	90	24.4	29.5	103.75	4.25
		48	90	24.5	30.7	107.97	4.41
		50	90	24.6	31.8	111.84	4.55
		40	95	25.4	17.7	62.25	2.45
		42	95	25.5	26.6	93.55	3.67
		44	95	25.6	27.7	97.42	3.81
		46	95	25.7	28.7	100.94	3.93
		48	95	25.8	29.9	105.16	4.08
		50	95	25	31	109.03	4.36

Trane	39.4	40	75	27.3	38	133.65	4.90
		42	75	27.4	39.5	138.92	5.07
		44	75	27.5	41.1	144.55	5.26
		46	75	27.6	42.6	149.82	5.43
		48	75	27.8	44.2	155.45	5.59
		50	75	27.9	45.9	161.43	5.79
		40	80	28.7	37.2	130.83	4.56
		42	80	28.8	38.7	136.11	4.73
		44	80	28.9	40.2	141.38	4.89
		46	80	29	41.7	146.66	5.06
		48	80	29.2	43.3	152.29	5.22
		50	80	29.3	44.9	157.91	5.39
		40	85	30.2	36.5	128.37	4.25
		42	85	30.3	37.8	132.94	4.39
		44	85	30.3	39.4	138.57	4.57
		46	85	30.6	40.8	143.49	4.69
		48	85	30.7	42.4	149.12	4.86
		50	85	30.8	43.9	154.40	5.01
		40	90	31.8	35.5	124.85	3.93
		42	90	32	36.9	129.78	4.06
		44	90	32.1	38.4	135.05	4.21
		46	90	32.3	39.9	140.33	4.34
		48	90	32.4	41.4	145.60	4.49
		50	90	32.5	42.9	150.88	4.64
		40	95	33.6	34.6	121.69	3.62
		42	95	33.8	36	126.61	3.75
		44	95	33.9	37.4	131.54	3.88
		46	95	34.1	38.9	136.81	4.01
		48	95	34.2	40.4	142.09	4.15
		50	95	34.3	41.9	147.36	4.30
Trane	48.6	40	75	34.1	47	165.30	4.85
		42	75	34.2	48.9	171.98	5.03
		44	75	34.4	50.8	178.66	5.19
		46	75	34.5	52.8	185.70	5.38
		48	75	34.6	54.7	192.38	5.56
		50	75	34.8	56.8	199.77	5.74
		40	80	35.8	46	161.78	4.52
		42	80	36	47.8	168.11	4.67
		44	80	35.1	49.7	174.79	4.98

		46	80	36.3	51.6	181.48	5.00
		48	80	35.4	53.6	188.51	5.33
		50	80	36.5	55.5	195.19	5.35
		40	85	37.7	44.9	157.91	4.19
		42	85	37.9	46.7	164.24	4.33
		44	85	37.8	48.6	170.93	4.52
		46	85	38.2	50.4	177.26	4.64
		48	85	38.3	52.3	183.94	4.80
		50	85	38.5	54.3	190.97	4.96
		40	90	39.7	43.8	154.04	3.88
		42	90	39.9	45.6	160.38	4.02
		44	90	40.1	47.4	166.71	4.16
		46	90	40.2	49.2	173.04	4.30
		48	90	40.4	51.1	179.72	4.45
		50	90	40.5	53	186.40	4.60
		40	95	41	42.7	150.18	3.66
		42	95	42.1	44.4	156.15	3.71
		44	95	42.3	46.2	162.49	3.84
		46	95	42.4	48	168.82	3.98
		48	95	42.6	49.8	175.15	4.11
		50	95	42.8	51.7	181.83	4.25
Trane	59.4	40	75	42.1	57.7	202.93	4.82
		42	75	42.3	59.9	210.67	4.98
		44	75	42.5	62.1	218.41	5.14
		46	75	42.6	64.4	226.49	5.32
		48	75	42.8	66.7	234.58	5.48
		50	75	43	69.1	243.02	5.65
		40	80	44.2	56.4	198.36	4.49
		42	80	44.4	58.5	205.74	4.63
		44	80	44.6	60.7	213.48	4.79
		46	80	44.8	63	221.57	4.95
		48	80	45	65.2	229.31	5.10
		50	80	45.1	67.6	237.75	5.27
		40	85	46.5	55	193.43	4.16
		42	85	46.7	57.2	201.17	4.31
		44	85	46.8	59.4	208.91	4.46
		46	85	47.1	61.5	216.30	4.59
		48	85	47.3	63.7	224.03	4.74
		50	85	47.5	66	232.12	4.89

40	90	49	53.7	188.86	3.85
42	90	49.2	55.7	195.90	3.98
44	90	49.4	57.9	203.63	4.12
46	90	49.6	60	211.02	4.25
48	90	49.8	62.2	218.76	4.39
50	90	50	64.5	226.85	4.54
40	95	51.7	52.3	183.94	3.56
42	95	51.9	54.3	190.97	3.68
44	95	52.1	56.4	198.36	3.81
46	95	52.3	58.5	205.74	3.93
48	95	52.5	60.7	213.48	4.07
50	95	52.8	62.9	221.22	4.19

APPENDIX F

Collection of manufacturers' part-load data used to model water-cooled scroll chillers.

Reference Capacity (tons)	Tcond,in (°F)	Tevap,out (°F)	PLR	EER	COP
52.4	75	44	1		6.068954
	75	44	0.75	18.5	5.4205
	75	44	0		0
	65	44	1		7.173893
	65	44	0.5	21.1	6.1823
	65	44	0		0
59.9	75	44	1		5.959733
	75	44	0.75	18.2	5.3326
	75	44	0		0
	65	44	1		7.059484
	65	44	0.5	20.9	6.1237
	65	44	0		0
67.8	75	44	1		5.758473
	75	44	0.722	18.5	5.4205
	75	44	0		0
	65	44	1		6.808729
	65	44	0.5	21.2	6.2116
	65	44	0		0
76.6	75	44	1		6.032295
	75	44	0.75	19.4	5.6842
	75	44	0		0
	65	44	1		7.169754
	65	44	0.5	23.9	7.0027
	65	44	0		0
85.9	75	44	1		6.201135
	75	44	0.726	20.3	5.9479
	75	44	0		0
	65	44	1		7.396035
	65	44	0.5	23.7	6.9441
	65	44	0		0
92.8	75	44	1		6.176823
	75	44	0.75	19.7	5.7721
	75	44	0		0

	65	44	1		7.348029
	65	44	0.5	23.3	6.8269
	65	44	0		0
110.5	75	44	1		6.735816
	75	44	0.718	20.2	5.9186
	75	44	0		0
	65	44	1		8.918359
	65	44	0.5	25	7.325
	65	44	0		0
127.4	75	44	1		6.949508
	75	44	0.75	19.7	5.7721
	75	44	0		0
	65	44	1		9.179751
	65	44	0.5	25.2	7.3836
	65	44	0		0
144	75	44	1		7.050248
	75	44	0.75	20	5.86
	75	44	0		0
	65	44	1		9.24186
	65	44	0.5	25.3	7.4129
	65	44	0		0

APPENDIX G

Collection of reported quasi-steady-state constants for water-cooled reciprocating chillers.

	Reference Capacity (kW)	Tevap,out (°F)	Tcond,in (°F)	A2	A1	A0
Carrier 30HKA015	47.6	49.73	94.73	39.53	0.2239	18.21
Carrier 30HKA020	64	49.73	94.73	42.52	0.2667	26.96
Carrier 30HKA030	82.4	49.73	94.73	80.27	0.3444	6.733
Carrier 30HK040	119	49.73	94.73	142.2	0.6226	15.1
Carrier 30HK050	160	49.73	94.73	183.7	0.8913	44.68
Carrier 30HK060	192	49.73	94.73	179.4	0.8986	51.91
Carrier 30HK080	238	49.73	94.73	284.3	1.24	28.72
Carrier 30HK100	315	49.73	94.73	310.2	1.437	56.12
Carrier 30HK120	358	49.73	94.73	424.6	1.855	43.55
Carrier 30HK140	440	49.73	94.73	460.7	2.161	93.13
Carrier 30HK160	481	49.73	94.73	566.6	2.446	50.14
Trane CGAV214	585.8	49.73	94.73	924	3.712	7.032
Trane CGAV422	852.4	49.73	94.73	1342	5.622	73.07
Trane CGAV426 o/s	930.6	49.73	94.73	1094	4.687	86.27
Trane CGAV426	1065	49.73	94.73	1456	5.855	7.727
Trane CGAV428	1172	49.73	94.73	1851	7.433	14.26
Trane CGAV430	1279	49.73	94.73	2256	9.059	25.01
Trane CCAC 70R C60	242.2	49.73	94.73	354.6	1.352	-21.93
Trane CCAC 70R C80	255.6	49.73	94.73	301	1.209	-2.832
Trane CCAC 80R C80	255.6	49.73	94.73	388.2	1.583	5.357
Trane CCAC 80R D10	295.33	49.73	94.73	352	1.458	9.861
Trane CGWC C70R	257.7	49.73	94.73	258	1.019	-12
Trane CGWC C80R	296.4	49.73	94.73	318.3	1.268	-10.71
Trane CGWC C90R	328.4	49.73	94.73	318.2	1.371	-16.53
Trane CGWC D10R	367.8	49.73	94.73	334.8	1.387	-1.012
Trane CGWC D11R	402.7	49.73	94.73	353.1	1.501	9.678
Trane CGWC D12R	445.6	49.73	94.73	430.2	1.913	44.37

APPENDIX H

Collection of water-cooled screw chiller coefficients obtained from EnergyPlus library.

	Capacity		EIRFPLR		
	kW	Tons	C1	C2	C3
York YS	781	221	0.25191	0.275691	0.472583
York YS	879	249	0.30295	0.322312	0.375195
York YS	1758	498	0.31499	0.317127	0.370977
Carrier 23XL	686	194	0.21139	0.419023	0.368614
Carrier 23XL	830	235	0.23075	0.778416	-0.007517
Carrier 23XL	862	244	0.22928	0.366272	0.403202
Carrier 23XL	1062	301	0.25763	0.341691	0.400767
Carrier 23XL	1108	314	0.13707	0.837482	0.025343
Carrier 23XL	1196	339	0.10611	0.730551	0.163288

	Capacity		EIRFT					
	kW	Tons	C1	C2	C3	C4	C5	C6
York YS	781	221	0.4476	-0.01055	0.000713	0.011586	0.000515	-0.00098
York YS	879	249	0.55953	-0.01088	0.000872	0.010103	0.000509	-0.00121
York YS	1758	498	0.63813	0.006304	0.000923	-0.00455	0.000826	-0.00156
Carrier 23XL	686	194	0.50141	0.001561	-0.000135	0.01525	0.00057	-0.00122
Carrier 23XL	830	235	0.4611	-0.0156	-0.000274	0.026506	-7.8E-05	0.000186
Carrier 23XL	862	244	0.54206	-0.0211	0.001514	0.020679	0.000529	-0.00163
Carrier 23XL	1062	301	0.26341	-0.00703	-0.000494	0.025169	0.000171	-0.00043
Carrier 23XL	1108	314	0.56683	-0.02801	0.000936	0.022108	0.000466	-0.0008
Carrier 23XL	1196	339	0.50778	-0.01608	0.000174	0.020939	0.000416	-0.00072

	Capacity		CAPFT					
	kW	Tons	C1	C2	C3	C4	C5	C6
York YS	781	221	1.00215	0.033002	0.000374	-0.00593	-2.6E-05	-0.00022
York YS	879	249	1.03143	0.033647	-0.000274	-0.00379	-0.00016	0.000278
York YS	1758	498	0.81302	-0.01425	-0.001618	0.026384	-0.00092	0.001696
Carrier 23XL	686	194	0.29035	-0.02677	-0.004772	0.081624	-0.00303	0.005713
Carrier 23XL	830	235	0.81985	0.0043	-0.000245	0.01431	-0.00036	0.000251
Carrier 23XL	862	244	-0.03646	-0.06061	-0.003709	0.1198	-0.00372	0.005369
Carrier 23XL	1062	301	1.0257	0.023275	-0.004694	-0.00709	-0.00038	0.002843
Carrier 23XL	1108	314	0.66313	-0.01027	-0.000539	0.033203	-0.0013	0.002169
Carrier 23XL	1196	339	0.57759	0.022061	-0.003342	0.039702	-0.00167	0.002763

Regression Functions (Henninger et al. 2010):

$$\text{EIRFPLR} = C1 + C2 * PLR + C3 * PLR^2$$

$$\text{EIRFT} = C1 + C2 * T_{CHW,out} + C3 * T^2{}_{CHW,out} + C4 * T_{CW,in} + C5 * T^2{}_{CW,in} + C6 * T_{CHW,out} * T_{CW,in}$$

$$\text{CAPFT} = C1 + C2 * T_{CHW,out} + C3 * T^2{}_{CHW,out} + C4 * T_{CW,in} + C5 * T^2{}_{CW,in} + C6 * T_{CHW,out} * T_{CW,in}$$

$T_{CHW,out}$ and $T_{CW,in}$ in °C

APPENDIX I

Collection of water-cooled centrifugal chiller coefficients obtained from EnergyPlus library.

		Capacity		EIRFPLR		
		kW	Tons	C1	C2	C3
York YT	vanes	960	272	0.27379	0.31411	0.411367
York YT	vanes	1023	290	0.23684	0.32864	0.434494
York YT	vanes	1048	297	0.15438	0.72761	0.116239
York YT	vanes	1396	395	0.3043	0.0372	0.659034
York YT	vanes	1758	498	0.36948	0.09552	0.534729
York YT	vanes	2110	597	0.24692	0.18627	0.56609
Carreir 19XR	vanes	823	233	0.29654	0.46897	0.233234
Carrier 19XR	vanes	1196	339	0.27245	0.27104	0.455236
Carrier 19XR	vanes	1259	356	0.22262	0.51993	0.257847
Carreir 19XR	vanes	1635	463	0.25816	0.27072	0.470743
Carrier 19XR	vanes	2391	677	0.30364	0.25249	0.442929
York YT	VSD	897	254	0.04709	0.0707	0.88022
York YT	VSD	1090	309	0.1432	-0.4921	1.341333
York YT	VSD	1368	387	0.09484	0.15211	0.754303
York YT	VSD	1758	498	0.0786	0.19503	0.724158
York YT	VSD	1881	532	0.06088	0.48422	0.457152
Carrier 19XR	VSD	742	210	0.12023	0.13964	0.739404
Carrier 19XR	VSD	897	254	0.20364	-0.3913	1.187172
Carreir 19XR	VSD	1143	324	0.14088	-0.1578	1.014316
Carrier 19XR	VSD	1558	441	0.16209	-0.2554	1.092232
Carrier 19XR	VSD	2391	677	0.09775	0.24901	0.653938

		Capacity		EIRFT					
		kW	Tons	C1	C2	C3	C4	C5	C6
York YT	vanes	960	272	0.57359	0.0227	-0.00333	0.00603	0.000325	3.23E-05

York YT	vanes	1023	290	0.5255	-0.0197	0.000344	0.01651	0.000201	-0.00032
York YT	vanes	1048	297	0.72556	-0.035	0.002213	0.00393	0.000554	-0.00086
York YT	vanes	1396	395	0.52075	-0.0091	-0.00018	0.02569	4.26E-05	-0.00059
York YT	vanes	1758	498	0.23112	0.09582	-0.00567	0.02766	-0.000141	-0.00101
York YT	vanes	2110	597	0.62709	-0.0412	0.001327	0.02661	-0.000186	0.000509
Carreir 19XR	vanes	823	233	0.80291	0.02171	0.000239	-0.01096	0.001065	-0.00206
Carrier 19XR	vanes	1196	339	0.95144	-0.0225	-1.1E-05	-0.00014	0.000391	8.13E-05
Carrier 19XR	vanes	1259	356	0.7582	0.0069	-0.00149	0.00225	0.000391	-0.00017
Carreir 19XR	vanes	1635	463	0.7356	-0.0108	-0.00092	0.01459	8.49E-06	0.000128
Carrier 19XR	vanes	2391	677	0.62666	-0.0237	0.000403	0.02828	-0.000199	-0.00015
York YT	VSD	897	254	0.55261	0.0033	-0.0008	0.04246	-0.000353	-0.00094
York YT	VSD	1090	309	0.9241	-0.0496	0.000129	0.03299	-0.000677	0.001693
York YT	VSD	1368	387	0.32275	-0.0142	-0.00509	0.04607	-0.000877	0.0026
York YT	VSD	1758	498	0.67945	0.06695	-0.00363	-0.01019	0.001066	-0.00211
York YT	VSD	1881	532	0.61753	-0.0391	0.000618	0.02776	-0.000215	0.000551
Carrier 19XR	VSD	742	210	0.99461	-0.0483	0.000467	-0.00116	0.000576	0.000215
Carrier 19XR	VSD	897	254	0.6511	0.04949	-0.00082	0.02323	0.000199	-0.00267
Carreir 19XR	VSD	1143	324	0.94756	-0.0119	8.8E-05	0.00023	0.000182	0.000218
Carrier 19XR	VSD	1558	441	1.09934	-0.0313	0.000411	-0.00738	0.000578	-0.00035
Carrier 19XR	VSD	2391	677	0.62301	-0.0237	0.0004	0.02875	-0.000212	-0.00015

		Capacity		CAPFT					
		kW	Tons	C1	C2	C3	C4	C5	C6
York YT	vanes	960	272	-0.22785	0.40559	-0.03247	0.00379	-0.000224	0.000672
York YT	vanes	1023	290	0.25712	-0.0157	-0.00304	0.08107	-0.002569	0.004247
York YT	vanes	1048	297	0.72382	0.01748	-0.00452	0.02138	-0.000934	0.002515
York YT	vanes	1396	395	0.51679	-0.0279	-0.00095	0.06693	-0.002728	0.004723
York YT	vanes	1758	498	0.89759	-0.0146	0.003647	0.03203	-0.00119	0.00033
York YT	vanes	2110	597	0.53592	0.01786	0.001579	0.04523	-0.001632	0.000601

Carreir 19XR	vanes	823	233	0.55732	0.08715	-0.00292	0.025	-0.000886	-0.00032
Carrier 19XR	vanes	1196	339	1.1268	-0.0042	-0.002	0.00736	-0.001157	0.003065
Carrier 19XR	vanes	1259	356	1.08207	0.03201	-0.00399	-0.00579	-0.000824	0.002934
Carreir 19XR	vanes	1635	463	0.76392	0.0116	-0.00534	0.03307	-0.002101	0.004921
Carrier 19XR	vanes	2391	677	0.36764	-0.0509	-0.00177	0.09518	-0.003404	0.004527
York YT	VSD	897	254	0.1198	0.1569	-0.00443	0.0345	-0.000816	-0.00224
York YT	VSD	1090	309	0.6769	0.05712	-0.00061	0.01657	-0.000809	0.00023
York YT	VSD	1368	387	0.38322	-0.0327	-0.00339	0.0858	-0.003513	0.006528
York YT	VSD	1758	498	0.45751	0.13135	-0.00441	0.0193	-0.000548	-0.00138
York YT	VSD	1881	532	0.50652	-0.0042	-0.00268	0.04763	-0.001951	0.003994
Carrier 19XR	VSD	742	210	0.97971	-0.0029	-0.0009	0.01031	-0.000743	0.001454
Carrier 19XR	VSD	897	254	0.55597	0.07631	-0.00143	0.02168	-0.000623	-0.00099
Carreir 19XR	VSD	1143	324	0.79395	0.04096	-0.00142	-0.00164	-0.000522	0.001349
Carrier 19XR	VSD	1558	441	1.03431	0.02391	-0.00122	-0.00535	-0.000218	0.000628
Carrier 19XR	VSD	2391	677	0.36764	-0.0509	-0.00177	0.09518	-0.003404	0.004527

Regression Functions (Henninger et al. 2010):

$$\text{EIRFPLR} = C1 + C2 * PLR + C3 * PLR^2$$

$$\text{EIRFT} = C1 + C2 * T_{CHW,out} + C3 * T^2{}_{CHW,out} + C4 * T_{CW,in} + C5 * T^2{}_{CW,in} + C6 * T_{CHW,out} * T_{CW,in}$$

$$\text{CAPFT} = C1 + C2 * T_{CHW,out} + C3 * T^2{}_{CHW,out} + C4 * T_{CW,in} + C5 * T^2{}_{CW,in} + C6 * T_{CHW,out} * T_{CW,in}$$

$T_{CHW,out}$ and $T_{CW,in}$ in °C

VITA

Name:	Steven James Rivera
Address:	Energy Systems Laboratory Texas Engineering Experiment Station The Texas A&M University System 3581 TAMU College Station, TX 77843
Email Address:	stevenrivera@tees.tamus.edu
Education:	B.S., Mechanical Engineering, The University of Notre Dame, 2010